

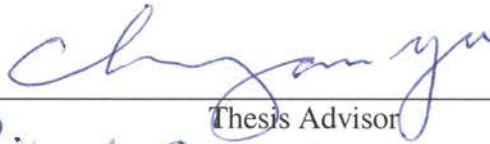
STRUCTURE AND FUNCTION STUDY OF THE
RHODOBACTER SPHAEROIDES
CYTOCHROME bc_1 COMPLEX

BY
KUNHONG XIAO
Bachelor of Medicine
Beijing Medical University
Beijing, P. R. China
1993

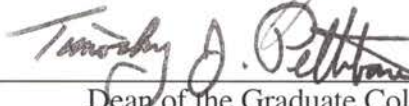
Submitted to the Faculty of the
Graduate College of the
Oklahoma State University
In partial fulfillment of
The requirements for the Degree of
DOCTOR OF PHILOSOPHY
May, 2003

STRUCTURE AND FUNCTION STUDY OF THE
RHODOBACTER SPHAEROIDES
CYTOCHROME bc_1 COMPLEX

Thesis Approved:



Thesis Advisor



Dean of the Graduate College

ACKNOWLEDGEMENTS

I wish to express sincere gratitude to my advisor Dr. Chang-An Yu for his guidance, inspiration and encouragement throughout my graduate program. I am also equally grateful to Dr. Linda Yu for her supervision, support and encouragement during my study. My sincere appreciation extends to my graduate committee members: Dr. Richard Essenberg, Dr. Robert Matts, and Dr. Robert Burnap, for their suggestions and assistance.

I would like to thank Dr. Frank Millett and Dr. Gregory Engstrom from University of Arkansas for their support and great collaboration.

I would also like to thank Dr. Hua Tian, Dr. Sudha K. Shenoy, Dr. Li Zhang, Dr. Xiaolin Wen, Dr. Zhaolong Li, Shi-jia Tso, Jian Zhu, Byron Quinn, other professors, postdoctors, staff, and students in Dr. Yu's lab and in the Biochemistry and Molecular Biology Department for their assistance and help in this study. My appreciation also goes to Dr. Roger Koeppel for the critical review of the manuscripts, and Ms. Jane Maxwell for spending time to read my dissertation and providing precious suggestions.

Finally, I would like to deeply thank my wife, Ke Liu, for her support and patience, my parents, Quanhua Xiao and Yucui Zeng and my sister, Yanjing Xiao for their inspiration and encouragement.

TABLE OF CONTENTS

Chapter	Page
I. Introduction.....	1
Bioenergetics and electron transfer chain.....	2
The cytochrome (cyt) bc_1 complex.....	5
References.....	37
II. Confirmation of the Involvement of Protein Domain Movement during the Catalytic Cycle of the Cytochrome bc_1 Complex by the Formation of an Intersubunit Disulfide Bond between Cytochrome b and the Iron-sulfur Protein	
Abstract.....	43
Introduction.....	44
Experimental Procedures.....	47
Results and discussion.....	52
References.....	71
III. Evidence for the Intertwined Dimer of the Cytochrome bc_1 Complex in Solution	
Abstract.....	75
Introduction.....	76
Experimental procedures.....	78
Results and discussion.....	81
References.....	97
IV. Photoinduced Electron Transfer between the Rieske Iron-Sulfur Protein and Cytochrome c_1 in the <i>Rhodobacter sphaeroides</i> Cytochrome bc_1 Complex --- Effects of pH, temperature, and driving force	
Abstract.....	100
Introduction.....	101
Experimental procedures.....	104
Results	107
Discussion.....	118
References.....	127
V. Effect of Famoxadone on Photoinduced Electron Transfer between the Iron-Sulfur Center and Cytochrome c_1 in the Cytochrome bc_1 Complex	
Abstract.....	132
Introduction.....	133
Experimental procedures.....	135
Results and Discussion.....	138

References.....	160
-----------------	-----

VI. The Extra Fragment of Iron-Sulfur Protein (Residues 96-107) of *R. sphaeroides*
Cytochrome *bc*₁ Complex is Required for Protein Stability

Abstract.....	164
Introduction.....	165
Experimental procedures.....	171
Results and discussion.....	174
References.....	187

LIST OF TABLES

	page
I-1. Properties of Bovine Heart Mitochondrial Electron Transfer Complexes	4
I-2. Effects of Q _o Site Inhibitors on the Relative Anomalous Peak Height of the 2Fe2S Cluster of ISP (normalized to heme b) in the Beef Cytochrome <i>bc</i> ₁ Complex	22
II-1. Characterization of ISP and Cytochrome <i>b</i> interface Cysteine Mutants.....	55
II-2. Effect of β-ME on the Cytochrome <i>bc</i> ₁ Activity in Chromatophores, ICM, and Purified Complexes from Wild Type and Mutants A185C(<i>cyt</i> <i>b</i>), K70C(ISP), and A185C/K70C.....	61
III-1. Characterization of ISP and cytochrome <i>b</i> Interface Cysteine Mutants.....	84
III-2. Effect of β-ME on the Cytochrome <i>bc</i> ₁ Activity in Chromatophores and Purified Complexes from Wild type, Single- and Double-cysteine Pair Mutants.....	91
IV-1. Kinetic Properties of <i>R. sphaeroides</i> Cyt <i>bc</i> ₁ Mutants.....	116
V-1. Spectral and Electrochemical Properties of Ruthenium Complexes.....	141
V-2. Kinetic Properties of <i>R. sphaeroides</i> Cyt <i>bc</i> ₁ Mutants.....	155
V-3. Effect of Famoxadone on Electron Transfer from 2Fe-2S to Cyt <i>c</i> ₁ in <i>R. sphaeroides</i> Cyt <i>bc</i> ₁ Mutants.....	156
VI-1. Characterization of the ISP Extra Fragment Mutants.....	178

LIST OF FIGURES

	Page
I-1. Mitochondrial electron transfer chain.....	3
I-2. The protonmotive Q-cycle.....	8
I-3. Structural formula of some representative inhibitors of the cytochrome bc_1 complex.....	9
I-4. The 3-D structure of mitochondrial cytochrome bc_1 complex.....	11
I-5. Structure of Rieske iron-sulfur protein (ISP).....	13
I-6. Ribbon representation of the cytochrome b structure	15
I-7. The intertwining dimer of cytochrome bc_1 complex.....	17
I-8. The distances of the redox centers in tetragonal $I4_122$ crystal of native oxidized bovine mitochondrial cyt bc_1 complex.....	19
I-9. Various positions of $[2Fe_2S]$ in crystals loaded with different Q_0 site inhibitors	21
I-10. Carton representation of the "moving Rieske" model in the protonmotive Q-cycle	26
I-11. The 3-D model of <i>R. sphaeroides</i> cytochrome bc_1 complex.....	36
II-1. Location of engineered cysteines and free endogenous cysteines in the structural model of the <i>R. sphaeroides</i> bc_1 complex.	53
II-2. SDS-PAGE of cysteine mutant cytochrome bc_1 complexes.	57
II-3. EPR spectra of the $2Fe_2S$ cluster in the cytochrome bc_1 complexes of wild type, A185C (cytb), K70C (ISP) and A185C (cytb)/K70C (ISP) with or without 100 mM β -ME treatment	64
II-4. pH induced reduction and oxidation of ISP and cytochrome c_1 in the partially reduced <i>R. sphaeroides</i> cytochrome bc_1 complex.....	67
II-5. Time trace of the redox change of cytochrome c_1 in the cytochrome bc_1 complex upon changing the pH from 6.9 to 8.9 or from 8.9 to 6.9.....	69
III-1. Location of engineered cysteines in the structural model of the <i>R. sphaeroides</i>	

<i>bc</i> ₁ complex.	83
III-2. SDS-PAGE of single- and double-cysteine-pair mutant cytochrome <i>bc</i> ₁ complexes	88
III-3. EPR spectra of the 2Fe2S cluster in the cytochrome <i>bc</i> ₁ complexes of wild type (WT) and indicated mutants, with (+) or without (-) 100 mM β-ME treatment.....	95
IV-1. X-ray crystal structures of cytochrome <i>bc</i> ₁ from chicken in the presence of stigmatellin and antimycin (<i>b</i> state), and in the beef P6 ₅ 22 crystals (<i>c</i> ₁ state).....	102
IV-2. Electron transfer within <i>R. sphaeroides</i> cyt <i>bc</i> ₁ following photooxidation of cyt <i>c</i> ₁	108
IV-3. Electron transfer within <i>R. sphaeroides</i> cyt <i>bc</i> ₁ following photooxidation of cyt <i>c</i> ₁	111
IV-4. pH dependence of the rate constant for electron transfer from 2Fe-2S to cyt <i>c</i> ₁	113
IV-5. Temperature dependence of rate constant for electron transfer from 2Fe-2S to cyt <i>c</i> ₁	115
IV-6. Structure of bovine cyt <i>bc</i> ₁ P6 ₅ 22 crystals in the <i>c</i> ₁ state.....	122
V-1. (A).X-ray crystal structure of bovine cyt <i>bc</i> ₁ in the presence of famoxadone	139
V-1. (B). X-ray crystal structure of bovine cyt <i>bc</i> ₁ P6 ₅ 22 crystals (<i>c</i> ₁ conformation)	140
V-2. Electron transfer from 2Fe-2S to cyt <i>c</i> ₁ in bovine cyt <i>bc</i> ₁ following photooxidation of cyt <i>c</i> ₁	142
V-3. Reverse electron transfer from cyt <i>c</i> ₁ to 2Fe-2S in bovine cyt <i>bc</i> ₁ following photoreduction of cyt <i>c</i> ₁	149
V-4. Temperature dependence of rate constant for electron transfer from cyt <i>c</i> ₁ to 2Fe-2S in bovine cyt <i>bc</i> ₁ inhibited with famoxadone.....	151
V- 5. Electron transfer from 2Fe-2S to cyt <i>c</i> ₁ in <i>R. sphaeroides</i> cyt <i>bc</i> ₁ following photooxidation of cyt <i>c</i> ₁	153
VI-1. Partial sequence comparison of various ISPs in the region of extra fragment	168

VI-2. The location of the extra fragment of ISP in the proposed structural model of <i>Rhodobacter sphaeroides</i> cytochrome bc_1 complex.....	169
VI-3. Photosynthetic growth of various <i>R. sphaeroides</i> strains.....	177
VI-4. Western blot analysis of ISP in complement and mutant membranes.....	180
VI-5. EPR spectra of the 2Fe2S cluster of Rieske iron-sulfur protein in membranes from the complement and mutants ISP Δ (96-107), ISP(96-107)A, ISP(96-99)A, ISP(100-103)A, and ISP(104-107)A.....	182
VI-6. Western blot analysis of ISP in broken cell suspension, 200,000 x g supernatant and 200,000 x g precipitate fractions from complement and mutant cells.....	183
VI-7. SDS-PAGE analysis of the purified cytochrome bc_1 complexes from complement and mutant membranes	185

NOMENCLATURE

ADP	adenosine diphosphate
ATP	adenosine triphosphate
β -ME	β -mercaptoethanol
cyt	cytochrome
DNA	deoxyribonucleic acid
<i>E. coli</i>	<i>Escherichia coli</i>
EPR	electron paramagnetic resonance
ISP	Iron sulfur protein
kDa	kilodaltons
kb	kilo base pairs
PAGE	polyacrylamide gel electrophoresis
PMSF	phenylmethylsulfonyl fluoride
Pi	phosphate
Q	ubiquinone
Q ₀ C ₁₀ Br	2,3-dimethoxy-5-methyl-6-(10-bromo)-decyl-1,4-benzoquinone
Rs.	<i>Rhodobacter sphaeroides</i>
SDH	succinate dehydrogenase
SDS	sodium dodecylsulfate
SMP	submitochondrial particle
UHDBT	5- <i>n</i> -undecyl-6-hydroxyl-4,7-dioxobenzothiazole
UV	ultra violet

CHAPTER I INTRODUCTION

Table of Contents

I. Bioenergetics and oxidative phosphorylation

II. The cytochrome bc_1 complex

1. The role of the cytochrome bc_1 complex in the electron transfer chain
2. The catalytic mechanism for the cytochrome bc_1 complex---protonmotive Q-cycle
3. The 3-dimensional structural study of bovine heart mitochondrial cytochrome bc_1 complex
 - 1). The crystal structure of cytochrome bc_1 complex
 - A. The overall structure of cytochrome bc_1 complex
 - B. The structure of Rieske iron-sulfur protein (ISP)
 - C. The structure of cytochrome b
 - D. New features deduced from the crystal structure of cytochrome bc_1 complex
 - 2). The crystal structures of cytochrome bc_1 complex loaded with Q_o site inhibitors
 - A. Conformational changes in ISP induced by Q_o site inhibitors
 - B. Conformational changes in cytochrome b induced by Q_o site inhibitors
4. The movement of the head domain of ISP during bc_1 catalysis
 - 1). The “moving Rieske” model
 - 2). The mobility of ISP head domain is essential for bc_1 catalysis
 - 3). The rate constants of electron transfer between 2Fe2S and heme c_1 and the rate-limiting step of ubiquinol oxidation
5. Study system
 - 1). Photosynthetic bacteria *Rhodobacter sphaeroides* cytochrome bc_1 complex
 - 2). Homology structural modeling of *Rhodobacter sphaeroides*

III. References

I. Bioenergetics and oxidative phosphorylation

More than 95% of the energy required for eukaryotic organisms is produced by the oxidative phosphorylation process that is carried out in the inner mitochondrial membrane by the electron transfer chain and a ATP synthase complex (Fig. 1). The mitochondrial electron transfer (ET) chain is composed of four multi-subunit electron transfer complexes: NADH-ubiquinone oxidoreductase (Complex I), succinate ubiquinone reductase (Complex II), ubiquinol-cytochrome *c* reductase (Complex III), and cytochrome *c* oxidase (Complex IV). Table I summarizes the subunit compositions and prosthetic groups in these four electron transfer complexes.

Electrons from NADH or succinate which are derived from the TCA cycle or lipid oxidation are passed through Complexes I, III and IV or II, III and IV, respectively, to molecular oxygen. The electrons that transfer through these complexes, except Complex II, are coupled to translocate protons across the mitochondrial inner membrane to generate a proton gradient and membrane potential for use by ATP synthase (Complex V) to synthesize ATP. ATP synthase is comprised of two basic units--- F_1 and F_0 . The water-soluble catalytic unit F_1 ($\alpha_3\beta_3\gamma\delta\epsilon$) binds ADP and Pi and synthesizes ATP. It consists of a hexagonal array of alternating α - and β -subunits with a centrally located γ -subunit, which has been shown to rotate during catalysis (1, 2). The detergent-soluble moiety F_0 delivers the energy from the electrochemical proton gradient, via the rotating γ -subunit, to the F_1 -ATP complex to induce the release of tightly bound ATP on one of the three β -subunits while promoting ATP synthesis from ADP and Pi on a second β -subunit and binding of ADP and Pi to a third (2, 3). The generation of a proton electrochemical

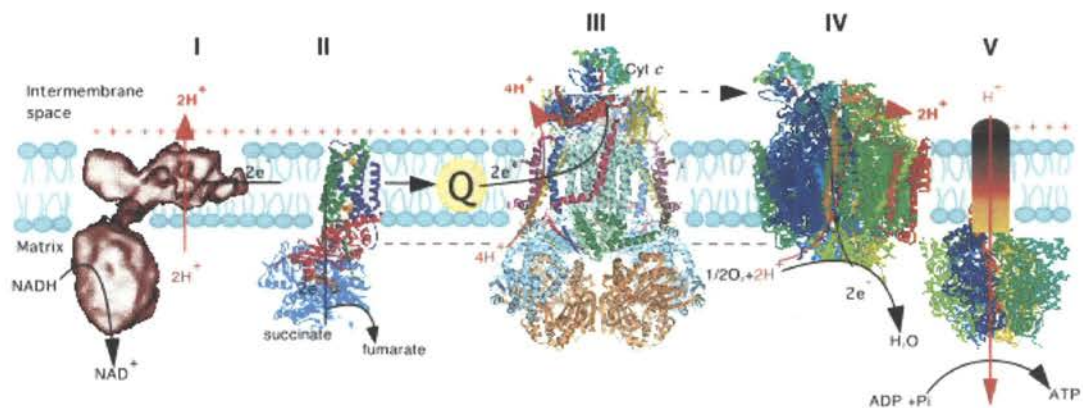


Fig. 1. Mitochondrial electron transfer chain.

Table I
*Properties of Bovine Heart Mitochondrial
 Electron Transfer Complexes*

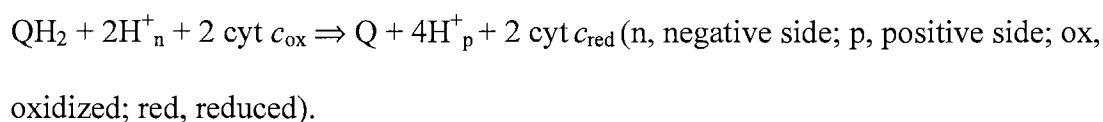
Complex	Other names	Subunits	Proton Pumping	Molecular weight (monomer) (kDa)	Prosthetic groups	Midpoint potential (mV)
I ⁽⁴⁾	NADH-UQ reductase (NQR)	43	Yes	907	FMN [2Fe2S]N-1a [2Fe2S]N-1b [2Fe2S]N-2 [2Fe2S]N-3,4 [2Fe2S]N-5,6	-245~-335 -375 -250 -150 -250 -260
II ⁽⁵⁻⁷⁾	Succinate-UQ reductase (SQR)	5	No	127	FAD [2Fe2S]S-1 [4Fe4S]S-2 [3Fe4S]S-3 <i>b</i> ₅₆₀	-40 0 -270 130 -185
III ⁽⁸⁾	UQH ₂ -cytochrome <i>c</i> reductase (QCR)	11	Yes	248	<i>b</i> ₅₆₂ (<i>b</i> _H) <i>b</i> ₅₆₆ (<i>b</i> _L) <i>c</i> ₁ 2Fe2S	+30 -30 230 280
IV ⁽⁹⁾	Cytochrome <i>c</i> oxidase (CcO)	13	Yes	204	<i>a</i> Cu _A Cu _B <i>a</i> ₃	210 245 340 385

membrane potential ($\Delta\mu_{\text{H}^+}$) across the energy-transducing membrane during electron transfer through the energy transducing electron transfer complexes is the central dogma of the chemiosmotic hypothesis, which was proposed by the Noble Prize laureate Peter Mitchell (10-14). To this date, the electron transfer and proton translocation in the electron transfer chain are the main points of bioenergetics.

II. The cytochrome (cyt) bc_1 complex

1. The role of the cytochrome bc_1 complex in the electron transfer chain

The cytochrome bc_1 complex, also known as ubiquinol-cytochrome c reductase or Complex III, is the central complex of the energy-conserving electron transfer system of mitochondria (Fig.1) and many respiratory and photosynthetic bacteria (15-17). The complex catalyzes electron transfer from quinol to cytochrome c or c_2 with concomitant generation of a proton gradient and membrane potential for ATP synthesis. The following equation describes the overall reaction catalyzed by the bc_1 complex:



All cytochrome bc_1 complexes contain three essential subunits to which the prosthetic groups bind (15-17). These three essential subunits are: cytochrome b , which houses two b-type hemes (b_{566} or b_{L} and b_{562} or b_{H}), cytochrome c_1 , which houses a c-type heme (c_1), and the Rieske iron-sulfur protein (ISP), which houses a high-potential [2Fe2S] cluster (15-17). Besides these three essential subunits, varied numbers of supernumerary subunits (subunits which contain no redox prosthetic groups) are present

in the cytochrome bc_1 complexes from different sources (16, 18). Although the functions of these supernumerary subunits are largely unknown, the complexes containing no supernumerary subunits are less stable and have lower activity than those with supernumerary subunits (19-21). Therefore, it is possible that the increased enzymatic activity for the mitochondrial complexes results from interaction of the essential subunits with supernumerary subunits. The study of the function of supernumerary subunits in the cytochrome bc_1 complex is one of the ongoing projects in our laboratory (19-21).

2. The catalytic mechanism for the cytochrome bc_1 complex---protonmotive Q-cycle

Although several models have been proposed for the electron and proton transfer in the cytochrome bc_1 complex, the “protonmotive Q-cycle” hypothesis proposed by Peter Mitchell (22, 23) is the most popular one.

There are two key features for this Q-cycle mechanism (8, 24-26) (Fig. 2): (i) The involvement of two separate binding sites for ubiquinone and ubiquinol: ubiquinol is first oxidized at the Q_o site near the positive side (P-side) of the inner mitochondrial membrane, and ubiquinone is reduced at the Q_i site near the negative side (N-side) of the membrane. (ii) The bifurcated electron transfer at the Q_o site---the two electrons from the ubiquinol (QH_2) diverge at the Q_o site. The first one electron is transferred to cytochrome c through a high redox potential chain; it goes to the $2Fe_2S$ cluster ($E_{m,7} = 280$ mV), heme c_1 , and then to heme c with concomitant formation of an ubisemiquinone anion at the Q_o site. The electron is then transferred to cytochrome c through cytochrome c_1 . The

second electron from the ubisemiquinone is transferred through a low redox potential pathway to heme b_L ($E_{m,7} = -30$ mV) and then to heme b_H ($E_{m,7} = 30$ mV). The heme b_H near the Q_i site then reduces ubiquinone to form a stable ubisemiquinone ($Q^{\cdot-}$). So far, the cycle is only half completed with only one electron from ubiquinol transferred to cytochrome c and two protons released to the P-side of the membrane. During the second turnover, a second molecule of QH_2 is oxidized at the Q_o site resulting in the transfer of another electron to ISP and a second electron passing to b_H , which then reduces the ubisemiquinone to QH_2 with the uptake of two protons from the N-side. As dictated in the Q-cycle model, in a completed turnover of the cytochrome bc_1 complex, two QH_2 molecules are oxidized at the Q_o site, one QH_2 is generated at the Q_i site, two molecules of cyt c are reduced, and four protons are deposited on the P-side of the membrane.

The protonmotive Q-cycle mechanism is supported by many biophysical and biochemical experimental results. (i) The protonmotive Q-cycle accounts for one of the most mysterious observations relating to cytochrome b oxidation and reduction---the oxidant-induced cytochrome b reduction phenomenon. Addition of reduced ubiquinol to cytochrome bc_1 complex completely reduces cytochrome c_1 , but only causes a 30% reduction of cytochrome b . Binding of antimycin A enhances the reduction of cytochrome b and prevents the reduction of cytochrome c_1 . When ferricyanide is added to oxidize the cytochrome bc_1 complex, cytochrome c_1 becomes oxidized as expected but cytochrome b becomes unusually reduced (27). No linear electron transfer scheme accounts for this oxidant-induced cytochrome b reduction phenomenon (26). The Q-cycle

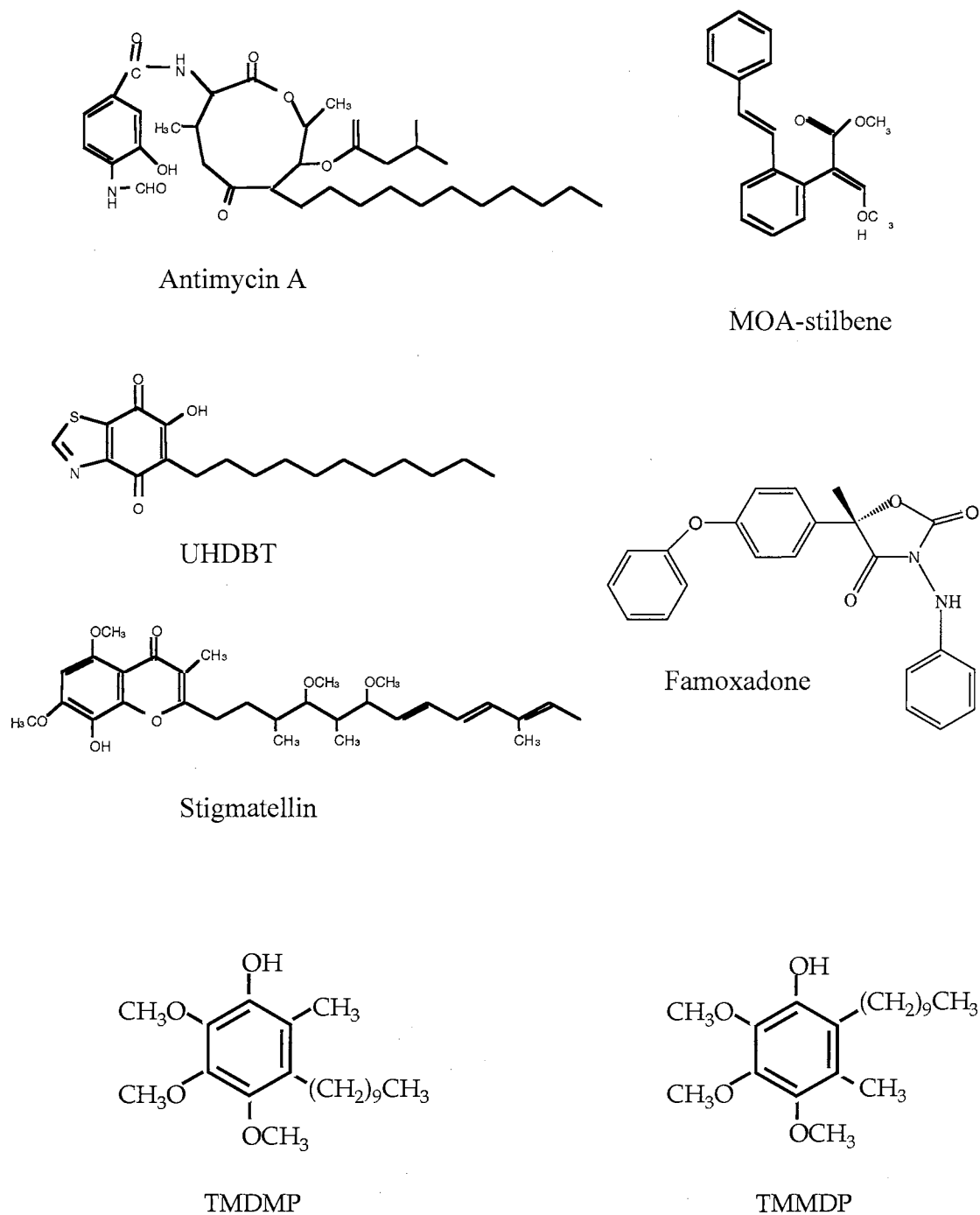


Fig. 3. Structure of some representative inhibitors of the cytochrome *bc*₁ complex.

mechanism explains the oxidant-induced cytochrome *b* reduction by postulating that ubiquinol is divergently oxidized by cytochrome *c*₁ and cytochrome *b*. Ubiquinol plays an integral role that undergoes a two-step oxidation and reduction via the free radical ubisemiquinone. The first electron from ubiquinol is transferred to 2Fe2S, and then to cytochrome *c*₁ and cytochrome *c*; and the second electron is transferred from ubisemiquinone in the Q_o site to heme b_L and then to heme b_H and ubiquinone in the Q_i site (14, 28, 29). (ii) The finding of two different sets of inhibitors also supports the Q-cycle mechanism. The inhibitors binding to the Q_o site, like stigmatellin, myxothiazol and UHDBT, block the oxidation of ubiquinol, whereas the inhibitors binding to the Q_i site, like antimycin A and HQNO, block ubiquinone reduction (18, 26, 30). Only use of these two classes of inhibitors simultaneously can the cytochrome *bc*₁ complex be completely inhibited. Fig. 3 lists the structures of some representative inhibitors of cytochrome *bc*₁ complex. (iii) The observation of two protons being translocated across the membrane per one electron oxidized by the complex (31). (iv) A stable ubisemiquinone radical was detected in isolated mitochondrial cytochrome *bc*₁ complex and this radical is antimycin A sensitive (32). (v) A transient, unstable ubisemiquinone radical which is not antimycin A sensitive was detected by de Vires, et. al. (33). However, the existence of this unstable ubisemiquinone radical was questioned by other groups (34, 35) because no Q_o site inhibitor-sensitive ubisemiquinone radical was detected under the same oxidant-induced condition. The failure to detect the ubisemiquinone radical might be due to the very rapid electron transfer in the Q_o site.

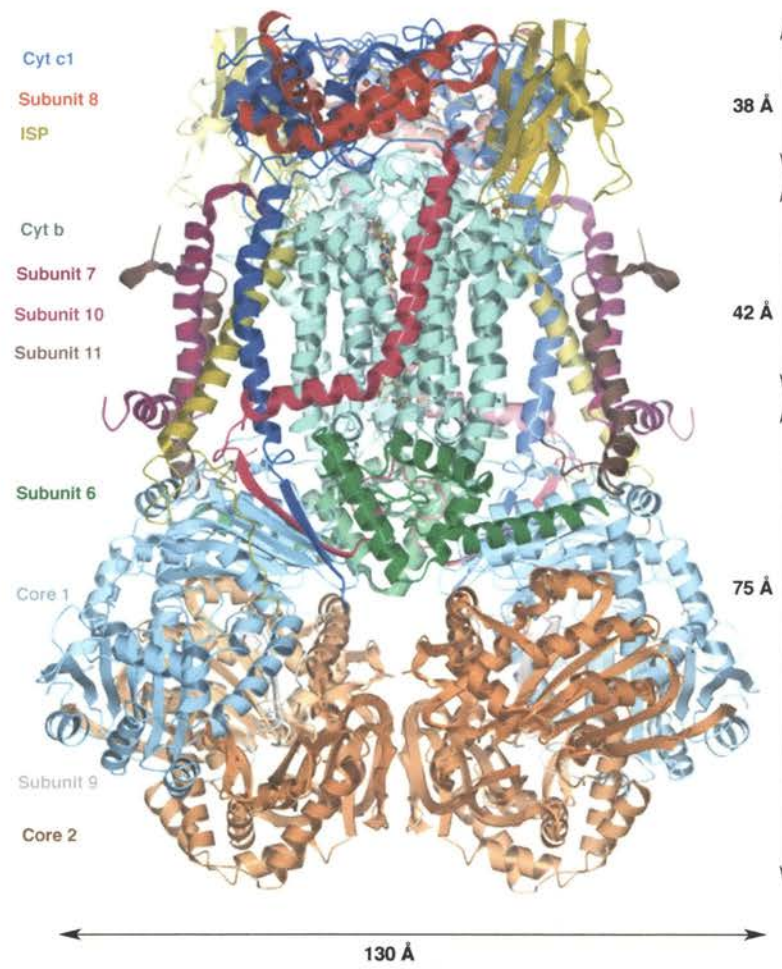


Fig. 4. The 3-D structure of mitochondrial cytochrome bc_1 complex.

3. The 3-dimensional structural study of bovine mitochondrial cytochrome bc_1 complex

1). The crystal structural of cytochrome bc_1 complex

A. The overall structure of cytochrome bc_1 complex

The structural information for the cytochrome bc_1 complex was primarily obtained from X-ray crystallographic investigations of eukaryotic mitochondrial cytochrome bc_1 complexes (37-40). The first bc_1 complex crystal structure, determined at 2.9Å resolution, from bovine heart mitochondria, was reported in 1997 by our group in collaboration with Deisenhofer's group (37). Since then, crystallographic structures of mitochondrial bc_1 complexes from other sources such as chicken and yeast have also become available from other groups (38-40). In our bovine $I4_122$ crystal structure, the cytochrome bc_1 complex is a pear-shaped, intertwined dimer with a maximal diameter of 130 Å in width and 155 Å in height. It can be divided into three regions: matrix, transmembrane, and intermembrane space regions (Fig. 4). More than one-half of the molecular mass is located in the matrix region of the molecule, extending 75 Å from the transmembrane helices. This region consists of subunits I, II, VI, IX, the N-terminal part of subunit VII and the C-terminal of ISP. The transmembrane region is about 42 Å thick, consisting of 13 transmembrane helices in each monomer, eight from cytochrome b , five from cytochrome c_1 , ISP, and subunits VII, X, and XI, respectively. The transmembrane region of cytochrome b houses heme b_L and b_H , and Q_o and Q_i pockets. The intermembrane space region, which extends 38 Å into intermembrane space from the membrane surface, houses the functional domains of cytochrome c_1 and ISP, as well as subunit VIII (37).

B. The structure of Rieske iron-sulfur protein (ISP)

The overall structure of Rieske iron-sulfur protein (ISP) can be divided into three domains: the membrane spanning N-terminal domain (tail domain) including residues 1-62, the soluble C-terminal domain (head domain) covering residues 73-196, and the flexible linking domain (neck region) covering residues 63-72 (42) (Fig. 5A). In tetragonal $I4_122$ crystals of native bc_1 complex, the head domain of ISP is represented by a weak, uninterpretable electron density indicating that this domain is highly mobile. However, this extramembrane soluble head domain (ISF) of ISP was crystallized individually and its structure was determined at 1.5 Å resolution (42) (Fig. 5B). It is a rigid, compact and flat-spherical-shaped structure that contains three layers of antiparallel beta sheets comprising 10 β -strands. The 2Fe2S cluster is located at the tip of the head domain. The cluster-binding fold is a small domain like structure comprised of approximately 46 amino acids. The loops between β_4 - β_5 and β_6 - β_7 each contribute one cysteine and one histidine to the cluster. Cysteines 139 and 158 are ligands of Fe-1 and are buried within the protein. Histidines 141 and 161 are ligands to the redox-active Fe-2 and are completely exposed to the solvent (Fig. 5C). The conserved cysteines 144 and 160 (one on each loop) form a disulfide bond to bring the two loops together and stabilize this region. A complex hydrogen bond network is formed around the 2Fe2S cluster in the structure (Fig. 5D). With the exception of cysteine 158, which has only one hydrogen bond to the nitrogen of cysteine 160, all sulfur atoms around the 2Fe2S cluster are involved in two hydrogen bonds each. The hydrogen bond network also includes residues Ser-163 and Tyr-165. The hydroxyl group of Ser-163 is hydrogen-bonded to S-1 and the hydroxyl group of Tyr-165 is hydrogen-bonded to S^r of cysteine 139 (42). The hydrogen

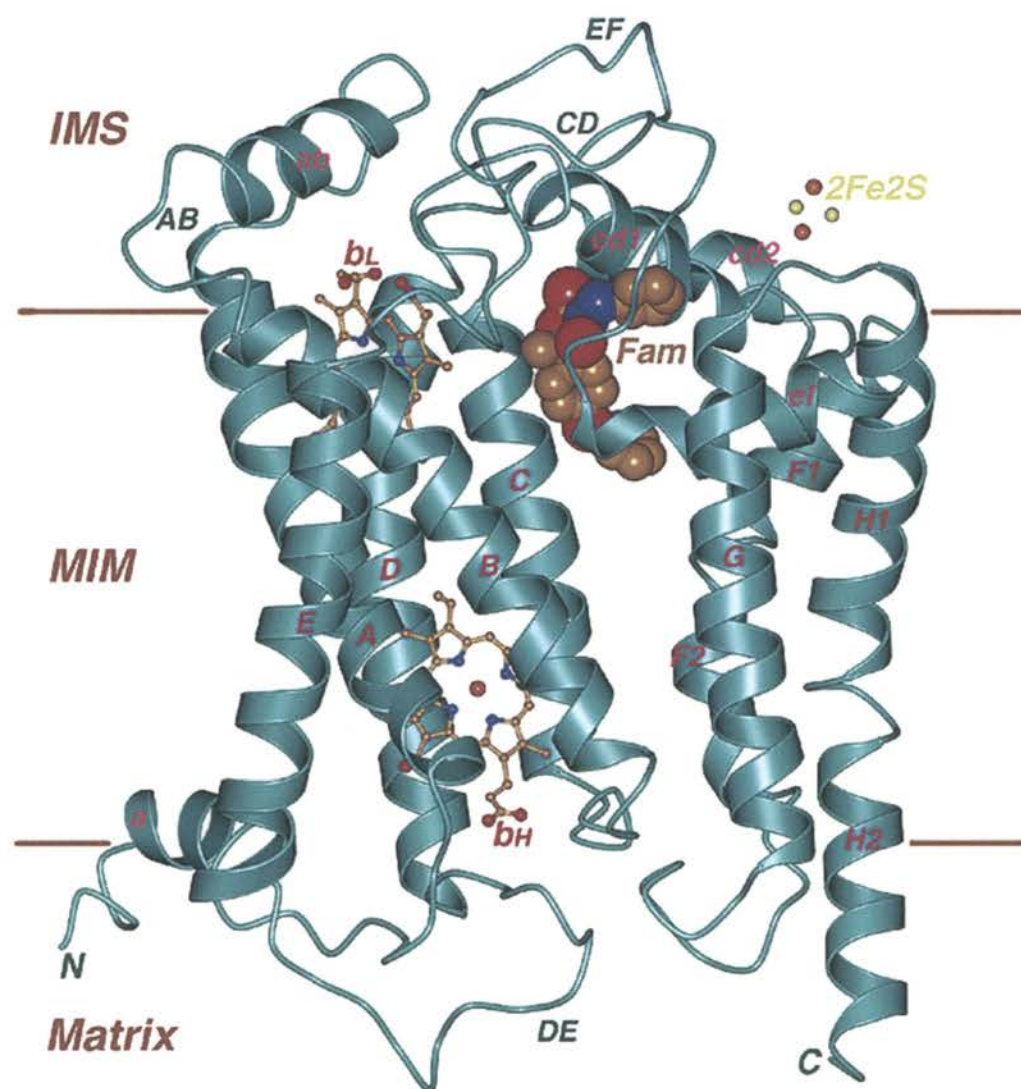


Fig. 6. Ribbon representation of the cytochrome *b* structure. A famoxadone (Fam) molecule is bound in the structure.

bond network is the main contribution to the high mid-point potential of 2Fe2S and its pH dependence, which is used for the kinetics analysis in this study.

C. The structure of cytochrome *b*

Cytochrome *b* is considered a key player in the function of cytochrome *bc*₁ complex, coordinating to the actions of various components of cytochrome *bc*₁ in the catalytic cycle. Eight out of the thirteen membrane-spanning helices belong to the cytochrome *b* subunit. They can be divided into two groups, with helices A, B, C, D, and E in one group, and helices F, G, and H in the other group. Four long loops (AB, CD, DE, and EF) and three short loops (BC, FG, and GH) connect these eight helices (37, 43) (Fig. 6). In the crystal structure, both N- and C- terminals are located in the matrix region. Heme *b*_L is near the P-side and heme *b*_H is near the N-side of the membrane. The distance of 21 Å (from iron to iron) between heme *b*_L and *b*_H is in good agreement with the predicted distance of 22 Å derived from the previous biochemical and biophysical studies (44). The observation of a distance of 21 Å between the two *b*_L hemes in the dimer indicates that rapid electron transfer between the two *b*_L hemes may occur. Heme *b*_L and *b*_H are bound within the four-helix bundle made by helices A, B, C, and D. As predicted, the axial ligands of both hemes are histidines: His 83 and His 182 for heme *b*_L, and His 97 and His 196 for heme *b*_H. The putative ubiquinol/ubiquinone binding sites, Q_o site and Q_i site, are located at the P-side and N-side and close to heme *b*_L and *b*_H, respectively.

D. New features deduced from the crystal structure of cytochrome *bc*₁ complex

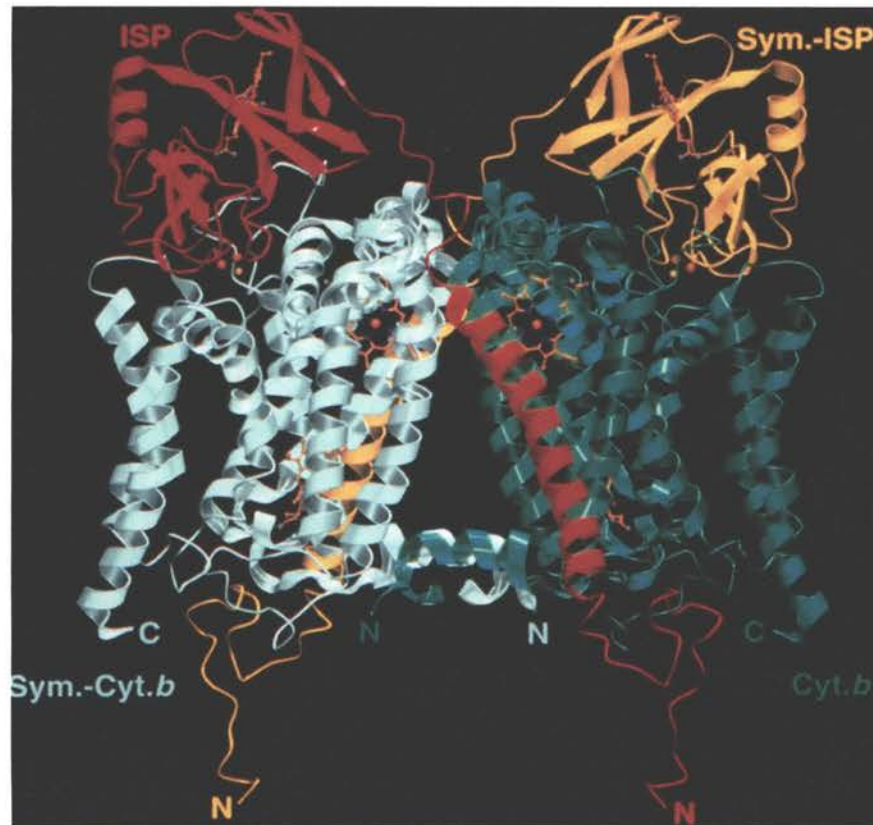


Fig. 7. The intertwinning dimer of cytochrome bc_1 complex.

One of the unexpected features observed in the X-ray crystallographic investigations is that the cytochrome bc_1 complex exists as a dimer in the crystal structure and the two ISPs from the two monomers are intertwined; the head domain of ISP in one monomer is close to cytochrome b and c_1 in the other monomer (Fig 7). In tetragonal $I4_122$ crystals of native oxidized bovine cytochrome bc_1 complex, the 2Fe2S cluster in one monomer is 27 Å from heme b_L of the other monomer and 40 Å from the heme b_L of the same monomer. This structural arrangement suggests that mitochondrial bc_1 complex functions as a dimer, since the distance between the 2Fe2S of ISP of one monomer and the low potential cytochrome b (b_L) of the other monomer is less than that between these groups in the same monomer. The shorter distance accommodates fast electron transfer from QH_2 to ISP and b_L . However, a complex that exists as a dimer in the crystal might exist and function as a monomer in solution. Evidence for the cytochrome bc_1 complex functioning as a dimer or a monomer has been reported (45-48). Therefore, it is important to establish whether or not the structure of the dimeric cytochrome bc_1 complex observed in the crystal also exists in solution. Chapter III of this thesis addresses this question by generating mutant bc_1 complexes that forms two intersubunit disulfide bonds, one at the interface between the head domain of ISP and cytochrome b and the other at the proximity of the tail domain of ISP and cytochrome b (49). An adduct protein with an apparent molecular mass of 128 kDa containing two cytochrome b and two ISP proteins is detected in the K70C(ISP)/A185C(cyt b)/P33C(ISP)/G89C(cyt b) and K70C(ISP)/A185C(cyt b)/N36C(ISP)/G89C(cyt b) mutant complexes, confirming that the bc_1 complex exists as a dimer with intertwining ISP's in solution.

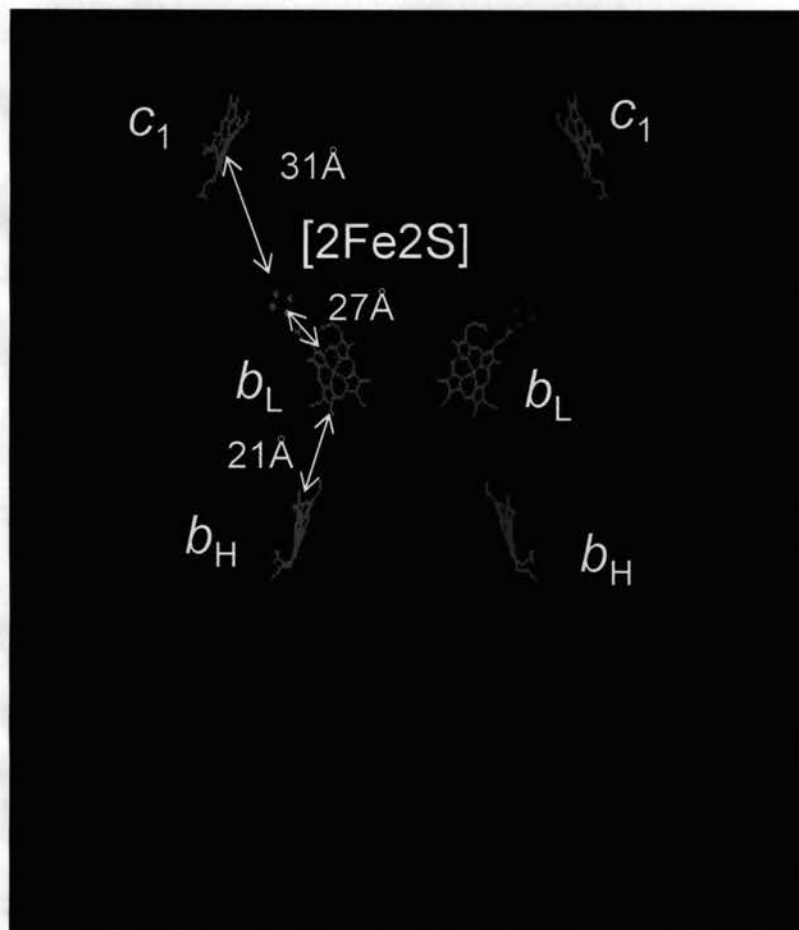


Fig. 8. The distances of the redox centers in tetragonal $I4_122$ crystal of native oxidized bovine mitochondrial cyt bc_1 complex.

Another unexpected feature derived from the extensive structural study is the movement of the head domain of the iron-sulfur protein (ISP) during bc_1 catalysis. In tetragonal $I4_122$ crystals of native oxidized bovine cytochrome bc_1 complex, the position of the 2Fe2S cluster is 27 Å from heme b_L and 31 Å from heme c_1 (the "fixed state" position) (Fig. 8) (37, 50). The distance of 27 Å between 2Fe2S and heme b_L accommodates well the observed fast electron transfer between these two redox centers. However, the distance of 31 Å between 2Fe2S and heme c_1 is difficult to explain due to the rapid electron transfer observed between these two redox centers. This structural observation provided an impetus for the idea that the head domain of ISP may undergo substantial movement during the catalytic cycle of the complex. The implication of the movement of the head domain of ISP arose from an observation of a particularly low electron density area in the intermembrane space portion of the complex, where the extramembrane domains of the ISP and cytochrome c_1 reside (37). The peak height for a 2Fe2S cluster is only half of that of b_H heme, which is consistent with the movement hypothesis. With a mobile ISP during bc_1 catalysis, it is possible to offset the long distance between 2Fe2S and heme c_1 , and thus allow fast electron transfer.

2). The crystal structures of cytochrome bc_1 complex loaded with Q_o site inhibitors

To further substantiate our movement hypothesis, structural studies of the cytochrome bc_1 complex loaded with different Q_o site inhibitors were conducted in our lab and other groups.

A. Conformational changes in ISP induced by Q_o site inhibitors

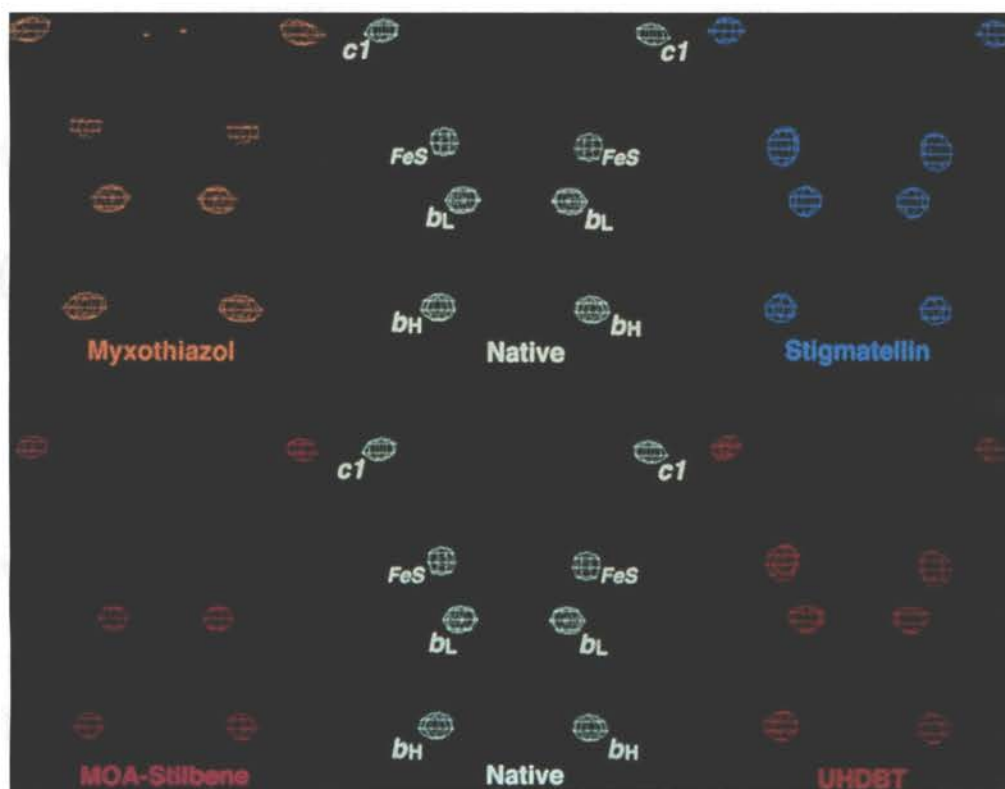


Fig. 9. Various positions of [2Fe₂S] in crystals loaded with different Q₀ site inhibitors.

Table II

Effects of Q_o site inhibitors on the relative anomalous peak height of the 2Fe2S cluster of ISP (normalized to heme b) in the beef cytochrome bc_1 complex⁽⁵¹⁾

Crystal preparation	Peak ratio (2Fe2S/ b_H)
Native cytochrome bc_1 complex (fully oxidized)	0.56
+ MOAS	-
+ Myxothiazol	0.38
+ Stigmatellin	1.18
+ UHDBT	0.97
+ Famoxadone	1.49
+ Azoxystrobin	1.07

Binding of Q_o site inhibitors has a considerable effect on the electron density of the anomalous scattering peak of a 2Fe2S cluster in the anomalous difference maps (Table II). Binding of stigmatellin or UHDBT enhances the electron density of the anomalous scattering peak of 2Fe2S, suggesting that these inhibitors arrest the mobility of ISP in the “fixed state” position (50). Conversely, binding of (E)- β -methoxyacrylate-stilbene (MOAS) or myxothiazol to the complex abolishes the electron density of the anomalous scattering peak of 2Fe2S, suggesting that these inhibitors increase the mobility of ISP in the crystal and that 2Fe2S has no predominant position (referred as “released” or “loose” position) in this inhibited state (Fig. 9) (50). In orthorhombic crystals ($P2_12_12_1$) of the chicken enzyme, binding of stigmatellin shifts 2Fe2S from the so-called “distal or c_1 -position” to the “proximal or b -position” (38). The b -position in the $P2_12_12_1$ crystal is believed to be the same as the “fixed state” position observed in $I4_122$ crystals. In bovine $P6_5$ crystals, 2Fe2S is located between the b -state and c_1 -state positions (the “intermediate” position) (39). Although the position of 2Fe2S in bovine $P6_5$ crystals might result from crystal contacts because the crystal contacts in $P6_5$ crystals are at the extramembrane domain of ISP, the observation of more than two positions of 2Fe2S supports the idea of one fixed position and other released (loose) positions, as suggested by the $I4_122$ structure.

B. Conformational changes in cytochrome b induced by Q_o site inhibitors

For the cytochrome b subunit, the overall structure does not have significant change upon inhibitor binding, reflecting the overall structure rigidity. Significant local conformational changes do occur when inhibitors are bound to cytochrome b . When

pairwise-comparisons of the structures of cytochrome *b* from four different bovine cytochrome *bc*₁ complex crystals were made (native structure, stigmatellin loaded structure, antimycin A loaded structure, and antimycin A + stigmatellin loaded structure), antimycin A was not found to induce significant conformational change for the mitochondrial cytochrome *b* except for less than 0.5-1 Å of the local changes near the Q_i pocket in order to accommodate the inhibitor (52). However, significant changes of up to 2.3 Å were found when stigmatellin was present. These conformational changes mainly involve α -cd1 and α -cd2 helices and the EF loop regions. The conformational changes in cytochrome *b* might be caused by the effects of the ISP in the b position and the opening of the Q_o pocket in order to accommodate stigmatellin. In the crystal structure loaded with famoxadone, there are two sets of residues involved in the conformational changes. The first set of residues (type I) are those in the immediate environment of the famoxadone binding pocket, directly contacting with or partially displaced by the bound famoxadone (43). These residues change their positions in order to accommodate the incoming inhibitor. The largest conformational changes in cytochrome *b* were observed in the second set of residues (type II) that are not in direct contact with famoxadone (43). These residues are located at the end of the CD loop and the proline-rich EF loop and are divided into three areas: the docking crater for ISP head domain, the contact surface with ISP neck region, and the region that contacts the Q_o site to these two regions. These findings may provide a possible control mechanism for ISP head domain movement. The cytochrome *b* could serve as a major driving force for ISP movement, and the type II residues may form a surface conformational strip serving as a signal transduction

pathway to amplify the inhibitor-binding signal to the position change of ISP head domain (43).

4. The movement of the head domain of ISP during bc_1 catalysis

1). The “moving Rieske” model

The 3-dimensional structural information indicates that the movement of ISP head domain is needed because of the long distance between ISP at b-position and cyt c_1 . Based on the extensive X-ray crystallographic structural studies, a “moving Rieske” model has been proposed to explain the electron transfer events at the Q_o site. The head domain of ISP changes its position from b-position, where oxidized 2Fe2S accepts an electron from ubiquinol in the Q_o site, to the c_1 -position, where the reduced 2Fe2S transfer an electron to heme c_1 (Fig. 10). One puzzling paradox of the protonmotive Q-cycle mechanism is why the ubisemiquinone, a very powerful reductant, transfers the second electron to lower midpoint potential heme b_L , but not the high midpoint potential 2Fe2S cluster, during the ubiquinone oxidation, even though this electron is thermodynamically favored to transfer to 2Fe2S. The "moving Rieske" model provided a feasible answer to explain this bifurcated electron transfer paradox of the protonmotive Q-cycle mechanism. It is possible that either the reduced 2Fe2S (reduced by the first electron of ubiquinol) is unable to leave the b-position to transfer an electron to heme c_1 before the second electron of ubiquinol is transferred to heme b_L (53), or the reoxidized ISP (assuming the reduced ISP can move to the c-position) cannot return to the its original b-position to be rereduced (54). It also proposed that the change of the

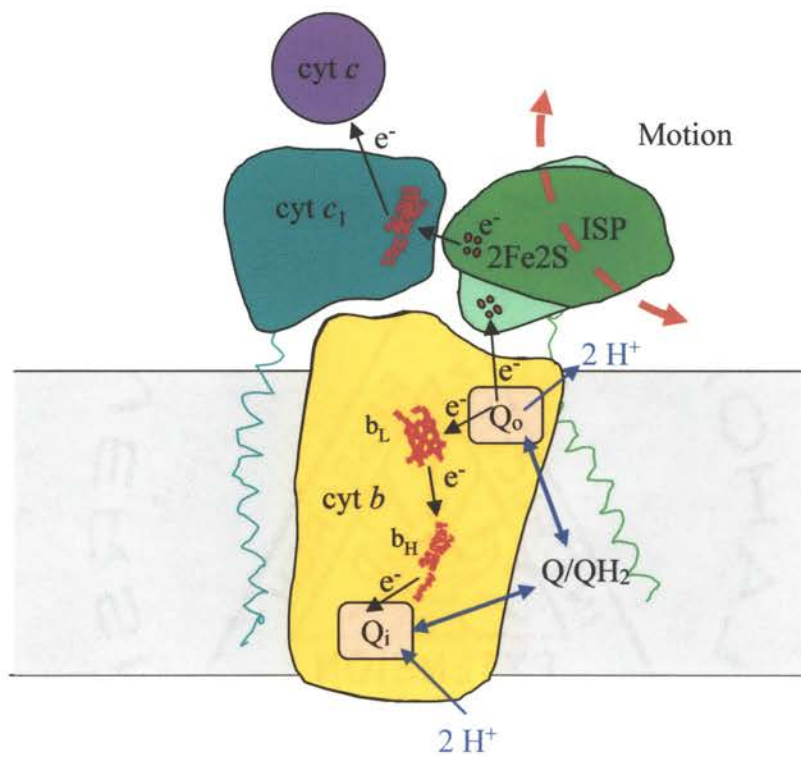


Fig. 10. Carton representation of the "moving Riske" model in the protonmotive Q-cycle.

ubiquinol-binding site to a ubisemiquinone-binding site, and reduction of heme b_L and b_H , might cause a conformational change in cytochrome b , which pushes or allows the ISP head domain to move to the c_1 -position to facilitate rapid electron transfer. However, without ubiquinol binding information, this hypothesis is still waiting for further evidences.

2). The mobility of ISP head domain is essential for bc_1 catalysis

The X-ray crystallographic structural information clearly shows that the 2Fe2S cluster assumes different positions in different crystal forms and in the presence of different Q_o site inhibitors; and the “moving Rieske” model well accommodates the protonmotive Q-cycle. However, the structural information does not provide direct proof of the functional significance of the ISP domain movement. Since the head domain and tail domain of ISP are rigid, movement of the ISP head domain requires flexibility in the neck domain (residues 63-72). By using molecular genetic manipulation of bacterial cytochrome bc_1 complex, the first functional evidence for ISP head domain movement was provided by our group (55, 56). Mutants with increased neck rigidity, generated by deletion, or double- or triple-proline substitution, have greatly reduced electron transfer activity with an increased activation energy (55). Formation of a disulfide bond between two engineered cysteines, having only one amino acid residue between them, in the neck region near the transmembrane helix, also drastically reduces electron transfer activity (56), presumably due to increased neck rigidity. Cleavage of the disulfide bond by reduction or alkylation restores activity to that of the wild type enzyme (56). These results not only demonstrate the critical role of the neck region flexibility for the

movement of the head domain of ISP, but also the essentiality of this movement. This conclusion was further confirmed by similar investigation from other groups (57-63).

Considering the movement of the head domain of ISP is essential for bc_1 catalysis, locking the head domain of ISP in a given position should abolish the bc_1 complex activity. Chapter II of this thesis further confirms the essentiality of the ISP head domain movement by locking the 2Fe2S cluster of ISP in a "fixed" position to form a disulfide bond between a pair of genetically engineered cysteines on the interface between the head domain of ISP and cytochrome *b* (64).

To understand the electron transfer mechanism in the cytochrome bc_1 complex, it is important to determine the electron transfer rate constants among the redox centers in this complex. Since the crystal structural analysis clearly shows that the 2Fe2S cluster assumes different positions in the presence of different Q_o site inhibitors, the electron transfer rate constants between 2Fe2S and heme c_1 must be different when different Q_o site inhibitors are used in the fast kinetics study. Binding of famoxadone or stigmatellin or UHDBT arrests the 2Fe2S cluster to the fixed b-position according to the anomalous peak height observed in the crystals loaded with these inhibitors (Table II). The electron transfer rates from 2Fe2S to heme c_1 should be drastically decreased or abolished in the cytochrome bc_1 complex loaded with these inhibitors due to the long distance between these two redox centers. Also, the electron transfer rates from 2Fe2S to heme c_1 should be greatly decreased or abolished in the mutant cytochrome bc_1 complex with the ISP head domain locked in a fixed position. In Chapter IV and V, a method of rereduction of photoactivated ruthenium complex induced oxidized cytochrome c_1 is used to determine the electron transfer rate constants of electron transfer between 2Fe2S and heme c_1 in

native, Q_o site inhibitor loaded, as well as mutant cytochrome *bc*₁ complexes (65, 66); and the essentiality of ISP head domain movement is again substantiated by the fast kinetics study.

3). The rate constants of electron transfer between 2Fe2S cluster and heme c₁ and the rate-limiting step of ubiquinol oxidation

Although the "moving Rieske" model provides a feasible solution for the puzzle concerning the bifurcated electron transfer at the Q_o site, several questions involving the ISP head domain movement are still unanswered. The reactions of ISP with its partners (heme c₁ and ubiquinol bound at the Q_o site of cytochrome *b*) require the movement of head domain of ISP (37-40, 67, 68). Determining whether or not this movement is the rate-limiting step for ubiquinol oxidation and therefore contributes to the activation energy barrier is very important to elucidate the mechanism of the protonmotive Q-cycle. The large domain movement of the ISP head domain has been proposed to contribute to the activation energy barrier (ΔG^0) of the ubiquinone oxidation (41). Its contribution to the activation energy was supported by the 3-fold increase of the activation energy of *R. sphaeroides* mutations with higher rigidity of the neck region (41). However, the activation energy of the partial reaction that contributes to the ISP head domain movement was measured to be lower than the high activation barrier associated with ubiquinol oxidation (67). In another experiment, the transient cytochrome *b* reduction kinetics observed in the head domain movement of impaired mutants was similar to those seen with the wild type strain (68). At this stage, it is difficult to rule out the other steps during ubiquinol oxidation from contributing to the activation energy.

Determination of the electron transfer rate constants among the redox centers in the cytochrome bc_1 complex is a very powerful method to understand the electron transfer mechanism for this complex. Fast kinetic analysis of electron transfer reactions of cytochrome bc_1 complex will help us to elucidate the rate-limiting step for the ubiquinol oxidation. Since the movement of the ISP head domain is essential for the cytochrome bc_1 catalysis, it is of importance to establish the rate constant of electron transfer between 2Fe2S cluster and heme c_1 and understand whether or not this movement controls the rate of electron transfer between these two redox centers. However, fast kinetic analysis of electron transfer rate constants involving cytochrome bc_1 complex has proven to be a formidable work, because these reactions are too fast to be measured by conventional techniques. The kinetics of cytochrome bc_1 electron transfer reactions have been studied extensively within chromatophores from *Rhodobacter sphaeroides* and *Rhodobacter capsulatus*, where the electron-transfer cycle can be initiated by a short light flash (68). However, the time resolution of this system is limited by the rate of diffusion of photooxidized cytochrome c_2 from the reaction center to the bc_1 complex ($k_{\text{diff}} = 5000 \text{ s}^{-1}$) (68). The rate constant for intracomplex electron transfer from 2Fe2S to heme c_1 has been estimated to be much larger than 10^5 s^{-1} using this method (68).

Recently, electron transfer between 2Fe2S and heme c_1 was studied using the ruthenium dimer, Ru_2D , to either photoreduce or photooxidize cytochrome c_1 within $1 \mu\text{s}$. Ru_2D has a charge of +4, which allows it to bind with high affinity to the cytochrome bc_1 complex. Flash photolysis of reduced *Rhodobacter sphaeroides* bc_1 , Ru_2D , and a sacrificial acceptor resulted in oxidation of cytochrome c_1 within $1 \mu\text{s}$, followed by

electron transfer from 2Fe2S to cytochrome c_1 . The reduction of photooxidized cytochrome c_1 is biphasic, with a fast phase having a rate constants of $80,000 \text{ s}^{-1}$ and with a slow phase having a rate constant of 1000 s^{-1} at $25 \text{ }^\circ\text{C}$. The fast phase is due to electron transfer from 2Fe2S to heme c_1 and the slow phase is due to electron transfer from QH_2 to 2Fe2S and then to heme c_1 . The slow phase of reduction of heme c_1 has the same rate constant as the reduction of heme b_H in the presence of antimycin A. Oxidant-induced reduction of heme b_H was observed with a rate constant of 1000 s^{-1} in the presence of antimycin A (69).

In order to elucidate whether or not the movement of ISP head domain is the rate limiting step for electron transfer between 2Fe2S and heme c_1 , in Chapter IV and V, we further characterize the electron transfer reaction between these two redox centers in *R. sphaeroides* cytochrome bc_1 . If the movements are slow as compared to electron transfer in the optimal c_1 state and the population of the c_1 state is small, then the observed rate constant is limited by the rate of the movements and the movement of ISP is the rate-limiting step of this reaction. On the other hand, if the movements are rapid as compared to electron transfer, then the observed rate constant is $k_{\text{obs}} = fk_{\text{et}}$, where f is the fraction of molecules in the c_1 state and the electron transfer is rate-limited by real electron transfer. Experiments were carried out to evaluate whether the reaction is rate-limited by true electron transfer, proton gating, or domain movement in Chapter IV. In Chapter V, the effects of famoxadone on electron transfer between 2Fe2S and heme c_1 are studied. It is concluded that movement of ISP head domain controls electron transfer between the Rieske iron-sulfur protein and cytochrome c_1 .

5. Study system

In this thesis study, we use the cytochrome bc_1 complex from a photosynthetic bacterium, *Rhodobacter(R.) sphaeroides*, as a model system. *R. sphaeroides* is an anoxygenic purple bacterium, in which ATP synthesis is through the cyclic or non-cyclic electron transfer pathways in the plasma membrane. The cyclic electron transfer pathway involves two membrane-bound components: the reaction center (RC), in which the initial light-dependent electron transfer steps occur, and the cytochrome bc_1 complex. After light absorption by the light-harvesting complex (LHC), the excitation energy is transferred to a dimer of bacteriochlorophyll P870 in the RC. The electron released from bacteriochlorophyll P870 then reduces a ubiquinone molecule to a ubiquinol by taking two protons from the cytochromeoplasm (70, 71). The reduced ubiquinol then leaves the RC and diffuses through the membrane to cytochrome bc_1 complex. The cytochrome bc_1 complex conducts a similar function as in the mitochondrial electron transfer chain to transfer the electrons and translocate two protons across the membrane per electron transfer. The electron returns to bacteriochlorophyll P870, via cytochrome c_2 , to complete the cyclic electrical circuit. The proton gradient formed in this process is used for ATP synthesis by a process known as photophosphorylation. Photophosphorylation takes place under a photosynthetic oxygen-deficient condition. However, when the environmental oxygen tension is high, *R. sphaeroides* can also undergo respiratory growth. Under this condition, the photosynthetic apparatus is repressed by the high oxygen tension, and the contents of oxidases in the cells increase. These changes increase the respiratory capacity of the cells and allow these facultative phototrophs to conserve energy via oxidative phosphorylation. The quinol oxidase branch is

independent of the cytochrome bc_1 complex among the multiple respiratory pathways. The electron transfer can go through this non-cyclic pathway in accompanying with the proton translocation across the membrane, allowing respiratory growth of the cytochrome bc_1 -deficient mutant cells (70, 71).

1). Photosynthetic bacteria *R. sphaeroides* cytochrome bc_1 complex

The photosynthetic bacterium *R. Sphaeroides* described previously was used as a study system for this thesis. *R. sphaeroides* provides several experimental advantages: (i), Simplicity --- the bc_1 complex from *R. sphaeroides* contains only four subunits. The three catalytic subunits: cytochrome b , cytochrome c_1 and ISP are homologous to their mitochondrial counterpart; (ii), Readily applied molecular engineering protocols --- in eukaryotic systems, such as yeast, cytochrome b is encoded in the mitochondria and is inconvenient for site-directed mutagenesis. In *R. sphaeroides*, the three catalytic subunits are encoded by genes organized in an *fbcFBC* operon, which has been deleted from the chromosome to facilitate the mutagenesis studies; (iii), Mutated bc_1 complex that cannot support photosynthetic growth of the cells can still be characterized by biochemical and biophysical methods. In photosynthetic bacteria, the bc_1 complex is not essential for aerobic cell growth because of the presence of ubiquinol oxidases that constitute the cytochrome bc_1 -independent branch of respiratory systems. Therefore, the bacterial strains over-expressing defective bc_1 complex are able to grow under a semiaerobic dark growth condition (to induce extensive intracytoplasmic membrane) (72-74). Intracytoplasmic membrane (ICM) with defective bc_1 complexes can be prepared for biochemical and biophysical studies to assess the reasons of the defect. Utilizing all

these advantages, this bacterial cytochrome bc_1 complex is an ideal model for structural and functional relationship of this particular electron transfer region.

2). Homology structural modeling of *R. sphaeroides* cytochrome bc_1 complex

The *R. sphaeroides* cytochrome bc_1 complex is functionally homologous to mitochondrial complex. This bacterial bc_1 complex offers many advantages for the structure-function studies as discussed above. The 3-D structure of the bacterial bc_1 complex will be very useful for designing mutants and allows for the ability to look directly at the structural consequences of mutations, and relate them to functional studies. Homology modeling is a practical way to predict the three-dimensional structure of this protein since the crystal structure of *R. sphaeroides* bc_1 complex has not yet been solved. Based on the assumption that sequence conservation is directly proportional to structural conservation, a structural model of the *R. sphaeroides* cytochrome bc_1 complex was built in our lab recently, using the bovine mitochondrial bc_1 complex as a template (Fig. 11). Alignment of the amino acid sequences of *R. sphaeroides* cytochrome b , cytochrome c_1 , and ISP with their counterparts in the beef heart mitochondrial complex reveals high sequence homology, except several extra fragments in the bacterial proteins. These extra fragments are: residues 96-107 of ISP; residues 1-15, 232-239, 309-326 and 422-445 of cytochrome b ; and residues 141-161 of cytochrome c_1 . By swapping coordinates from template to model in all regions where there is a corresponding match in the sequence alignment, the majority of cytochrome b , cytochrome c_1 and ISP are modeled. Subunit IV and the extra fragments of cytochrome b , c_1 , and ISP were modeled with the coordinates from the corresponding supernumerary subunits in the bovine bc_1 complex.

The feasibility of using the beef supernumerary subunit's coordinates for modeling the extra fragments of the bacterial core subunits into the bc_1 structure encouraged us to explore the possible association of supernumerary subunit function with these extra fragments and to study the interaction between these supernumerary subunit function-associated extra fragments and the mitochondrial-like core subunits. To investigate the role of the extra fragment of ISP in the bc_1 complex, in Chapter VII, we generated *R. sphaeroides* mutants expressing His₆-tagged bc_1 complexes with deletion or substitution at various positions of this fragment. The photosynthetic behavior of mutants are examined and compared with those of the complement strain to see whether or not this extra fragment of ISP is critical to the bc_1 complex and to identify the critical amino acid residue(s). The bc_1 activity, the amount of ISP protein, and EPR characteristics of ISP in membrane and purified state from complement and mutants are examined and compared. The study of the role of the extra fragment(s) from *R. sphaeroides* cytochrome *b* and cytochrome *c*₁ are the ongoing projects in our lab.

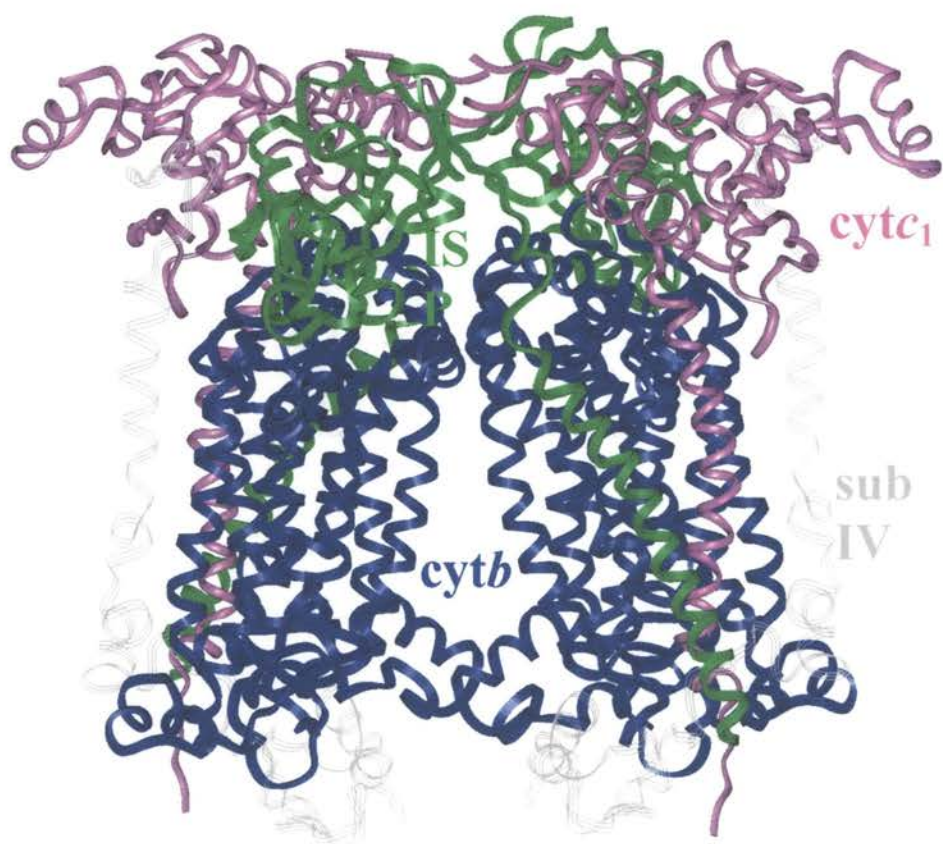


Fig. 11. The 3-D model of *R. sphaeroides* cytochrome *bc*₁ complex.

III References

1. Duncan, T. M., Bulygin, V. S., Zhou, Y., Hutcheon, M. L., and Cross, R. L. (1995) *Proc. Natl. Acad. Sci. U. S. A.* **92**, 10964-8.
2. Noji, H., Yasuda, R., Yoshida, M., and Kinosita, K., Jr. (1997) *Nature* **386**, 299-302.
3. Pedersen, P. L. Ko, and Hong, S. (2000) *J. Bioenerg. Biomembr.* **32**, 325-32.
4. Fearnley, I. M., and Walker, J. E. (1992) *Biochim. Biophys. Acta.* **1140**, 105-34.
5. Yu, L., Xu, J-X., Haley, P. E., and Yu, C. A. (1987) *J. Biol. Chem.* **262**, 1137-43.
6. Ohnishi, T., Salerno, J. C., Winter, D. B., Lim, J., Yu, C. A., Yu, L. and King, T. E. (1976) *J. Biol. Chem.* **251**, 2094-104.
7. Ackrell, B. A. C., Kearney, E. B., Mins, W. B., Peisach, J. and Beinert, H. (1984) *J. Biol. Chem.* **259**, 4015-8.
8. Rich, P. R. (1986) *J. Bioenerg. Biomembr.* **18**, 145-56.
9. Tsukihara, T., Aoyama, H., Yamashita, E., Tomiraki, T., Yamguchi, H., Shinzawa-Itoh, K., Nakashima, R., Yaono, R., and Yoshikawa, S. (1996) *Science* **272**, 1136-44.
10. Mitchell, P. (1961) *Nature* (London) **191**, 144-8.
11. Mitchell, P. (1966) *Chemiosmotic Coupling in Oxidative and Photosynthetic Phosphorylation*, Glynn Research, Bodmin.
12. Mitchell, P. (1968) *Chemiosmotic Coupling and Energy Transduction*, Glynn Research, Bodmin.
13. Greville, G. (1969) *Curr. Top. Bioenerg.* **3**, 1-78.
14. Mitchell, P. (1976) *J. Theor. Biol.* **62**, 327-67.
15. Yu, C. A. (1999) *J. Bioenerg. Biomembr.* **31**, 167-8.
16. Yu, C. A. and Yu, L. (1993) *J. Bioenerg. Biomembr.* **25**, 259-73.

17. Yu C. A., Xia J. Z., Kachurin A. M., Yu L., Xia D., Kim H., Deisenhofer J. (1996) *Biochim. Biophys. Acta.* **1275**, 47-53.
18. Trumpower, B.L. and Gennis, R.B. (1994) *Annu. Rev. Biochem.* **63**, 675-716.
19. Chen, Y.R., Yu, C.A., Yu, L. (1996) *J. Biol. Chem.* **271**, 2057-62.
20. Yu, L., Tso, S. C., Shenoy, S. K., Quinn, B. N., Xia, D. (1999) *J. Bioenerg. Biomembr.* **31**, 251-7.
21. Tso, S. C., Shenoy, S. K., Quinn, B. N., Yu, L. (2000) *J. Biol. Chem.*, **275**, 15287-94.
22. Mitchell, P. (1975) *FEBS Lett.* **59**, 137-9.
23. Mitchell, P. (1976) *J. Theor. Biol.* **62**, 327-67.
24. Trumpower, B. L. (1976) *Biochem. Biophys. Res. Commun.* **70**, 73-80.
25. Crofts, A. R., Meinhardt, S. W. (1982) *Biochem. Soc. Trans.* **10**, 201-3.
26. Trumpower, B. L. (1990) *J. Biol. Chem.* **265**, 11409-12.
27. Rieske, J. S. (1971) *Arch. Biochem. Biophys.* **145**, 179-93.
28. Wikstrom, M. K. F., and Berden, J. A. (1972) *Biochim Biophys Acta.* **283**, 403-20.
29. Mitchell, P. (1975) *FEBS Lett.* **56**, 1-6.
30. von Jagow, G., and Link, T. (1986) *Methods in Enzymology* **126**, 253-71.
31. Brand, M. D., Reynafarje, B. and Lehninger, A. L. (1976) *J. Biol. Chem.* **251**, 5670-5.
32. Yu, C. A., Nagoaka, L., Yu, L., and King, T. E. (1978) *Biophys. Res. Commun.* **82**, 1070-3.
33. de Vires, S., Albracht, S. P. J., Berden, J. A., and Slater, E. C., (1981) *J. Biol. Chem.* **256**, 1996-8.
34. Junemann, S., Heathcote, P., and Rich, P.R. (1998) *J. Biol. Chem.* **273**, 21603-7.
35. Crofts, A. R., and Wang, Z. (1989) *Photosynth. Res.* **22**, 69-87.

36. Yu, C. A., Tian, H., Zhang, L., Deng, K. P., Shenoy, S. H., Yu, L., Xia, D., Kim, H. and Deisenhofer, J. (1999) *J. Bioenerg. Biomembr.* **31**, 191-9.
37. Xia, D., Yu, C. A., Kim, H., Xia, J.Z., Kachurin, A.M., Zhang, L., Yu, L. and Deisenhofer, J. (1997) *Science* **277**, 60-6.
38. Zhang, Z., Huang, L., Shulmeister, V.M., Chi, Y.-I., Kim, K.K., Hung, L.-W., Crofts, A.R., Berry, E.A. and Kim, S.-H. (1998) *Nature* **392**, 677-84.
39. Iwata, S., Lee, J.W., Okada, K., Lee, J.K., Iwata, M., Rasmussen, B., Link, T.A., Ramaswamy, S. and Jap, B.K. (1998) *Science* **281**, 64-71.
40. Hunte, C., Koepke, J., Lange, C., Rossmann, T., Michel, H. (2000) *Structure Fold Des.* **8**, 669-84.
41. Tian, H., Yu, L., Mather, M.W., Yu, C.A. (1998) *J. Biol. Chem.* **273**, 27953-9.
42. Link, T. A., Iwata, S. (1996) *Biochim Biophys Acta.* **1275**, 54-60.
43. Gao, X., Wen, X., Yu, C., Esser, L., Tsao, S., Quinn, B., Zhang, L., Yu, L., Xia, D. (2002) *Biochemistry* **39**, 11692-702.
44. Ohishi, T. H., Schagger, H., Meinhardt, S. W., Lobrutto, R., Link, T., A., and von Jagow, G. (1989) *J. Biol. Chem.* **264**, 735-44.
45. Von Jagow, G., Schagger, H., Ricco, P., Klingenberg, M., and Kolb, H. J. (1977) *Biochim. Biophys. Acta.* **462**, 549-58.
46. Nalecz, M. J., Azzi, A. (1985) *Arch. Biochem. Biophys.* **240**, 921-31.
47. Musatov, A., and Robison, N. (1994) *Biochemistry* **33**, 13005-12.
48. Jungas, C., Ranck, J-L., Rigaud, J-L., Jiliet, P., and Vermeiglio, A. (1999) *EMBO J.* **18**, 534-42.

49. Xiao, K., Chandrasekaran, A., Yu, L., and Yu, C.A. (2001) *J. Biol. Chem.* **276**, 46125-31.
50. Kim, H., Xia, D., Yu, C. A., Xia, J. Z., Kachurin, A. M., Zhang, L., Yu, L., Deisenhofer, J. (1998) *Proc. Natl. Acad. Sci. U. S. A.* **95**, 8026-33.
51. Yu, C. A., Wen, X., Xiao, K., Xia, D., and Yu, L. (2002) *Biochim. Biophys. Acta* **1555**, 65-70.
52. Crofts, A. R., Barquera, B., genneis, R. B., Kuras, R., Guergova-Kuras, M., and Berry, E.A. (1999) *Biochemistry* **38**, 1186-9.
53. Yu, C. A., Xia, D., Kim, H., Deisenhofer, J., Zhang, L., Kachurin, A. M., and Yu, L. (1998) *Biochim. Biophys. Acta* **1365**, 151-8.
54. Brandt, U. (1998) *Biochim Biophys Acta.* **1365**, 261-8.
55. H. Tian, L. Yu, W. Michael and C.A. Yu (1998) *J. Biol. Chem.* **273**, 27953–9.
56. H. Tian, S. White, L. Yu and C.A. Yu (1999) *J. Biol. Chem.* **274**, 7146–52.
57. E. Darrouzet, M. Valkova-Valchanova and F. Daldal (2000) *Biochemistry* **39** 15475–83.
58. E. Darrouzet, M. Valkova-Valchanova, T. Ohnishi and F. Daldal (1999) *J. Bioenerg. Biomembr.* **31**, 275–88.
59. V.H. Obungu, Y. Wang, S.M. Amyot, C.B. Gocke and D.S. Beattie (2000) *Biochim. Biophys. Acta.* **1457**, 36–44.
60. J.H. Nett, C. Hunte and B.L. Trumpower (2000) *Eur. J. Biochem.* **267**, 5777–82.
61. E. Darrouzet and F. Daldal (2002) *J. Biol. Chem.* **277**, 3471–3476.
62. S. Heimann, M.V. Ponamarev and W.A. Cramer (2000) *Biochemistry* **39**, 2692–9.

63. E.A. Berry, M. Guergova-Kuras, L.S. Huang and A.R. Crofts (2000) *Ann. Rev. Biochem.* **69**, 1005–75.
64. Xiao, K., Yu, L., and Yu, C. A. (2000) *J. Biol. Chem.* **275**, 38597-604.
65. Enfstrom, G., Xiao, K., Yu, C. A., Yu, L., Durham, B., and Millett, F. (2002) *J. Biol. Chem.* **277**, 31072-8.
66. Xiao, K., Enfstrom, G., Rajagukguk, S., Yu, C. A., Yu, L., Durham, B., and Millett, F. (2002) *J. Biol. Chem.* In press.
67. Crofts, A. R., Hong, S., Zhang, Z., Berry, E. A. (1999) *Biochemistry* **38**, 15827-39.
68. Crofts, A.R. and Wang, Z. (1989) *Photosynth. Res.* **22**, 69-87.
69. Sodoski, R. C., Engstrom, G. Tian. H., Zhang, L., Yu, C.A., Yu, L., Burham, B., and Millett. F. (2000) *Biochemistry* **39**, 4231-6.
70. Clayton, R. K. and Sistrom, W. R. (1979) “The Photosynthetic Bacteria”. Plenum, New York.
71. Voet, D. and Voet, J. G. (1995) Chapter 22, Photosynthesis. In “*Biochemistry*” (Voet, D. and Voet, J. G. eds.), John Wiley & Sons, Inc. pp. 626-61.
72. Knaff, D.B. (1990) *Trends Biochem. Sci.* **15**, 289-91.
73. Gennis, R.B., Barquera, B., Hacker, B., Van Doren, S.R., Arnaud, S., Crofts, A.R., Davidson, E., Gray, K.A. and Daldal, F. (1993) *J. Bioenerg. Biomembr.* **25**, 195-209.
74. Thöny-Meyer, L. (1997) *Microbiol. Mol. Biol. Rev.* **61**, 337-76.
75. Quinn, B. N. (2000), thesis.

CHAPTER II

**Confirmation of the Involvement of Protein Domain
Movement during the Catalytic Cycle of the Cytochrome *bc*₁
Complex by the Formation of an Intersubunit Disulfide Bond
between Cytochrome *b* and the Iron-sulfur Protein**

Kunhong Xiao, Linda Yu, and Chang-An Yu

The Journal of Biological Chemistry, 275, 38597-604 (2000)

ABSTRACT

To study the essentiality of head domain movement of the Rieske iron-sulfur protein (ISP) during bc_1 catalysis, *Rhodobacter sphaeroides* mutants expressing His-tagged cytochrome bc_1 complexes with three pairs of cysteines engineered (one cysteine each) on the interface between cytochrome b and ISP: A185C(cytb)/K70C(ISP), I326C(cytb)/G165C(ISP), and T386C(cytb)/K164C(ISP), were generated and characterized. Formation of an intersubunit disulfide bond between cytochrome b and ISP is detected in membrane (intracytoplasmic membrane and air-aged chromatophore) and purified bc_1 complex prepared from the A185C(cytb)/K70C(ISP) mutant cells. Formation of the intersubunit disulfide bond in this cysteine pair mutant complex is concurrent with the loss of its bc_1 activity. Reduction of this disulfide bond by β -mercaptoethanol restores activity, indicating that mobility of the head domain of ISP is functionally important in the cytochrome bc_1 complex. The rate of intramolecular electron transfer, between 2Fe2S and heme c_1 , in the A185C(cytb)/K70C(ISP) mutant complex is much lower than that in the wild type or in their respective single cysteine mutant complexes, indicating that formation of an intersubunit disulfide bond between cytochrome b and ISP arrests the head domain of ISP in the "fixed state" position, which is too far for electron transfer to heme c_1 .

INTRODUCTION

The cytochrome bc_1 complex (also known as ubiquinol-cytochrome c reductase or Complex III) is an essential segment of the energy-conserving electron transfer chains of mitochondria and many respiratory and photosynthetic bacteria (1). This complex catalyzes electron transfer from ubiquinol to cytochrome c and concomitantly translocates protons across the membrane to generate a membrane potential and pH gradient for ATP synthesis. Recently the cytochrome bc_1 complexes from bovine (2, 3) and chicken (4) heart mitochondria, which contain 11 non-identical protein subunits, were crystallized and their structures solved at 2.9 Å resolution. The structural information obtained not only answered a number of questions concerning the arrangement of the redox centers, transmembrane helices, and inhibitor binding sites but also suggested movement of the head domain of the iron-sulfur protein (ISP) during bc_1 catalysis. This suggestion arose from observation of a particularly low electron density area in the intermembrane space portion of the complex, where the extramembrane domains of ISP and cytochrome c_1 reside (2). This movement hypothesis was further supported by the observation of various positions for 2Fe2S in the different crystal forms (3, 4) and in complexes loaded with different inhibitors (4, 5).

In tetragonal $I4_122$ crystals of native oxidized bovine cytochrome bc_1 complex the position of the 2Fe2S cluster is 27 Å from heme b_L and 31 Å from heme c_1 (the "fixed state" position) (2, 5). Binding of stigmatellin or 5-*n*-undecyl-6-hydroxy-4,7-dioxobenzothiazole (UHDBT) enhances the electron density of the anomalous scattering peak of 2Fe2S, suggesting that these inhibitors arrest the mobility of ISP in the "fixed state" position (5). Conversely, binding of (E)- β -methoxyacrylate-stilbene (MOAS) or

myxothiazol to the complex abolishes the electron density of the anomalous scattering peak of 2Fe2S, suggesting that these inhibitors increase the mobility of ISP in the crystal and that 2Fe2S has no predominant position (referred as “released” or “loose” position) in this inhibited state (5). In orthorhombic crystals ($P2_12_12_1$) of the chicken enzyme, binding of stigmatellin shifts 2Fe2S from the so-called “distal or c_1 -position” to the “proximal or b -position” (4). The b -position in the $P2_12_12_1$ crystal is believed to be the same as the “fixed state” position observed in $I4_122$ crystals. In bovine $P6_5$ crystals 2Fe2S is located between the b -state and c_1 -state positions (the “intermediate” position) (3). The observation of more than two positions (intermediate- and c_1 - positions) of 2Fe2S in $P6_5$ crystals (3) supports the idea of one fixed position and other released (loose) positions, suggested by the $I4_122$ structure.

If movement of the head domain of ISP is required for bc_1 catalysis, locking the head domain of ISP in a given position should abolish the bc_1 complex activity. One way to lock the 2Fe2S cluster of ISP in a “fixed” position is to form a disulfide bond (disulfide bridge) between a pair of genetically engineered cysteines on the interface between the head domain of ISP and cytochrome b . However, genetic manipulation of bovine heart mitochondria is not practical. *Rhodobacter sphaeroides* is an ideal system for studying the intersubunit disulfide bond formation by molecular genetics. The four-subunit bacterial complex is functionally analogous to the mitochondrial enzyme; the largest three subunits (cytochrome b , cytochrome c_1 , and ISP) are homologous to their mitochondrial counterparts; and this system is readily manipulated genetically. In addition, *R. sphaeroides* expressing (His)₆-tagged cytochrome bc_1 complex has been

prepared (6, 7). This greatly speeds up the isolation of the bc_1 complex from wild type or mutant cells.

In fact, the study of the neck region of ISP using this system (6, 8) provided the first functional evidence for movement of the head domain of ISP during bc_1 catalysis. The molecule of ISP can be divided into three domains: head, tail, and neck, with the 2Fe2S cluster located at the tip of the head (9, 10). Since the 3-D structures of the head and tail domains are rigid and are the same in the fixed and released states, a bending of the neck is required for movement of the head domain. For the neck region to bend, some flexibility is imperative. Mutants with increased neck rigidity, generated by deletion, or double- or triple-proline substitution, have greatly reduced electron transfer activity with an increased activation energy (6). Formation of a disulfide bond between two engineered cysteines, having only one amino acid residue between them, in the neck region near the transmembrane helix, also drastically reduces electron transfer activity (8), presumably due to increased neck rigidity. Cleavage of the disulfide bond by reduction or alkylation restores activity to that of the wild type enzyme (8). These results clearly demonstrate a need for neck flexibility in catalysis.

To further establish that movement of the head domain of ISP is essential for the bc_1 complex we generated mutants expressing (His)₆-tagged bc_1 complex with pairs of cysteine substituted (one cysteine each) at the interface between cytochrome *b* and the head domain of ISP. We predicted that formation of an intersubunit disulfide bond between the engineered cysteine pair would arrest the mobility of ISP to the "fixed state" and decrease electron transfer activity. Herein we report procedures for generating three cysteine-pair mutants with one each on cytochrome *b* and ISP in close proximity

(interface) to each other. Mutants with single cysteine substitutions at indicated positions were also generated and characterized to confirm that the generated cysteine-pair mutants are not at critical positions in the bc_1 complex and, hence, are suitable for this study. The photosynthetic growth behavior, cytochrome bc_1 complex activity, SDS-PAGE patterns and EPR characteristics of the 2Fe2S cluster in purified complexes from wild type and mutant strains were examined and compared as were the rates of pH induced intramolecular electron transfer between 2Fe2S and heme c_1 .

EXPERIMENTAL PROCEDURES

Materials-- Cytochrome c (horse heart, Type-III) was purchased from Sigma. N-Dodecyl- β -D-maltoside (LM) and N-octyl- β -D-glucoside (OG) were from Anatrace. 2,3-Dimethoxy-5-methyl-6-geranyl-1,4-benzoquinol (Q_2H_2) was prepared in our laboratory as previously reported (11). All other chemicals were of the highest purity commercially available.

Generation of *R. sphaeroides* Strains Expressing the bc_1 Complexes with Single or Pairs of Cysteine Substitutions on Cytochrome b and ISP-- Mutations were constructed by site-directed mutagenesis using the Altered Sites system from Promega. The oligonucleotides used for mutagenesis were as follows: K70C (ISP), GTCAAGTTCCTCGGCTGCCCGATCTTCATCCGCCGCCGCACCGAGGCCGACATCG; G165C (ISP), CCGTATCCGGAAGTGCCCCGCGCCCGAGAACC; K164C (ISP), ACAGTGCCGGCCGTATCCGGTGCGGCCCCGCGCCCGAGAACC; A185C (cytb), GCTGCTCGGCGGCCCGTGCGTGGACAATGCCA; I326C (cytb),

CATCAGCTTCGGCATCTIGCGACGCCAAGTTCTTCGGCGTGCTCGCGATGT;
 T386C (cytb),
 GGGTCGGCGCCCAGCAGACCTIGCTTCCCCTACGACTGGATCTCG.

The single-stranded pSELNB3503 (12) was used as the template for mutagenesis. A plate-mating procedure (12) was used to mobilize the pRKD*fb*C_mB_mC_HQ plasmid in *E. coli* S17-1 cells into *R. sphaeroides* BC17 cells. The presence of engineered mutations was confirmed by DNA sequencing before and after photosynthetic or semi-aerobic growth of the cells. Expression plasmid pRKD*fb*C_mB_mC_HQ was purified from an aliquot of a photosynthetic or semi-aerobic culture using the Qiagen Plasmid Mini Prep kit. Since *R. sphaeroides* cells contain four types of endogenous plasmids, the isolated plasmids lack the purity and concentration needed for direct sequencing. Therefore, a 2.5-kilobase pair DNA segment, containing the mutation sequence, was amplified from the isolated plasmids by the polymerase chain reaction (PCR) and purified by 1% agarose gel electrophoresis. The 2.5-kilobase pair polymerase chain reaction product was recovered from the gel with an extraction kit from Qiagen. DNA sequencings and oligonucleotide syntheses were performed by the Recombinant DNA/Protein Core Facility at the Oklahoma State University.

Growth of Bacteria-- *E. coli* cells were grown at 37°C in LB medium. For photosynthetic growth of the plasmid-bearing *R. sphaeroides* BC17 cells, an enriched Siström's medium containing 5 mM glutamate and 0.2% casamino acids was used. Photosynthetic growth conditions for *R. sphaeroides* were essentially as described previously (6). Cells harboring mutated *fb* genes on the pRKD*fb*C_HQ plasmid were grown photosynthetically for one or two serial passages to minimize any pressure for

reversion. For semi-aerobic growth of *R. sphaeroides*, an enriched Siström's medium supplemented with 20 amino acids and extra rich vitamins was used. These semi-aerobic cultures were grown in 500 ml of enriched Siström's medium in 2-liter Bellco flasks with vigorous shaking (220 rpm) for 26 hours at 30°C. The inoculation volumes used for both photosynthetic and semi-aerobic cultures were at least 5% of the total volume.

Antibiotics were added to the following concentrations: ampicillin, 125 µg/ml;

Kanamycin sulfate, 30 µg/ml ; tetracycline (10 µg/ml for *E. coli* and 1 µg/ml for *R.*

sphaeroides); Trimethoprim (100 µg/ml for *E. coli* and 30 µg/ml for *R. sphaeroides*).

Enzyme Preparations and Activity Assay-- Chromatophore and intracytoplasmic membrane (ICM) were prepared as described previously (6) and stored at -80°C in the presence of 20% glycerol until use. The (His)₆-tagged cytochrome *bc*₁ complexes were purified from frozen chromatophores by the method of Tian *et al.* (6). Purified cytochrome *bc*₁ complexes were stored at -80°C in the presence of 20% glycerol. To assay ubiquinol-cytochrome *c* reductase activity, chromatophores, ICM, or purified cytochrome *bc*₁ complexes were diluted with 50 mM Tris-Cl, pH 8.0, containing 200 mM NaCl to a final concentration of cytochrome *b* of 5 µM. Five-µl of the diluted samples were added to 1-ml of assay mixture containing 100 mM of Na⁺ /K⁺ phosphate buffer, pH 7.4, 0.3 mM of EDTA, 100 µM of cytochrome *c*, and 25 µM of Q₂H₂. Activities were determined by measuring the reduction of cytochrome *c* (the increase of the absorbance at wavelength 550 nm) in a Shimadzu UV 2101 PC spectrophotometer at 23°C, using a millimolar extinction coefficient of 18.5 for calculation. The nonenzymatic oxidation of Q₂H₂, determined under the same conditions, in the absence of enzyme, was subtracted during specific activity calculations.

Determination of pH-induced Reduction and Oxidation of ISP and Cytochrome c_1 in the Partially Reduced Wild type and Mutant bc_1 Complexes-- The wild type or mutant bc_1 complex was diluted in 3 ml of 20 mM Tris-Cl buffer, pH 8.0, containing 200 mM NaCl and 0.01% dodecylmaltoside. The concentration of cytochrome c_1 was adjusted to about 10 μ M. Different amounts of NaOH or HCl were added to give indicated pHs. Fully oxidized or reduced cytochrome c_1 and ISP was obtained by addition of $K_3Fe(CN)_6$ or sodium ascorbate. Reduction of cytochrome c_1 was followed by measuring the increase of the α -absorption (553 nm - 545 nm) in a Shimadzu UV 2101 PC spectrophotometer. Reduction of ISP was followed by measuring the negative circular dichroism (CD) peak, at 500 nm, of partially reduced ISP minus fully oxidized complex in a JASCO J-715 spectropolarimeter (13-15). The same samples were used for the absorption and CD measurements. Instrument settings for the spectropolarimeter were: scan speed, 100 nm/min; step resolution, 1 nm; accumulation, 10 traces for averaging; response, 1s; bandwidth, 1.0 nm; sensitivity, 10 mdeg; and slit width, 500 μ m.

Determination of Redox Potentials of the 2Fe2S Cluster in Wild type and Mutant bc_1 Complexes-- The redox status of heme c_1 or the 2Fe2S cluster was determined as described above. The cytochrome c_1 partially reduced wild type and mutant bc_1 complexes were prepared and used for the absorption and CD measurements. The redox potentials of ISP were calculated from the redox statuses of heme c_1 and 2Fe2S, at pH 8.0, using 230 mV for the redox potential of heme c_1 (16).

Determination of Electron Transfer Rates between the 2Fe2S Cluster and Heme c_1 in Wild type and Mutant bc_1 Complexes-- The method used is essentially the same as that previously reported (15). The (His)₆-tagged, cytochrome c_1 -half reduced cytochrome

bc_1 complex was prepared as described for the preparation of the oxidized complex (6) except the cytochrome c_1 in the dodecylmaltoside-solubilized chromatophore was reduced 50% with sodium ascorbate before being applied to a Ni-NTA column. The cytochrome c_1 -half reduced complex was diluted in 20 mM Tris-Cl buffer, pH 6.8 or 8.9, containing 200 mM NaCl and 0.01% dodecylmaltoside to a cytochrome c_1 concentration of around 10 μ M and mixed with buffers of various pHs at room temperature in an Olis stopped-flow rapid scanning spectrophotometer. Oxidation or reduction of cytochrome c_1 was monitored by the decrease or increase of absorption at 553 nm minus 545 nm.

Other Biochemical and Biophysical Techniques-- Protein concentration was determined by the method of Lowry *et al.* (17). Cytochrome b (18) and cytochrome c_1 (16) contents were determined according to published methods. Sodium dodecylsulfate-polyacrylamide gel electrophoresis (SDS-PAGE) was performed according to Laemmli (19) using a Bio-Rad Mini-Protean dual slab vertical cell. Samples were digested with 10 mM Tris-Cl buffer, pH 6.8, containing 1% SDS, and 3% glycerol in the presence and absence of 0.4% β -ME for 2 hr at 37 °C before being subjected to electrophoresis. The intersubunit disulfide bond linked adduct protein was obtained by electrophoretic elution (20) of a protein band, with an apparent molecular weight of 64 kDa, from SDS-PAGE of the purified A185C(cytb)/K70C(ISP) mutant complex without β -ME treatment. Western blotting was performed with rabbit polyclonal antibodies against cytochrome b , cytochrome c_1 , and ISP of the *R. sphaeroides* bc_1 complex (6). The polypeptides separated by SDS-PAGE gel were transferred to polyvinylidene difluoride membrane for immunoblotting. Goat anti-rabbit IgG conjugated to alkaline phosphatase or protein A conjugated to horseradish peroxidase was used as the second antibody. EPR spectra were

recorded in a Bruker ER 200D apparatus equipped with liquid Nitrogen Dewar, at 77 K. The instrument settings are detailed in the figure legends.

RESULTS AND DISCUSSION

Photosynthetic Growth Behaviors of Mutants Carrying Cysteine Substitutions in the Interface between Cytochrome *b* and the Head Domain of ISP-- Three pairs of amino acid residues: A185(cytb)/K70(ISP), I326(cytb)/G165(ISP), and T386(cytb)/K164(ISP) were selected for mutation to cysteines. These choices were based on the 3-D structural model of the four-subunit cytochrome *bc*₁ complex of *R. sphaeroides* (see Fig 1A) constructed with coordinates from bovine cytochromes *b* and *c*₁, ISP, and subunit XII (21). The distances between these three cysteine pairs are 6.1, 6.1, and, 7.5 Å, respectively, in the bacterial complex (see Fig. 1B). They are 6.5, 6.8, and 6.4 Å (see Table I), respectively, when calculations are based on corresponding residues in the bovine enzyme. Mutants with a single cysteine substitution, at positions Ala¹⁸⁵(cytb), Ile³²⁶(cytb), Thr³⁸⁶(cytb), Lys⁷⁰(ISP), Gly¹⁶⁵(ISP), or Lys¹⁶⁴(ISP), were also generated and used as controls.

For a cysteine pair mutant to be useful in this study, the engineered cysteine positions must not be critical for cytochrome *bc*₁ complex activity. Because the *bc*₁ complex is absolutely required for the photosynthetic growth of *R. sphaeroides*, whether or not the engineered cysteine positions are critical to the complex can be determined by assaying photosynthetic growth. Mutants with cysteine substitutions at critical positions in the complex will not grow photosynthetically, whereas mutants with substitutions at non-critical positions will grow.

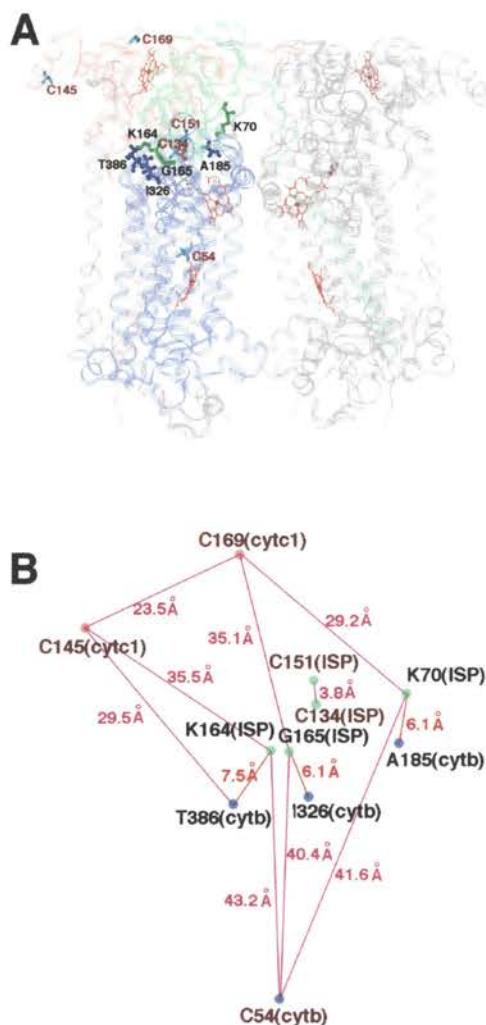


Fig. 1. Location of engineered cysteines and free endogenous cysteines in the structural model of the *R. sphaeroides* *bc*₁ complex. (A), the left monomer of cytochrome *b* is shown in blue ribbon, ISP (from the other monomer) in green and cytochrome *c*₁ in pink. Subunit IV and the other monomer are shown in gray. Positions of engineered cysteines are shown as the wild type amino acid being replaced, in ball and stick format, in the same color as the appropriate subunit. The free endogenous cysteines are shown in light blue sticks. The 2Fe2S clusters are marked as small red dots. (B), the distances between the various engineered and endogenous free cysteines. The colors are the same as in (A).

When mid-log phase, aerobically dark grown wild type and mutant cells were inoculated into enriched Siström's medium and subjected to anaerobic photosynthetic growth conditions, the A185C(cytb), K70C(ISP), A185C(cytb)/K70C(ISP), I326C(cytb), and T386C(cytb) mutants grew at rates comparable with that of wild type cells, the K164C(ISP) and T386C(cytb)/K164C(ISP) mutants grew at a retarded rate (60%), and the G165C(ISP) and I326C(cytb)/G165C(ISP) did not grow photosynthetically (Table I).

Because Gly¹⁶⁵ of ISP is a critical position, mutant I326C(cytb)/G165C(ISP) does not support photosynthetic growth and cannot be used to study the effect of disulfide bond formation on the *bc*₁ complex. The structural importance of Gly¹⁶⁵ was further investigated by substituting alanine or threonine at this position. The ISP:G165A or G165T substitution also results in cells which do not grow photosynthetically, indicating that the size of the amino acid side chain at position 165 of ISP is critical. A similar size-activity relationship was previously observed for G158 of cytochrome *b* in *R. capsulatus* (22) and Ser¹⁵⁵ of cytochrome *b* in *R. sphaeroides* (23).

On the other hand, mutants A185C (cytb)/K70C (ISP) and T386C(cytb)/K164C(ISP) support photosynthetic growth, indicating that the engineered cysteine positions are noncritical to the complex. Therefore, formation of an intersubunit disulfide bond between cytochrome *b* and the ISP head domain was examined with these two cysteine pair mutants.

Formation of a Disulfide Bond between Cytochrome *b* and ISP in the A185C (cytb)/K70C (ISP) Mutant *bc*₁ Complex-- Chromatophores freshly prepared from the A185C(cytb), K70C(ISP), A185C(cytb)/K70C(ISP), T386C(cytb), K164C(ISP), and

Table I.

Characterization of ISP and cytochrome b interface Cysteine Mutants

Mutants	Single mutation		Double mutant residues distance(Å) ^a		Ps ^b	Enzymatic activity ^c	
	Corresponding residues in bovine	Location	In bovine structure	In bacterial modeling		Chromatophore	Purified complex ^d
Wild type					++	2.3 (100%)	2.5 (100%)
A185C(cytb)	S169	Cd2			++	2.3 (100%)	2.5 (100%)
K70C(ISP)	K95	β3			++	1.3 (57%)	1.4 (56%)
A185C(cytb)/K70C(ISP)			6.5	6.1	++	1.3 (57%)	0.3 (12%) ^e
I326C(cytb)	I284	ef loop			++	0.8 (35%)	0.8 (32%)
G165C(ISP)	G174	Pro loop			-	NA*	NA
I326C(cytb)/G165C(ISP)			6.8	6.1	-	NA	NA
T386C(cytb)	E344	gh loop			++	0.9 (39%)	1.0 (40%)
K164C(ISP)	K173	Pro loop			+	1.0 (43%)	1.0 (40%)
T386C(cytb)/K164C(ISP)			6.4	7.5	+	0.8 (35%)	0.8 (32%)

*NA, not applicable

^aThe distances were measured from C-β to C-β (except with glycine which is to C-α).

^bPs, photosynthetic growth. ++, the cells growth rate is essentially the same as that of the wild type cells; +, the cells can grow photosynthetically but at a rate slower than that of the wild type cells; -, no photosynthetic growth in 4 days.

^cEnzymatic activity is expressed as μmol cytochrome *c* reduced/min/nmol cytochrome *b* at room temperature.

^dThe cytochrome *bc*₁ complex was in 50 mM Tris-Cl, pH 8.0 containing 200 mM NaCl, 200 mM histidine and 0.5% octyl glucoside.

^eThe cytochrome *bc*₁ complex activity of the A185C/K70C mutant complex was measured immediately after preparation.

T386C(cytb)/K164C(ISP) mutant cells have, respectively, 100, 57, 57, 39, 43, and 35% of the bc_1 activity found in wild type chromatophores (see Table I). When these chromatophore preparations were subjected to western blot analysis using antibodies against *R. sphaeroides* cytochrome *b* and ISP, no protein band corresponding to the adduct of cytochrome *b* and ISP was observed, indicating that no disulfide bond is formed between the two engineered cysteines in mutants A185C(cytb)/K70C(ISP) and T386C(cytb)/K164C(ISP) during anaerobic photosynthetic growth. The lack of disulfide bond formation is expected because photosynthetic growth is under strict anaerobic conditions whereas disulfide bond formation is an oxidative process. Without oxygen no disulfide bond can be formed even if the two cysteines are in favorable positions.

When the (His)₆-tagged bc_1 complexes were purified from these six freshly prepared cysteine mutant chromatophores, all but the A185C(cytb)/K70C(ISP) mutant complex have the same bc_1 activity found in their respective chromatophores (see Table I), based on cytochrome *b* content. The A185C(cytb)/K70C(ISP) mutant complex, when assayed immediately after preparation, has about 23% of the bc_1 complex activity found in its freshly prepared chromatophores. Activity in this cysteine-pair mutant complex decreased during storage at 0°C. About 7% of the activity remained after 24 hrs. Under identical conditions, no activity loss was observed for wild type and mutant complexes of A185C(cytb), K70C(ISP), T386C(cytb), K164C(ISP), and T386C(cytb)/K164C(ISP).

To see whether or not the loss of bc_1 complex activity observed for mutant A185C(cytb)/K70C(ISP) results from disulfide bond formation during purification, SDS-PAGE patterns of these purified mutant complexes, with and without β -ME treatment, were examined (see Fig. 2). When purified complexes were treated with SDS at 37°C for

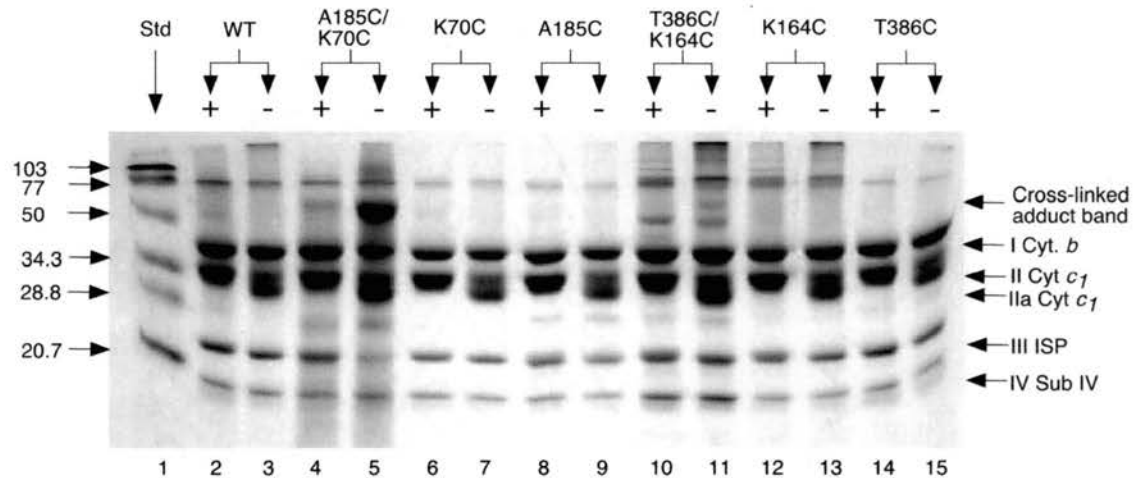


Fig. 2. SDS-PAGE of cysteine mutant cytochrome *bc*₁ complexes. Aliquots of wild type, A185C (cytb)/K70C (ISP), K70C (ISP), A185C (cytb), T386C (cytb)/K164C, K164C (ISP), and T386C (cytb) were incubated with 1% SDS with (+) or without (-) 1% β -ME at 37°C for 2 hr. Digested samples containing 150 pmoles of cytochrome *b* were subjected to electrophoresis. Lane 1, protein standard containing: Phosphorylase B (103K), Bovine serum albumin (77K), Ovalbumin (50K), Carbonic anhydrase (34.3K), Soybean trypsin inhibitor (28.8K) and Lysozyme (20.7k).

2 hr and subjected to electrophoresis in the absence of β -ME (see Fig. 2, lanes marked with -), the A185C(cytb), K70C(ISP), T386C(cytb), and K164C(ISP) mutants have the same electrophoretic pattern as that of the wild type complex. They all contain five protein bands with apparent molecular weights of 41, 33, 31, 23, and 14 kDa. Western blot analysis with antibodies against *R. sphaeroides* cytochrome *b*, cytochrome *c*₁, ISP, and subunit IV identified these five protein bands, with decreasing molecular masses, as band I, cytochrome *b*; band II and IIa, cytochrome *c*₁; band III, ISP; and band IV, subunit IV. The lack of any protein band with an apparent molecular weight of 64 kDa, the size of an adduct band of cytochrome *b* and ISP, indicates that no intersubunit disulfide bond is formed between an engineered cysteine in cytochrome *b* (A185C or T386C) or ISP (K70C or K164C) and an endogenous cysteine in ISP or cytochrome *b*, respectively.

This lack of intersubunit disulfide bond formation between an engineered cysteine in cytochrome *b* or ISP and an endogenous cysteine in ISP or cytochrome *b* is as expected. The *R. sphaeroides* cytochrome *bc*₁ complex has nine endogenous cysteine residues: one in cytochrome *b*, four in cytochrome *c*₁, and four in the ISP. It has been established that two cysteines (Cys129 & Cys149) in the ISP serve as ligands for the 2Fe2S cluster (24) and two cysteines (Cys37 & Cys40) in cytochrome *c*₁ are covalently bonded to heme *c*₁ (25). Thus, there are five endogenous free cysteines in the complex: two in ISP (Cys 134 and Cys151), one in cytochrome *b* (Cys54), and two in cytochrome *c*₁ (Cys 145 and Cys169). In the 3-D structural model, Cys134 is on the loop β 4- β 5 and Cys151 is on the loop β 6- β 7 of ISP (21). They form an intra-subunit disulfide bond which brings the two loops together and stabilizes this region. Therefore, they are not available for intersubunit disulfide bond formation with the engineered cysteines on cytochrome *b*. Since the

endogenous cysteine in cytochrome *b* (Cys54) is, respectively, 41.6 Å, and 43.2 Å from the engineered cysteines at positions 70 and 164 of ISP (see Fig. 1B), formation of an intersubunit disulfide bond between this endogenous free cysteine and the engineered cysteines on ISP is unlikely.

The presence of two bands (II and IIa) for cytochrome c_1 in SDS-PAGE of the bc_1 complex, in the absence of β -ME, may result from the formation of an intramolecular disulfide bond between Cys-145 and Cys-169 in some of the cytochrome c_1 molecules. The cytochrome c_1 molecules with the intramolecular disulfide bond move faster (band IIa) than those without this bond. This explanation is consistent with the presence of a single protein band, with slower electrophoretic mobility, in SDS-PAGE patterns obtained after treating the complex with SDS and β -ME prior to electrophoresis (see Fig. 2, lanes marked +). No doubt β -ME reduces the intramolecular disulfide bond present in some cytochrome c_1 molecules, thus converting the fast moving band to the slower one. Probably intramolecular disulfide bond formation occurs only after the complex has been dissociated with SDS. The cytochrome bc_1 complex, in its native state, with or without β -ME treatment, has the same electron transfer activity. Moreover, the distance between Cys-169 and Cys-145 of cytochrome c_1 , in the structural model of this bacterial complex, is 23.5 Å (see Fig. 1B), too large for disulfide bond formation.

The electrophoretic pattern of the T386C(cytb)/K164C(ISP) mutant complex, in the absence of β -ME (see Fig. 2, lane 11), shows a faint band with an apparent molecular weight of 64 kDa which disappears in the presence of β -ME (Fig. 2, lane 10). The failure of this 64 kD protein to react with antibodies against cytochrome *b* and ISP, and the lack of β -ME effect on cytochrome bc_1 activity of this mutant complex lead us to assign this

protein as a contaminant, rather than an adduct of ISP and cytochrome *b*. Thus, no intersubunit disulfide bond is formed between cytochrome *b* and ISP in the T386C(cytb)/K164C(ISP) mutant complex.

The electrophoretic pattern of the A185C(cytb)/K70C(ISP) mutant complex (see Fig. 2, lane 5), in the absence of β -ME, differs from those of wild type and mutant complexes of A185C(cytb), K70C(ISP), T386C(cytb), K164C(ISP), and T386C(cytb)/K164C(ISP) in two aspects: the appearance of a protein band with an apparent molecular weight of 64 kDa and a decrease in the band intensities of cytochrome *b* and ISP. The Mr=64 kDa protein band is established as an adduct of cytochrome *b* and ISP, resulting from intersubunit disulfide bond formation between these two subunits, by the following experimental results. First, the Mr=64 kDa protein band reacts with antibodies against cytochrome *b* and ISP (data not shown); second, when the mutant complex is treated with SDS and β -ME and then subjected to SDS-PAGE in the presence of β -ME, the Mr=64 kDa protein band disappears and the band intensities of cytochrome *b* and ISP increase (see Fig. 2, lane 4); and third, the protein isolated from the Mr=64 kDa gel slice, after treatment with β -ME, can be resolved into cytochrome *b* and ISP (data not shown).

Although the Mr=64 kDa protein band which reacts with antibodies against cytochrome *b* and ISP is absent from freshly prepared chromatophores from A185C(cytb)/K70C(ISP) mutant cells, it appears in ICM preparations obtained from cells grown semi-aerobically. The A185C(cytb)/K70C(ISP) mutant ICM has no cytochrome *bc*₁ complex activity (see Table II). Also, when freshly prepared mutant chromatophores are incubated at 0 °C under air, the Mr=64 kDa protein band intensity increases as the *bc*₁ activity decreases. It usually takes more than a week for the loss in activity to reach 50%.

Table II.

Effect of β -ME on the cytochrome bc_1 activity in chromatophores, ICM, and purified complexes from wild type and mutants A185C(cytb), K70C(ISP), and

A185C/K70C

mutants	Enzymatic activity ^c					
	Chromatophore		ICM		Purified bc_1	
	(+) ^a	(-) ^b	(+)	(-)	(+)	(-)
Wild type	2.3	2.3	2.4	2.4	2.5	2.5
A185C	2.3	2.3	2.4	2.4	2.5	2.5
K70C	1.3	1.3	1.4	1.4	1.4	1.4
A185C/K70C	1.3	1.3	1.4	0	1.4	0.1 ^d

^a(+) samples were prepared with buffers containing 100mM β -ME (Mercaptoethanol).

^b(-) samples were prepared in the absence of β -ME.

^cEnzymatic activity is expressed as μ mol cytochrome c reduced/min/nmol cytochrome b .

^dThe bc_1 activity was measured after the sample had been stored on ice for one day.

These results confirm that formation of a disulfide bond from the two engineered cysteines on cytochrome *b* and ISP in the A185C(cytb)/K70C(ISP) mutant complex is promoted by oxygen and is directly related to the loss of bc_1 activity in this mutant complex.

Effect of β -ME on the Disulfide Bond Formation and bc_1 Activity -- To further confirm that the formation of a disulfide bond between cytochrome *b* and ISP causes the A185C(cytb)/K70C(ISP) mutant complex to lose bc_1 complex activity, the effect of β -ME on bc_1 complex activity and disulfide bond formation was examined. When purified A185C(cytb)/K70C(ISP) mutant complex, which has been incubated at 0°C for 24 hrs, was treated with β -ME, the activity was restored to the same level as that in freshly prepared chromatophores (Table II). No adduct of cytochrome *b* and ISP was detected in the β -ME treated A185C(cytb)/K70C(ISP) mutant complex. When this complex was purified from the freshly prepared chromatophores in the presence of 100 mM β -ME, it had the same activity as that found in the chromatophores and no cytochrome *b*-ISP adduct was detected. A similar β -ME effect is observed for the cytochrome bc_1 complex in mutant ICM (see Table II). It should be emphasized that the observed activity restoration or preservation is not due to nonenzymatic reduction of cytochrome *c* by β -ME, because only antimycin sensitive cytochrome *c* reduction is used for activity calculations. Under identical conditions, β -ME has no effect on the bc_1 activities in the A185C(cytb), K70C(ISP), T386C(cytb), K164C(ISP), and T386C(cytb)/K70C(ISP) mutant complexes.

Effect of Disulfide Bond Formation between Cytochrome *b* and ISP on EPR Characteristics and Redox Potential of the 2Fe2S Cluster-- Although evidence

presented above clearly demonstrates that the loss of bc_1 complex activity in the A185C(cytb)/K70C(ISP) mutant correlates with the formation of a disulfide bond between the two engineered cysteines in cytochrome b and ISP, unknown is how disulfide bond formation causes the activity loss. Since this disulfide bond is formed in the interface between cytochrome b and ISP, it is possible that the microenvironments or the redox potential of the ISP cluster are altered thus leading to activity loss. To test this possibility, EPR characteristics and redox potentials of the 2Fe2S cluster in the A185C(cytb)/K70C(ISP), with and without β -ME treatment, are compared.

As shown in Fig. 3, the 2Fe2S in the A185C(cytb)/K70C(ISP) mutant complex, with or without β -ME treatment, has the same EPR spectrum, with the g_x signal at 1.775, g_y at 1.900, and g_z at 2.020. This result indicates that the microenvironments of the ISP cluster in the A185C(cytb)/K70C(ISP) mutant complex are not affected by disulfide bond formation between the two engineered cysteines in cytochrome b and ISP. Therefore, the loss of bc_1 activity is not due to a change of microenvironments in the ISP.

However, it should be noted that replacing the K70 of ISP with cysteine in the A185C(cytb)/K70C(ISP) mutant complex shifts the g_x signal of the 2Fe2S cluster from 1.800 to 1.775. This is deduced from the observation that the 2Fe2S cluster in the A185C(cytb) mutant complex has an EPR spectrum identical to that observed in the wild type complex, with resonance at $g_x=1.800$, $g_y=1.900$, and $g_z=2.020$ (see Fig. 3), whereas the 2Fe2S in the K70C(ISP) mutant complex has a broadened g_x signal which is shifted to 1.768. The g_x signal of 2Fe2S in the A185C(cytb)/K70C(ISP) mutant complex is sharper than that in the K70C(ISP) bc_1 complex but broader than that in the wild type or

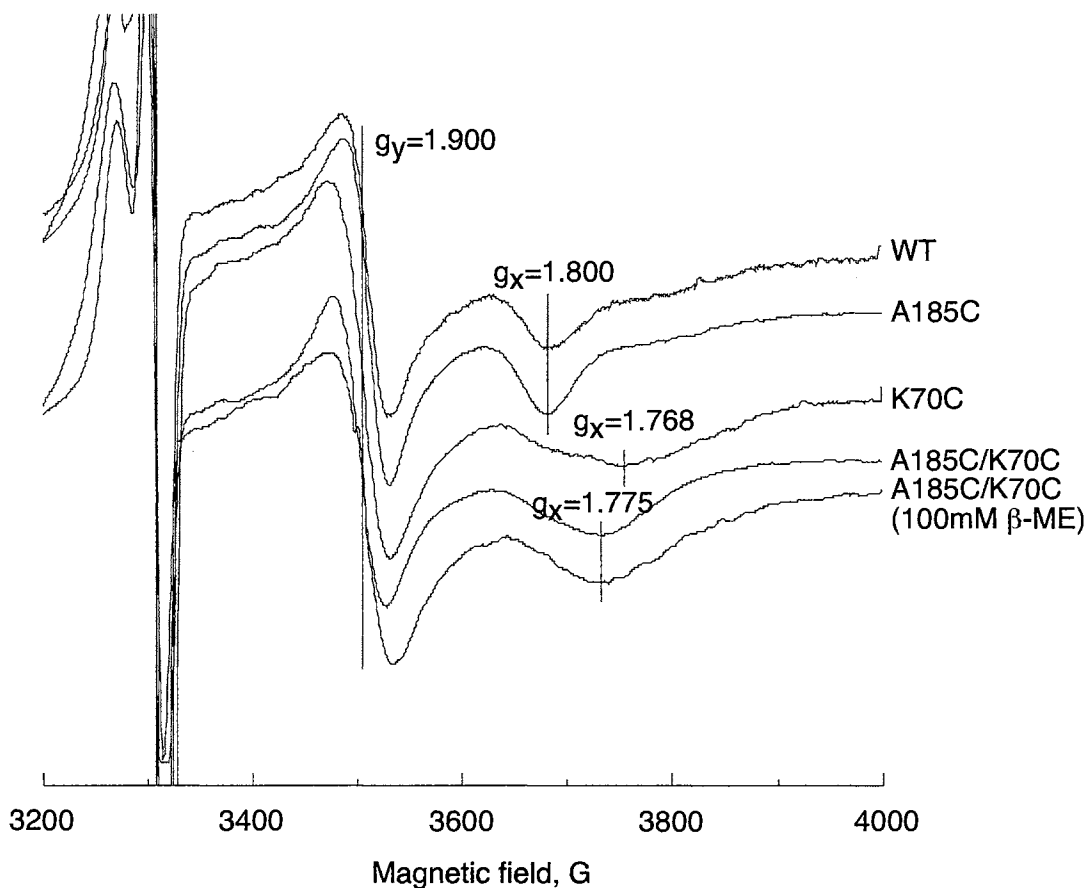


Fig. 3. EPR spectra of the 2Fe₂S cluster in the cytochrome *bc*₁ complexes of wild type, A185C (cytb), K70C (ISP) and A185C (cytb)/K70C (ISP) with or without 100 mM β-ME treatment. The complexes were incubated with 5 mM sodium ascorbate on ice for 30 minutes and frozen in liquid nitrogen. EPR spectra were recorded at 77 K with the following instruments settings: microwave frequency, 9.28 GHz; microwave power, 20 milliwatts; modulation amplitude, 20 G; modulation frequency, 100 kHz; time constants, 0.1 s; and scan rate, 20 G/s.

A185C(cytb) mutant complex. As expected, the effect on the bc_1 complex is small since the K70C(ISP) and β -ME treated A185C(cytb)/K70C(ISP) mutant complexes retain more than 50% of the bc_1 activity found in the wild type.

The line shape of the g_x signal of the 2Fe2S cluster is thought to be mediated by the oxidation state of ubiquinone present in the Q_o site (26-30). The g_x of bc_1 from *R. sphaeroides* is at $g=1.800$ when ubiquinone is present, but shifts to 1.750 and broadens when ubiquinol is present. When ubiquinone is extracted from chromatophore membranes, the g_x signal of the "depleted state" is at $g=1.765$ and is considerably broadened than those seen in the presence of either ubiquinone or ubiquinol. The change in the g_x signal due to oxidation-reduction state of Q in the Q_o site of the bc_1 complex is similar to that observed for the substitution of Leu for Phe-144 (F144L) in the cytochrome *b* from *R. capsulatus* (29). The F144L bc_1 complex in *R. capsulatus* chromatophores was reported to have a very low turnover rate with a broadened, redox state-insensitive, g_x value at 1.765. It was suggested that these properties of the F144L complex resulted from a reduced affinity for quinone and quinol exhibited by the Q_o center of the mutated complex. Since the K70 of ISP is in the vicinity of the putative Q_o pocket of cytochrome *b*, perhaps substitution of K70 with cysteine, as in the K70C and β -ME treated A185C/K70C mutant complexes, reduces the affinity of the Q_o site of cytochrome *b* for quinone and quinol and thus decreases activity.

The redox potentials of the 2Fe2S clusters in wild type and mutant complexes A185C(cytb), K70C(ISP), and A185C(cytb)/K70C(ISP) are 231, 228, 234, 232 mV, respectively. Since the redox potentials are similar, the loss of activity in the cysteine-

pair mutant cannot be attributed to a change of the redox potential of the 2Fe2S cluster of ISP.

Effect of the Disulfide Bond Formation between Cytochrome *b* and ISP on the Rate of Intramolecular Electron Transfer between 2Fe2S and heme c_1 — One way to unambiguously establish that formation of an intersubunit disulfide bond between cytochrome *b* and ISP arrests the movement of the head domain of ISP to the "fixed state" is to compare the rate of intramolecular electron transfer between 2Fe2S and heme c_1 in wild type and cysteine-pair mutant complexes.

It has been reported that intramolecular electron transfer between heme c_1 and the 2Fe2S cluster in the bovine complex can be induced by changing the pH of the enzyme solution (15). This is based on the fact that the redox potential of heme c_1 is independent of pH whereas the redox potential of 2Fe2S is pH-dependent (higher the pH lower the redox potential). At pH 8.0 heme c_1 and 2Fe2S have the same redox potentials. Thus, when the pH of the enzyme solution is raised above 8.0, the 2Fe2S becomes less reduced than heme c_1 if the preparation is 50% reduced at pH 8.0. However, when the pH is adjusted to a lower value than 8.0, the 2Fe2S becomes more reduced than heme c_1 . Electron shuffling between 2Fe2S and heme c_1 , in the partially reduced complex, is pH dependent.

To be sure that the electron transfer between heme c_1 and 2Fe2S in the *R. sphaeroides* bc_1 complex can also be induced by a change of pH, the redox status of heme c_1 and 2Fe2S in a cytochrome c_1 half-reduced wild type bc_1 complex was monitored at various pHs (see Fig. 4). Similar to results obtained with the bovine complex, at pH 8.1, heme c_1 has the same redox potential as the 2Fe2S cluster in the *R.*

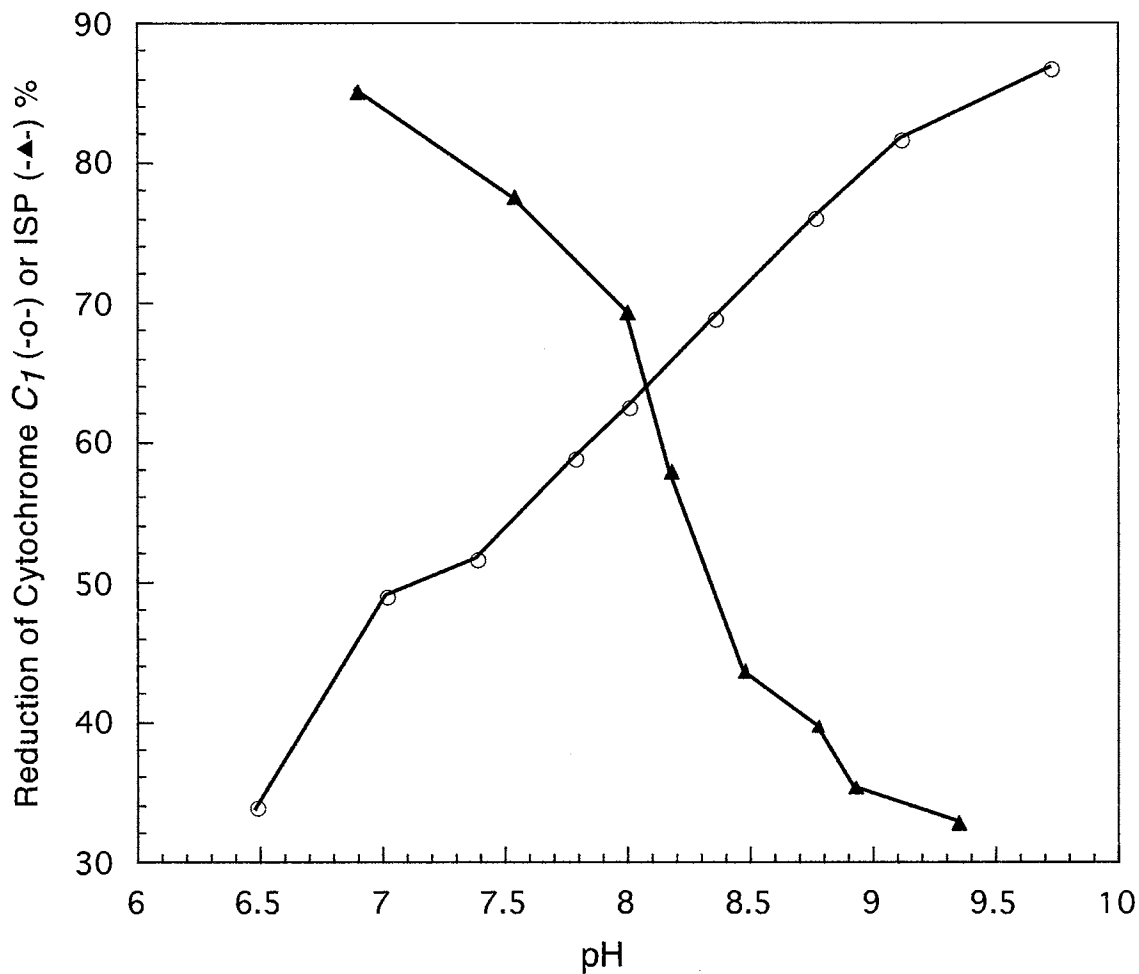


Fig. 4. pH induced reduction and oxidation of ISP and cytochrome c_1 in the partially reduced *R. sphaeroides* cytochrome bc_1 complex. The experimental conditions and instrument settings are detailed in the "Experimental Procedure". Purified His₆-tagged wild type cytochrome bc_1 complex was used.

sphaeroides bc₁ complex. When the pH is increased, 2Fe2S becomes less reduced, when it is lowered 2Fe2S becomes more reduced; heme c₁ changes in opposite directions.

Figure 5 shows time trace of acidification and alkalization-induced intramolecular electron transfer between 2Fe2S and heme c₁ in wild type and A185C (cytb)/K70C (ISP) mutant complexes. The rates of electron transfer from heme c₁ to 2Fe2S induced by acidification (reverse) and from 2Fe2S to heme c₁ (forward) induced by alkalization of wild type bacterial complex both have a $t_{1/2}$ of about 1-2 ms (Fig. 5 A & C). The rates of pH induced electron transfer between 2Fe2S and heme c₁ in the A185C (cytb)/K70C (ISP) mutant complex are very slow; the $t_{1/2}$ for the forward and backward reactions are 100 seconds and 10 seconds, respectively (Fig. 5 D & B). The rates of electron transfer between 2Fe2S and heme c₁ in mutant complexes of A185C(cytb) and K70C(ISP) are the same as those observed in the wild type complex (data not show). These results confirm that formation of a disulfide bond between the two engineered cysteines on cytochrome *b* and ISP in the A185C(cytb)/K70C(ISP) mutant complex arrests the movement of the head domain of ISP, required for *bc₁* catalysis, to a "fixed state". When the 2Fe2S cluster of ISP is in the "fixed state", it is about 31 Å away from heme c₁, too far for electron transfer.

The observation that the rates of electron transfer between 2Fe2S and heme c₁ in mutant complexes of A185C(cytb) and K70C(ISP), which have, respectively, 100% and 53% of the ubiquinol-cytochrome *c* reductase activity found in the wild type complex, are the same as that observed in the wild type complex, suggests that electron transfer between 2Fe2S and heme c₁ is not the rate limiting step in the electron transfer reaction catalyzed by the *bc₁* complex (from ubiquinol to cytochrome *c*). This suggestion is also

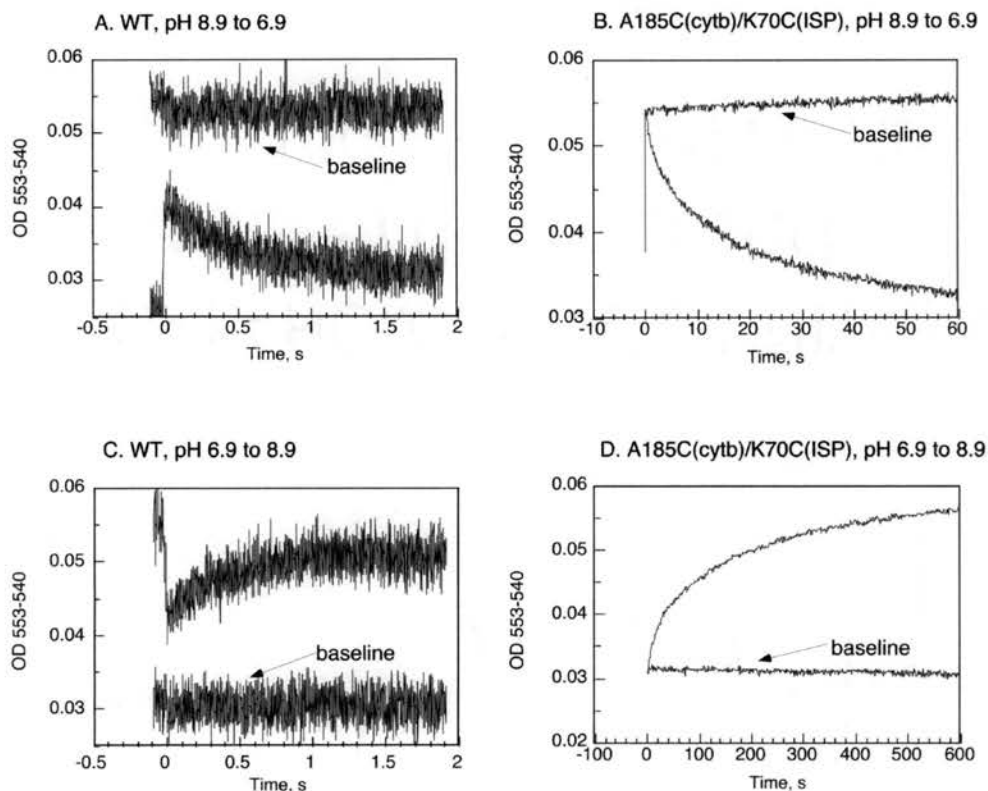


Fig. 5. Time trace of the redox change of cytochrome c_1 in the cytochrome bc_1 complex upon changing the pH from 6.9 to 8.9 or from 8.9 to 6.9. Purified cytochrome bc_1 complexes were diluted in 20 mM Tris-Cl buffer, pH 6.9 (for the alkalization experiment), or 8.9 (for the acidification experiment), containing 200 mM NaCl, 0.01% DM to a cytochrome c_1 concentration of about 10 μ M. The diluted complex was rapidly mixed with an equal volume of buffer containing enough NaOH or HCl to cause the desired pH changes, at room temperature, in an Olis stopped-flow rapid scanning spectrophotometer. A & B, oxidation of cytochrome c_1 in wild type and A185C (cytb)/K70C (ISP) mutant complexes, respectively; C & D, reduction of cytochrome c_1 in wild type and A185C (cytb)/K70C (ISP) mutant complexes, respectively. The reaction was monitored at 553 nm minus 545 nm. Complex diluted with an equal volume of the same buffer was used as a base line.

consistent with the observation that the rate of electron transfer from 2Fe2S to heme c_1 in the wild type bacterial complex is comparable to that in the bovine complex (15), even though the rate of electron transfer from ubiquinol to cytochrome c catalyzed by the bacterial complex is only one-tenth that of the bovine complex.

The fact that formation of an intersubunit disulfide bond between the engineered cysteines at the position 185 of cytochrome b and 70 of ISP results in loss of bc_1 activity suggests that movement of the head domain of ISP is independent from cytochrome b , at least in the cd2 region where the A185C is located. However, some regions of cytochrome b may have a synchronous movement with the head domain of ISP and may even provide the driving force for the movement of the ISP head. Formation of an intersubunit disulfide bond between such a region and the head domain of ISP should not have an adverse effect on electron transfer activity.

REFERENCES

1. Trumpower, B. L. and Gennis, R. B. (1994) *Annu. Rev. Biochem.* **63**, 675-716.
2. Xia, D., Yu, C. A., Kim, H., Xia, J. Z., Kachurin, A. M., Zhang, L., Yu, L., and Deisenhofer, J. (1997) *Science* **277**, 60-66.
3. Iwata, S., Lee, J. W., Okada, K., Lee, J. K., Iwata, M., Rasmussen, B., Link, T. A., Ramaswamy, S., and Jap, B. K. (1998) *Science* **281**, 64-71.
4. Zhang, Z. L., Huang, L-S., Shulmeister, V. M., Chi, Y-I., Kim, K. K., Huang, L-W., Crofts, A. R., Berry, E. A. and Kim, S-H (1998) *Nature* **392**, 677-684.
5. Kim, H., Xia, D., Yu, C. A., Kachurin, A., Zhang, L. Yu, L. and Deisenhofer, J. (1998) *Proc. Natl. Acad. Sci. USA* **95**, 8026-8033.
6. Tian, H., Yu, L., Michael, W., and Yu, C. A. (1998) *J. Biol. Chem.* **273**, 27953-27959.
7. Guergova-Kuras, M., Salcedo-Hernandez, R., Bechmann, G., Kuras, R., Gennis, R. B., and Crofts, A. R. (1999) *Protein Expr Purif.* **15**, 378-380.
8. Tian, H., White, S., Yu, L., and Yu, C. A. (1999) *J. Biol. Chem.* **274**, 7146-7152.
9. Iwata, S., Saynovits, M., Link, T. A., and Michel, H. (1996) *Structure* **4**, 567-579.
10. Link, T. A., Saynovits, M., Assmann, C., Iwata, S., Ohnishi, T., and Von Jagow, G. (1996) *Eur. J. Biochem.* **237**, 71-75.
11. Yu, C. A., and Yu, L. (1982) *Biochemistry* **21**, 4096-4101.
12. Mather, M. W., Yu, L., and Yu, C. A. (1995) *J. Biol. Chem.* **270**, 28668-28675.
13. Link, T. A., Hatzfeld, O. M., Unalkat, P., Shergill, J. K., Cammack, R., and Mason, J. R. (1996) *Biochemistry* **35**, 7546-7552.
14. Crofts, A. R., and Ugulava, N. B. (1998) *FEBS Lett.* **440**, 409-413.

15. Zhang, L., Tai, C-H., Yu, L., and Yu, C. A. (2000) *J. Biol. Chem.* **275**, 7656-7661.
16. Yu, L., Dong, J. H., and Yu, C. A. (1986) *Biochim. Biophys. Acta* **852**, 203-211.
17. Lowry, O. H., Rosebrough, N. J., Farr, A. L., and Randall, R. J. (1951) *J. Biol. Chem.* **193**, 265-275.
18. Berden, J. A., and Slater, E. C. (1970) *Biochim. Biophys. Acta* **216**, 237-249.
19. Laemmli, U. K. (1970) *Nature* **227**, 680-685.
20. Yu, L., Wei, Y-Y., Usui, S., and Yu, C. A. (1992) *J. Biol. Chem.* **267**, 24508-24515.
21. Tso, S-C., Shenoy, S. K., Quinn, B., and Yu, L. (2000) *J. Biol. Chem.* **275**, 15287-15294.
22. Atta-Asafo-Adjei, E., and Daldal, F. (1991) *Proc. Natl. Acad. Sci. U.S. A.* **88**, 492-496.
23. Tian, H., Yu, L., Mather, M. W., and Yu, C. A. (1997) *J. Biol. Chem.* **272**, 23722-23728.
24. Davidson, E., Ohnishi, T., Atta-Asafo-Adjei, E., and Daldal, F. (1992) *Biochemistry* **29**, 3342-3351.
25. Gray, K. A., Davidson, E., and Daldal, F. (1992) *Biochemistry* **31**, 11864-11873.
26. Meinhardt, S. W., Yang, X., Trumpower, B. L., and Ohnishi, T. (1987) *J. Biol. Chem.* **262**, 8702-8706.
27. McCurley, J. P., Miki, T., Yu, L., and Yu, C. A. (1990) *Biochim. Biophys. Acta* **1020**, 176-186.

28. Andrews, K. M., Crofts, A. R., and Gennis, R. B. (1990) *Biochemistry* **29**, 2645-2651.
29. Roberson, D. E., Daldal, F., and Dutton, P. L. (1990) *Biochemistry* **29**, 11249-11260.
30. Ding, H., Robertson, D. E., Daldal, F., and Dutton, P. L. (1992) *Biochemistry* **31**, 3144- 3152.

CHAPTER III

Evidence for the Intertwined Dimer of the Cytochrome bc_1 Complex in Solution

Kunhong Xiao, Ananda Chandrasekaran, Linda Yu, and Chang-An Yu
The Journal of Biological Chemistry, 276,46125-31 (2001)

ABSTRACT

To confirm that the cytochrome bc_1 complex exists as a dimer with intertwining Rieske iron sulfur proteins in solution, four *Rhodobacter sphaeroides* mutants expressing His-tagged cytochrome bc_1 complexes containing two pairs of cysteine substitutions, one in the interface between the head domain of iron-sulfur protein (ISP) and cytochrome b and the other between the tail domain of ISP and cytochrome b , were generated and characterized. They are: K70C(ISP)/A185C(cytb)·P33C(ISP)/G89C(cytb), K70C(ISP)/A185C(cytb)·P33C(ISP)/M92C(cytb), K70C(ISP)/A185C(cytb)·L34C(ISP)/V64C(cytb), and K70C(ISP)/A185C(cytb)·N36C(ISP)/G89C(cytb). The K70C(ISP)/A185C(cytb) cysteine pair cross-links the head domain of ISP and cytochrome b ; the P33C(ISP)/G89C(cytb), P33C(ISP)/M92C(cytb), L34C(ISP)/V64C(cytb), and N36C(ISP)/G89C(cytb) cysteine pairs cross-link the tail domain of ISP and cytochrome b . An adduct protein with an apparent molecular mass of 128 kDa containing two cytochrome b and two ISP proteins is detected in the K70C(ISP)/A185C(cytb)·P33C(ISP)/G89C(cytb) and K70C(ISP)/A185C(cytb)·N36C(ISP)/G89C(cytb) mutant complexes, confirming that the bc_1 complex exists as a dimer with intertwining ISPs. The loss of activity in these two double-cysteine-pair mutant complexes was attributed to the disulfide bond between the head domain of ISP and cytochrome b , and not the one between the tail domain of ISP and cytochrome b .

INTRODUCTION

The cytochrome bc_1 complex (also known as ubiquinol-cytochrome c reductase or Complex III) is an essential segment of the electron transfer chains of mitochondria and many respiratory and photosynthetic bacteria (1). This complex catalyzes electron transfer from ubiquinol to cytochrome c and concomitantly translocates protons across the membrane to generate a membrane potential and pH gradient for ATP synthesis. The polypeptide composition of cytochrome bc_1 complexes from different sources varies from three to eleven subunits. The redox subunits: cytochrome b , cytochrome c_1 , and the Rieske iron-sulfur protein (ISP), are conserved in all cytochrome bc_1 complexes.

Recently, mitochondrial cytochrome bc_1 complexes from beef (2, 3), chicken (4), and yeast (5) were crystallized and their 3-D structure determined. These 3-D structures not only established the location of the redox centers, transmembrane helices, and inhibitor binding sites, but also showed an unexpected dimeric structural arrangement of this complex in the crystal (2-5). The two ISPs from the two monomers are intertwined; the head domain of ISP in one monomer is close to the cytochrome b and cytochrome c_1 in the other monomer.

The molecule of ISP can be divided into three domains: head, tail, and neck, with the 2Fe-2S cluster located at the tip of the head (6, 7). In tetragonal $I4_122$ crystals of native oxidized bovine cytochrome bc_1 complex, the 2Fe-2S cluster in one monomer is 27 Å from heme b_L of the other monomer and 40 Å from the heme b_L of the same monomer (2). This structural arrangement suggests that mitochondrial bc_1 complex functions as a dimer, since the distance between the 2Fe-2S of ISP of one monomer and the low potential cytochrome b (b_L) of the other monomer is less than that between these

groups in the same monomer. The shorter distance accommodates fast electron transfer from QH₂ to ISP and *b_L*. However, a complex that exists as a dimer in the crystal might exist and function as a monomer in solution. Evidence for the cytochrome *bc₁* complex functioning as a dimer or a monomer has been reported (8-11). Therefore, it is important to establish whether or not the structure of the dimeric cytochrome *bc₁* complex observed in the crystal also exists in solution.

One way to address this question is to generate a mutant *bc₁* complex that forms two intersubunit disulfide bonds, one at the interface between the head domain of ISP and cytochrome *b* and the other at the proximity of the tail domain of ISP and cytochrome *b*. If the complex exists as a dimer with intertwining ISPs of the two monomers in solution, formation of these two intersubunit disulfide bonds should yield an adduct protein with an apparent molecular mass of 128 kDa containing two cytochrome *b* and two ISP proteins. If the complex exists as a dimer, but without intertwining of the two ISPs in the two monomers, or it exists as a monomer, formation of two intersubunit disulfide bonds would yield an adduct protein with an apparent molecular mass of 64 kDa containing only one cytochrome *b* and one ISP.

Because genetic manipulation of bovine heart mitochondria is not practical, *R. sphaeroides* is a better system for studying structural based functions of the *bc₁* complex by molecular genetics. The four-subunit *R. sphaeroides bc₁* complex is functionally analogous to the mitochondrial complex; the largest three subunits (cytochrome *b*, cytochrome *c₁*, and ISP) are homologous to their mitochondrial counterparts; and this system is readily manipulated genetically. In addition, *R. sphaeroides* expressing (His)₆-tagged cytochrome *bc₁* complex has been prepared (12). This greatly facilitates the

isolation of the bc_1 complex from wild-type or mutant cells. Recently, our laboratory has used this bacterial system to provide evidence for movement of the head domain of ISP during bc_1 catalysis (12-14). Such movement was suggested by the 3-D structure of the mitochondrial bc_1 complex (2-4, 15).

Herein we report procedures for generating four double-cysteine-pair *R. sphaeroides* mutants with one pair at the interface between the head domain of ISP and cytochrome *b* and the other at the proximity between the tail domain of ISP and cytochrome *b*. Mutants with single cysteine and single-cysteine-pair substitutions at indicated positions were also generated and characterized to confirm that the generated double-cysteine-pair mutants are not at critical positions in the bc_1 complex and, hence are suitable for this study. The photosynthetic growth behavior, cytochrome bc_1 complex activity, SDS-PAGE patterns and EPR characteristics of the 2Fe-2S cluster in purified complexes from wild type and mutant strains were examined and compared, as were the thermotropic properties.

EXPERIMENTAL PROCEDURES

Materials-- Cytochrome *c* (horse heart, Type-III) was purchased from Sigma. N-Dodecyl- β -D-maltoside and N-octyl- β -D-glucoside were from Anatrace. Ni-NTA gel and Qiaprep Spin Miniprep kit were from Qiagen. 2,3-Dimethoxy-5-methyl-6-geranyl-1,4-benzoquinol (Q_2H_2) was prepared in our laboratory as previously reported (16). All other chemicals were of the highest purity commercially available.

Generation of *R. sphaeroides* Strains Expressing the bc_1 Complexes with Single- or Double- Cysteine-Pair Substitutions on ISP and Cytochrome *b* -- Mutations were constructed by site-directed mutagenesis using the Altered Sites system from Promega.

For generation of single-cysteine-pair substitutions, the single stranded pSELNB3503 (17) was used as the template for mutagenesis, and oligonucleotides used were as follows: K70C (ISP)/A185C (cytb),

GTCAAGTTCCTCGGCTTGCCGATCTTCATCCGCCGCCGCACCGAGGCCGACATCG/GCTGCTCGGCCGCCCGTTGCGTGGACAATGCCA; P33C(ISP)/G89C(cytb),

GGGGCCGCCGTCTGGTTGCCTGATCAACCAAATG/AACGTGAACTTGCGGCTTCA TGCT; P33C(ISP)/M92C(cytb),

GGGGCCGCCGTCTGGTTGCCTGATCAACCAAATG/AACGGCGGCTTCTTGCCTGC GCTACCTGCATGC; L34C(ISP)/V64C(cytb),

GCCGTCTGGCCGTTGCATCAACCAAATG/GTCACCGGCATCTTGCCTTGCATGC AT; and N36C(ISP)/G89C,

TGGCCGCTGATCTTGCCAAATGAATCCGTC/AACGTGAACTTGCGGCTTCATGCT.

For generation of double-cysteine-pair substitutions, the single stranded

pSelect $fbcF_{K70C}B_{A185C}C_HQ$ was used as template for mutagenesis and oligonucleotides used were as follows: K70C(ISP)/A185C(cytb)//P33C(ISP)/G89C(cytb),

GGGGCCGCCGTCTGGTTGCCTGATCAACCAAATG/AACGTGAACTTGCGGCTTCA TGCT; K70C(ISP)/A185C(cytb)//P33C(ISP)/M92C(cytb),

GGGGCCGCCGTCTGGTTGCCTGATCAACCAAATG/AACGGCGGCTTCTTGCCTGC GCTACCTGCATGC; K70C(ISP)/A185C(cytb)//L34C(ISP)/V64C(cytb),

GCCGTCTGGCCGTTGCATCAACCAAATG/GTCACCGGCATCTTGCCTTGCATGC AT; K70C(ISP)/A185C(cytb)//N36C(ISP)/G89C(cytb),

TGGCCGCTGATCTTGCCAAATGAATCCGTC/AACGTGAACTTGCGGCTTCATGCT.

A plate-mating procedure (17) was used to mobilize the pRKD $fb_cF_mB_mC_HQ$ plasmid in *E. coli* S17-1 cells into *R. sphaeroides* BC17 cells. The presence of engineered mutations was confirmed by DNA sequencing before and after photosynthetic or semi-aerobic growth of the cells as previously reported (17). DNA sequencing and oligonucleotide synthesis were performed by the Recombinant DNA/Protein Core Facility at Oklahoma State University.

Growth of Bacteria-- *E. coli* cells were grown at 37°C in LB medium.

Photosynthetic growth conditions for *R. sphaeroides* were essentially as described previously (14). The concentrations of antibiotics used were: ampicillin, 125 µg/ml; Kanamycin sulfate, 30 µg/ml; tetracycline (10 µg/ml for *E. coli* and 1 µg/ml for *R. sphaeroides*); Trimethoprim (100 µg/ml for *E. coli* and 30 µg/ml for *R. sphaeroides*).

Enzyme Preparations and Activity Assay-- Chromatophores were prepared as described previously (12). The (His)₆-tagged cytochrome bc_1 complexes were purified from chromatophores as previously reported (12). To assay ubiquinol-cytochrome c reductase activity, chromatophores, or purified cytochrome bc_1 complexes were diluted with 50 mM Tris-Cl, pH 8.0, containing 200 mM NaCl and 0.01% LM to a final concentration of cytochrome b of 5 µM. Five-µl of the diluted samples were added to 1-ml of assay mixture containing 100 mM of Na⁺ /K⁺ phosphate buffer, pH 7.4, 300 µM of EDTA, 100 µM of cytochrome c , and 25 µM of Q₂H₂. Activities were determined by measuring the reduction of cytochrome c (the increase of the absorbance at wavelength 550 nm) in a Shimadzu UV 2101 PC spectrophotometer at 23 °C, using a millimolar extinction coefficient of 18.5 for calculation. The nonenzymatic oxidation of Q₂H₂,

determined under the same conditions, in the absence of enzyme, was subtracted during specific activity calculations.

Differential Scanning Calorimetry-- Calorimetric measurements were performed with a CSC 6100 NanoII DSC. All reference and sample solutions were degassed prior to use. A 0.33 ml of bc_1 solution, 2 mg/ml, in 50 mM K/Na phosphate buffer, pH 7.4, containing 100 mM KCl and 0.5% octylglucoside was placed in the sample capillary cell, and the same amount of buffer was placed in the reference capillary cell. The scanning rate was 1 °C /min for both heating and cooling. All thermodynamic analyses were according to the program known as CpCalc from the Nano DSC program group.

Other Biochemical and Biophysical Techniques-- Protein concentration was determined by the method of Lowry *et al.* (18). Cytochrome *b* (19) and cytochrome c_1 (20) contents were determined according to published methods. Sodium dodecylsulfate-polyacrylamide gel electrophoresis (SDS-PAGE) was performed according to Laemmli (21) using a Bio-Rad Mini-Protean dual slab vertical cell. Samples were digested with 10 mM Tris-Cl buffer, pH 6.8, containing 1% SDS, and 3% glycerol in the presence and absence of 0.4% β -ME for 2 hr at 37 °C before being subjected to electrophoresis.

EPR spectra were recorded in a Bruker ER 200D apparatus equipped with liquid Nitrogen Dewar, at 77 K. The instrument settings are detailed in the figure legends.

RESULTS AND DISCUSSION

Photosynthetic Growth Behaviors of Mutants Carrying Double-Cysteine-Pair Substitutions in ISP and Cytochrome *b*-- Four *R. sphaeroides* mutants carrying double-cysteine-pair substitutions, one pair in the interface between the head domain of ISP and cytochrome *b* and the other pair in the close proximity between the tail domain of ISP

and cytochrome *b*, were generated for this study. They are:

K70C(ISP)/A185C(cytb)//P33C(ISP)/G89C(cytb), K70C(ISP)/

A185C(cytb)//P33C(ISP)/M92C(cytb),

K70C(ISP)/A185C(cytb)//L34C(ISP)/V64C(cytb), and

K70C(ISP)/A185C(cytb)//N36C(ISP)/G89C(cytb). All of these double-cysteine-pair

mutants contain the K70C(ISP)/A185C(cytb) substitution, which was selected for cross-

linking the head domain of ISP and cytochrome *b*. This selection is based on our

previous finding (14) that the cysteine-pair of K70 of ISP and A185 of cytochrome *b*,

forms a spontaneous intersubunit disulfide bond between the head domain of ISP and

cytochrome *b* in the *bc*₁ complex. Other cysteine-pair substitutions:

P33C(ISP)/G89C(cytb), P33C(ISP)/M92C(cytb), L34C(ISP)/V64C(cytb), and

N36C(ISP)/G89C(cytb), were selected for possible cross-linking of the tail domain of ISP

with cytochrome *b*, based on the 3-D structural model of the four-subunit cytochrome *bc*₁

complex of *R. sphaeroides* (Fig. 1) constructed with coordinates from the bovine

cytochrome *bc*₁ complex (22). The distances between these four cysteine pairs are 3.4,

6.2, 6.5, and 4.9 Å, respectively, in the bacterial complex. They are 4.5, 6.3, 6.5, and 6.8

Å, when calculations are based on corresponding residues in the bovine enzyme (Table

I). Mutants with a single cysteine substitution, at positions, P33 (ISP), L34(ISP),

N36(ISP), K70(ISP), V64(cytb), G89(cytb), M92(cytb), and A185(cytb), and with single-

cysteine-pair substitution, at positions, K70(ISP)/A185(cytb), P33(ISP)/G89(cytb),

P33(ISP)/M92(cytb), L34(ISP)/V64(cytb), and N36(ISP)/G89(cytb) were also generated

and used as controls (see Table I).

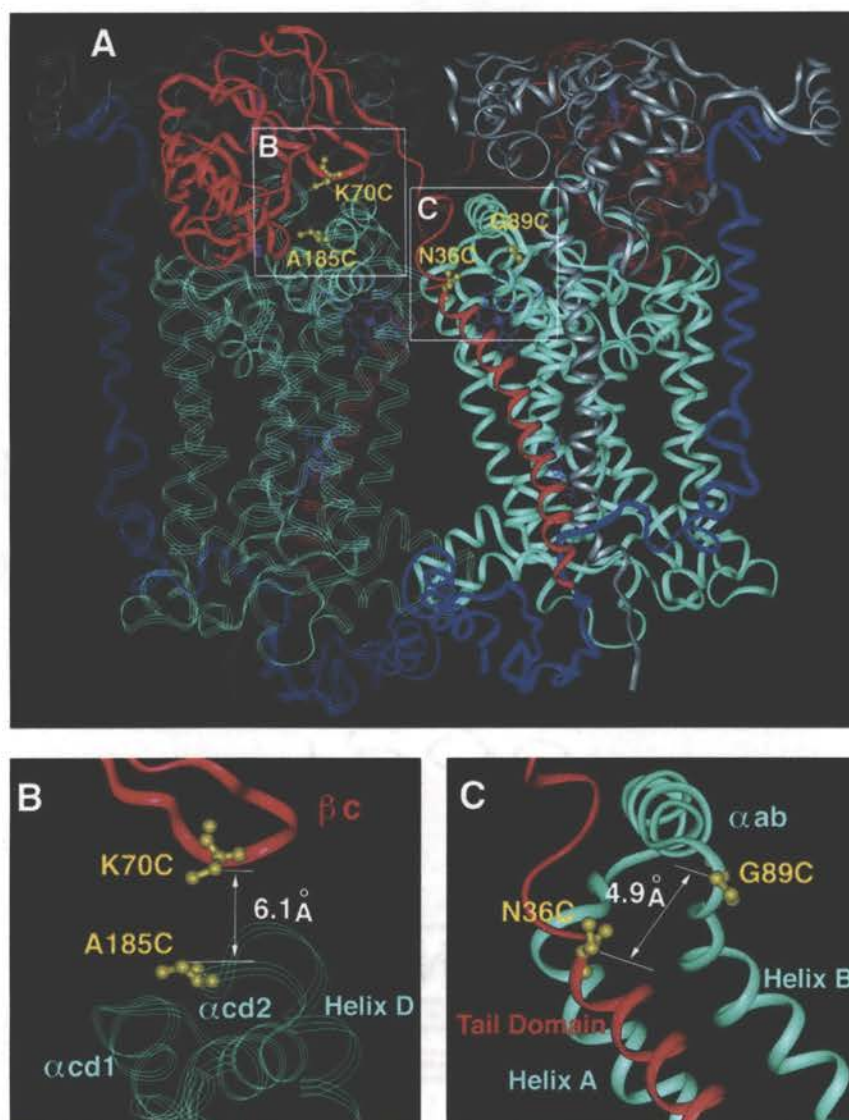


Fig. 1. Location of engineered cysteines in the structural model of the *R. sphaeroides* bc₁ complex. In the upper panel (A), one monomer (right) is displayed in solid ribbons and the symmetric monomer (left) is displayed in three-thread-line ribbons. Cytochrome *b* is in turquoise color, ISP in red, cytochrome *c*₁ in gray and subunit IVs in blue. The mutated residues are indicated by yellow balls and sticks. The 2Fe2S clusters are marked as small purple dots. The lower panels show the residues in the head-domain (B) and the tail-domain (C) of ISP that involve in the disulfide formation with residues of cytochrome *b* protein from different monomers. Some peptide sequences have been omitted for clarity. The distances between the engineered cysteines are measured from Cβ to Cβ.

Table I.
Characterization of ISP and cytochrome b interface Cysteine Mutants

Mutants	Single mutation		Double mutant residues distance ^a		Ps ^b	Enzymatic activity ^c	
	Corresponding residues in bovine	Location	In bovine structure	In bacterial modeling		Chromatophore	Purified complex ^d
			Å	Å			
Wild type					++	2.3 (100%)	2.5 (100%)
K70C(ISP)	K95	head			++	1.3 (57%)	1.4 (56%)
A185C(cytb)	S169	cd2			++	2.3 (100%)	2.5 (100%)
K70C(ISP)/A185C(cytb)			6.5	6.1	++	1.3 (57%)	0.3 (12%) ^e
P33C(ISP)	Q57	tail			++	1.3 (57%)	1.4 (56%)
G89C(cytb)	Y75	ab loop			++	2.4 (100%)	2.4 (96%)
P33C(ISP)/G89C(cytb)			4.5	3.4	++	1.3 (57%)	1.4 (56%)
K70C(ISP)/A185C(cytb)// P33C(ISP)/G89C(cytb)			6.5//4.5	6.1//3.4	+	0.4 (17%)	0.1 (4%) ^e
M92C(cytb)	I78	helix B			++	2.3 (100%)	2.5 (100%)
P33C(ISP)/M92C(cytb)			6.3	6.2	++	1.9 (83%)	2.0 (80%)
K70C(ISP)/A185C(cytb)// P33C(ISP)/M92C(cytb)			6.5//6.3	6.1//6.2	-	-	-
L34C(ISP)	F58	tail			++	1.6 (70%)	1.7 (68%)
V64C(cytb)	F50	helix A			++	2.3 (100%)	2.5 (100%)
L34C(ISP)/V64C(cytb)			6.5	6.5	++	1.4 (61%)	1.6 (64%)
K70C(ISP)/A185C(cytb)// L34C(ISP)/V64C(cytb)			6.5//6.5	6.1//6.5	-	-	-
N36C(ISP)	S60	tail			++	2.3 (100%)	2.5 (100%)
N36C(ISP)/G89C(cyb)			6.8	4.9	++	2.2 (96%)	2.5 (100%)
K70C(ISP)/A185C(cytb)// N36C(ISP)/G89C(cytb)			6.5//6.8	6.1//4.9	++	0.5 (22%)	0.1 (4%) ^e

^aThe distances were measured from C-β to C-β (except with glycine which is to C-α).

^bPs, photosynthetic growth. ++, cell growth rate is essentially the same as that of the wild type cells; +, cell grow photosynthetically but at a rate slower than that of the wild type; -, no photosynthetic growth in 4 days.

^cEnzymatic activity is expressed as μmol cytochrome *c* reduced/min/nmol cytochrome *b* at room temperature.

^dThe cytochrome *bc*₁ complex was in 50 mM Tris-Cl, pH 8.0, containing 200 mM NaCl, 200 mM histidine and 0.5% octyl glucoside.

^eThe cytochrome *bc*₁ complex activity was measured immediately after preparation.

For double-cysteine-pair mutants to be useful in this study, the resulting mutant bc_1 complexes must be active. Since the bc_1 complex is absolutely required for the photosynthetic growth of *R. sphaeroides*, whether or not the engineered cysteine positions result in inactive bc_1 complexes can be determined by assaying photosynthetic growth. Mutants with cysteine substitutions at critical positions in the complex will not grow photosynthetically; mutants with substitutions at noncritical positions will grow.

When mid-log phase, aerobically dark grown wild type and mutant cells were inoculated into enriched Sistrom's medium and subjected to anaerobic photosynthetic growth conditions, all the single cysteine substitution mutants, all the single-cysteine-pair mutants, and the K70C(ISP)/A185C(cytb)/N36C(ISP)/G89C(cytb) double-cysteine-pair mutant grew at rates comparable with that of wild-type cells. The K70C(ISP)/A185C(cytb)·P33C(ISP)/G89C(cytb) mutant grew at a retarded rate (30%), and K70C(ISP)/A185C(cytb)·P33C(ISP)/M92C(cytb) and K70C(ISP)/A185C(cytb)·L34C(ISP)/V64C(cytb) did not grow photosynthetically (Table I).

The finding that the K70C(ISP)/A185C(cytb)·P33C(ISP)/M92C(cytb) and K70C(ISP)/A185C(cytb)·L34C(ISP)/V64C(cytb) double-cysteine-pair mutants cannot grow photosynthetically is rather surprising, since mutants with single cysteine substitutions or single-cysteine-pair substitutions at the respective positions of ISP and cytochrome *b* have the same photosynthetic growth rate as that of wild-type cells. The inability of these two double-cysteine-pair mutants to support photosynthetic growth is not due to the formation of two intersubunit disulfide bonds from engineered cysteines because no disulfide bond formation is expected in the absence of oxygen. Perhaps introduction of an additional cysteine-pair in these two double-cysteine-pair mutants changes the

conformation of the bc_1 complex, causing inactivation. In any case, the failure of these two double-cysteine-pair mutants to support photosynthetic growth makes them unsuitable for this study.

On the other hand, the K70C(ISP)/A185C(cytb)//P33C(ISP)/G89C(cytb) and K70C(ISP)/A185C(cytb)//N36C(ISP)/G89C(cytb) support photosynthetic growth, indicating that the engineered cysteine pairs are not impairing the complex. Therefore, formation of two intersubunit disulfide bonds between ISP and cytochrome *b* was examined in these two double-cysteine-pair mutants.

Production of a 128-kDa Adduct Protein by Formation of Two Disulfide Bonds between ISP and Cytochrome *b* in the K70C(ISP)/A185C(cytb)// P33C(ISP)/G89C(cytb) and K70C(ISP)/A185C(cytb)//N36C(ISP)/G89C(cytb) Mutant Complexes--

Chromatophores freshly prepared from these two double-cysteine-pair mutants, and their respective single-cysteine pair mutants, K70C(ISP)/A185C(cytb), P33C(ISP)/G89C(cytb), and N36C(ISP)/G89C(cytb), have, respectively, 17, 22, 57, 57, and 96% of the bc_1 activity found in wild type chromatophores (see Table I). When these chromatophore preparations were subjected to Western blot analysis using antibodies against *R. sphaeroides b* and ISP, no protein band corresponding to the adduct of cytochrome *b* and ISP was observed, indicating that no disulfide bond is formed between the engineered cysteines during anaerobic photosynthetic growth. No disulfide bond formation is expected because photosynthetic growth is under strict anaerobic conditions. Without oxygen no disulfide bond can be formed even if the two cysteines are in favorable positions.

When the His₆-tagged *bc*₁ complexes were purified from these five freshly prepared mutant chromatophores, the P33C(ISP)/G89C(cytb) and N36C(ISP)/G89C(cytb) single-cysteine-pair mutant complexes have the same activity the same as that found in their respective chromatophores, based on cytochrome *b* content (see Table I). Activities in these two single-cysteine-pair mutant complexes remained unchanged during storage at 0 °C. On the other hand, the single-cysteine-pair mutant complex of K70C(ISP)/A185C(cytb) and double-cysteine-pair mutant complexes of K70C(ISP)/A185C(cytb)·P33C(ISP)/G89C(cytb) and K70C(ISP)/A185C(cytb)·N36C(ISP)/G89C(cytb) have about 20% of the *bc*₁ activity found in their respective chromatophores (Table I). Activities in these three mutant complexes decreased during storage at 0 °C. Almost no activity remained after 30 hr. Under identical conditions, no activity loss was observed for the wild type complex.

When these purified mutant complexes were treated with SDS at 37 °C for 2 h and subjected to electrophoresis in the absence of β-ME, an adduct protein band with an apparent molecular mass of 64 kDa, the size of one cytochrome *b* and one ISP, was detected in the single-cysteine-pair mutant complexes. Meanwhile an adduct protein band with an apparent molecular mass of 128 kDa, the size of two cytochrome *b* and two ISP, was detected in the double-cysteine-pair mutant complexes (see Fig. 2).

The 64-kDa protein band is an adduct of one cytochrome *b* and one ISP and the 128-kDa protein band an adduct of two cytochrome *b* and two ISP. These two adduct proteins result from the formation of one and two disulfide bonds between cytochrome *b* and ISP in the single- and double-cysteine-pair mutant complexes, respectively. Experimental results supporting this conclusion are as follows: first, the appearance of

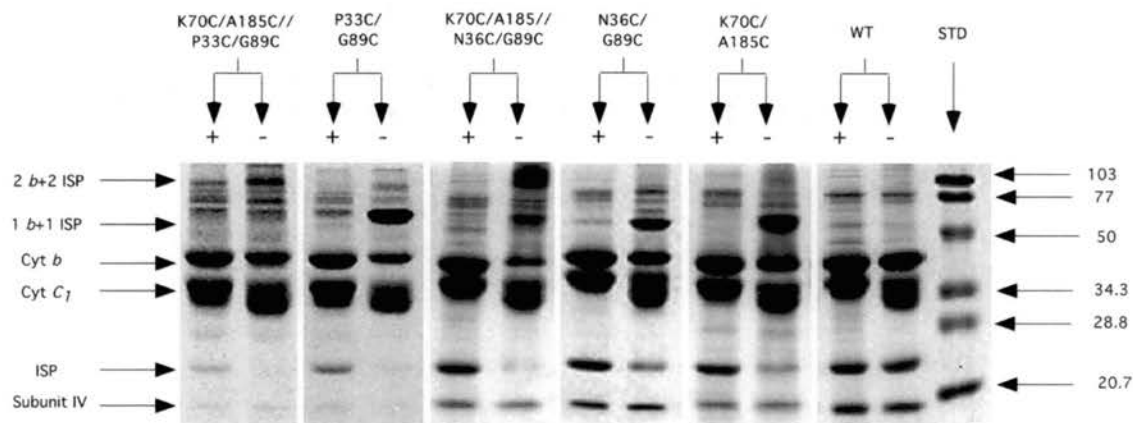


Fig. 2. SDS-PAGE of single- and double-cysteine-pair mutant cytochrome *bc*₁ complexes. Aliquots of purified *bc*₁ complexes of wild type and indicated mutants were incubated with 1% SDS with (+) or without (-) 0.4% β-ME at 37°C for 2 h. Digested samples containing 150 pmoles of cytochrome *b* were subjected to electrophoresis. Protein standard (STD) contains: phosphorylase B (103 kDa), bovine serum albumin (77 kDa), ovalbumin (50 kDa), carbonic anhydrase (34.3 kDa), soybean trypsin inhibitor (28.8 kDa) and lysozyme (20.7 kDa). WT, wild type.

the 64- kDa or 128-kDa protein band is accompanied by a decrease in the band intensities of cytochrome *b* and ISP (see Fig. 2); second, the Mr=64 kDa and Mr=128 kDa protein bands react with antibodies against cytochrome *b* and ISP; third, when these mutant complexes were treated with SDS and β -ME and then subjected to SDS-PAGE in the presence of β -ME, the 64 kDa and 128-kDa protein bands disappear, and the band intensities of cytochrome *b* and ISP increase; and fourth, protein isolated from the 64-kDa and 128-kDa gel slice, after treatment with β -ME, can be resolved into cytochrome *b* and ISP.

Formation of two intersubunit disulfide bonds, one between the tail domain of ISP and one cytochrome *b* and the other between the head domain of the same ISP and other cytochrome *b*, in double-cysteine pair mutant complexes of K70C(ISP)/A185C(cytb)·N36C(ISP)/G89C(cytb)/ and K70C(ISP)/A185C(cytb)·P33C(ISP)/G89C(cytb) yields an adduct protein with an apparent molecular weight of 128-kDa, containing two cytochrome *b* and two ISP, the cytochrome *bc*₁ complex must exist as a dimer with intertwining ISPs, in solution. This structural arrangement must be similar to that observed in the crystal state.

Effect of Disulfide Bond Formation on *bc*₁ Activity of Double-Cysteine-Pair Mutant Complexes-- The loss of activity in double-cysteine-pair mutant complexes of K70C(ISP)/A185C(cytb)//P33C(ISP)/G89C(cytb) and K70C(ISP)/A185C(cytb)//N36C(ISP)/G89C(cytb) is apparently due to the formation of two intersubunit disulfide bonds between ISP and cytochrome *b* (see Table I and Fig. 2). It is important to know which of the two, or both, bonds are responsible for activity loss. Because purified K70C(ISP)/A185C(cytb) mutant complex lost the *bc*₁ activity, while the

purified P33C(ISP)/G89C(cytb) or N36C(ISP)/G89C(cytb) mutant complex had the same activity as that in their respective chromatophores (see Fig. 2 and Table I), we conclude that the disulfide bond between cysteines K70C(ISP)/A185C(ISP), but not the one between cysteines P33C(ISP)/G89C(cytb) or N36C(ISP)/G89C(cytb), is responsible for the activity loss in these two double-cysteine-pair mutant complexes. This deduction is consistent with the recent finding that mobility of the ISP head is essential for the bc_1 complex (12-14, 23, 24). The cysteines at Lys-70 of ISP and Ala-85 of cytochrome *b* are between the head domain of ISP, where 2Fe-2S cluster resides, and cytochrome *b*. Formation of an intersubunit disulfide bond between these two cysteines would render the ISP head immobile, causing a loss of activity. The cysteines at Pro-33 or Asn-36 of ISP and Gly-89 of cytochrome *b* are between the tail domain of ISP and cytochrome *b*. Formation of an intersubunit disulfide bond here has no effect on activity, suggesting that movement of the head domain of ISP, which is required for bc_1 catalysis, does not involve the tail domain.

To further substantiate this deduction, the effect of β -ME on bc_1 activity and disulfide bond formation was examined in these two double-cysteine-pair mutant complexes and their respective single-cysteine-pair complexes. When purified K70C(ISP)/A185C(cytb)·N36C(ISP)/G89C(cytb) and K70C(ISP)/A185C(cytb)·P33C(ISP)/G89C(cytb) mutant complexes, which had little bc_1 activity, were treated with β -ME, the activities were restored to the same level as those in their respective chromatophores prepared in the presence or absence of β -ME (Table II). No adduct protein with an apparent molecular mass of 128 kDa containing 2 cytochrome *b* and 2 ISP subunits was detected in these β -ME treated complexes (see Fig. 2). These

Table II

Effect of β -ME on the cytochrome bc_1 activity in chromatophores and purified complexes from wild type, single- and double-cysteine pair mutants

Mutants	Enzymatic activity ^a			
	Chromatophore		Purified bc_1 complex	
	- ^b	+ ^c	- ^d	+ ^e
Wild type	2.3	2.3	2.5	2.5
K70C(ISP)/A185C(cytb)	1.3	1.3	0.1	1.4
P33C(ISP)/G89C(cytb)	1.3	1.3	1.4	0.8
N36C(ISP)/G89C(cytb)	2.2	2.2	2.5	1.5
K70C(ISP)/A185C(cytb)//P33C(ISP)/G89C(cytb)	0.4	0.4	0	0.4
K70C(ISP)/A185C(cytb)//N36C(ISP)/G89C(cytb)	0.5	0.5	0	0.6

^a Enzymatic activity is expressed as μ mol of cytochrome c reduced/min/nmol cytochrome b at room temperature.

^b - samples prepared in the absence of β -ME.

^c + samples prepared with buffers containing 100 mM β -ME.

^d - samples stored at 0 °C for 30 hr after preparation.

^e + stored samples treated with 100 mM β -ME.

results confirm that the loss of activity in these two mutant complexes results from the formation of two intersubunit disulfide bonds between ISP and cytochrome *b*.

Activity restoration by β -ME was also observed with the K70C(ISP)/A185C(cytb) single-cysteine-pair mutant complex (Table II). This reactivation was accompanied by the disappearance of the 64-kDa ISP-cyt *b* adduct protein (Fig. 2). Thus disulfide bond formation between the head domain of ISP and cytochrome *b* arrests the mobility of the ISP head, causing the bc_1 activity loss.

When the N36C(ISP)/G89C(cytb) and P33C(ISP)/G89C(cytb) mutant complexes, which had the same activity as that in their respective chromatophores and showed the 64 kDa ISP-cytb adduct protein, were treated with 100 mM β -ME, about 70% of the bc_1 activity was lost and the 64 kDa adduct protein disappeared. The loss of activity in these two β -ME treated mutant complexes is rather surprising, since their respective mutant chromatophores, prepared in the absence and presence of β -ME, have the same bc_1 activity (Table II) and contain no intersubunit disulfide bond. Spectral analysis revealed that the β -ME-treated N36C(ISP)/G89C(cytb) and P33C(ISP)/G89C(cytb) mutant complexes had only 50% of the cytochrome *b* content found in their respective untreated complexes, indicating that β -ME causes the release of heme *b* from its apoprotein, and thus loss the activity. Under identical conditions no heme *b* release was observed in the wild-type complex, double-cysteine-pair mutant complexes of K70C(ISP)/A185C(cytb)·N36C(ISP)/G89C(cytb) and K70C(ISP)/A185C(cytb)·P33C(ISP)/G89C(cytb), single-cysteine-pair mutant complex of K70C(ISP)/A185C(cytb), and single cysteine substitution mutant complexes of A185C(cytb), K70C(ISP), N36C(ISP), G89C(cytb), and P33C(ISP). Why cytochrome *b* in the N36C(ISP)/G89C(cytb) and

P33C(ISP)/G89C(cytb) mutant complexes is more labile toward β -ME treatment, is unknown. Nevertheless, the effect of disulfide bond formation on bc_1 activity in the N36C(ISP)/G89C(cytb) and P33C(ISP)/G89C(cytb) mutant complexes cannot be assessed by β -ME treatment.

Effect of Disulfide Bond Formation between Cytochrome *b* and ISP on EPR

Characteristics of the 2Fe-2S Cluster -- Although the loss of bc_1 complex activity in K70C(ISP)/A185C(cytb)·N36C(ISP)/G89C(cytb) and K70C(ISP)/A185C(cytb)·P33C(ISP)/G89C(cytb) is attributed to the formation of the disulfide bond between cysteines K70C(ISP) and A185C(cytb), making the ISP head immobile, perhaps formation of two intersubunit disulfide bonds in these two complexes altered the microenvironment of ISP, thus leading to activity loss. To test this possibility, EPR characteristics of the 2Fe-2S in these two complexes, with and without β -ME treatment, were compared. It has been reported that the g_x signal of the 2Fe-2S cluster of ISP in the cytochrome bc_1 complex depends on the environment (25) and the quinone occupancy (25, 26).

As shown in Fig. 3, the 2Fe-2S cluster in the K70C(ISP)/A185C(cytb)·N36C(ISP)/G89C(cytb) mutant complex, with or without β -ME treatment, has the same EPR spectrum, with the g_x signal at 1.77. An identical EPR spectrum was obtained for the K70C(ISP)/A185C(cytb)·P33C(ISP)/G89C(cytb) mutant complex (data not shown). These results indicate that the microenvironments of the ISP cluster in these two mutant complexes are not affected by the formation of two disulfide bonds. Therefore, the loss of bc_1 activity is not due to a change of microenvironment in ISP.

The 2Fe-2S cluster in the N36C(ISP)/G89C(cytb) mutant complex has an EPR spectrum identical to that observed in the wild type complex with the g_x at 1.80, suggesting that formation of an intersubunit disulfide bond between the tail domain of ISP and cytochrome *b* has no effect on ISP. The 2Fe-2S in the K70C(ISP)/A185C(cytb) mutant complex, with and without β -ME treatment, has the same EPR spectrum with a g_x at 1.78 (see Fig. 3). This coupled with the fact that the 2Fe-2S cluster in the A185C(cytb) mutant complex has an EPR spectrum identical to that observed in the wild type complex with the g_x at 1.80, whereas the 2Fe-2S in the K70C(ISP), mutant complex has a broadened g_x signal that is shifted to 1.77, suggests that the shift of the g_x signal of 2Fe-2S in the K70C(ISP)/A185C(cytb)·N36C(ISP)/G89C(cytb) complex is due to replacing K70 of ISP with cysteine.

Effect of disulfide bond formation on thermotropic Properties of Single- and Double-cysteine-Pair Mutant Cytochrome bc_1 Complexes -- Differential scanning calorimetry has been widely used to study protein stability. The thermodenaturation temperature (T_m) and the change of enthalpy (ΔH) are the two parameters used to assess this thermostability. Since the bc_1 complex purification involves detergents and the amount and type of detergents used greatly affect the protein stability, for systematic comparison of protein stability, all bc_1 preparations used in these DSC studies were in 0.5% octylglucoside.

When purified, wild-type cytochrome bc_1 complex underwent thermodenaturation it showed a T_m at 37.8 °C and ΔH of 33.1 kcal/mol. Under identical conditions the mitochondrial bc_1 complex has a T_m of 63.3 °C and ΔH of 749.3 kcal/mol (data not shown), indicating that the mitochondrial bc_1 complex is more stable than the bacterial

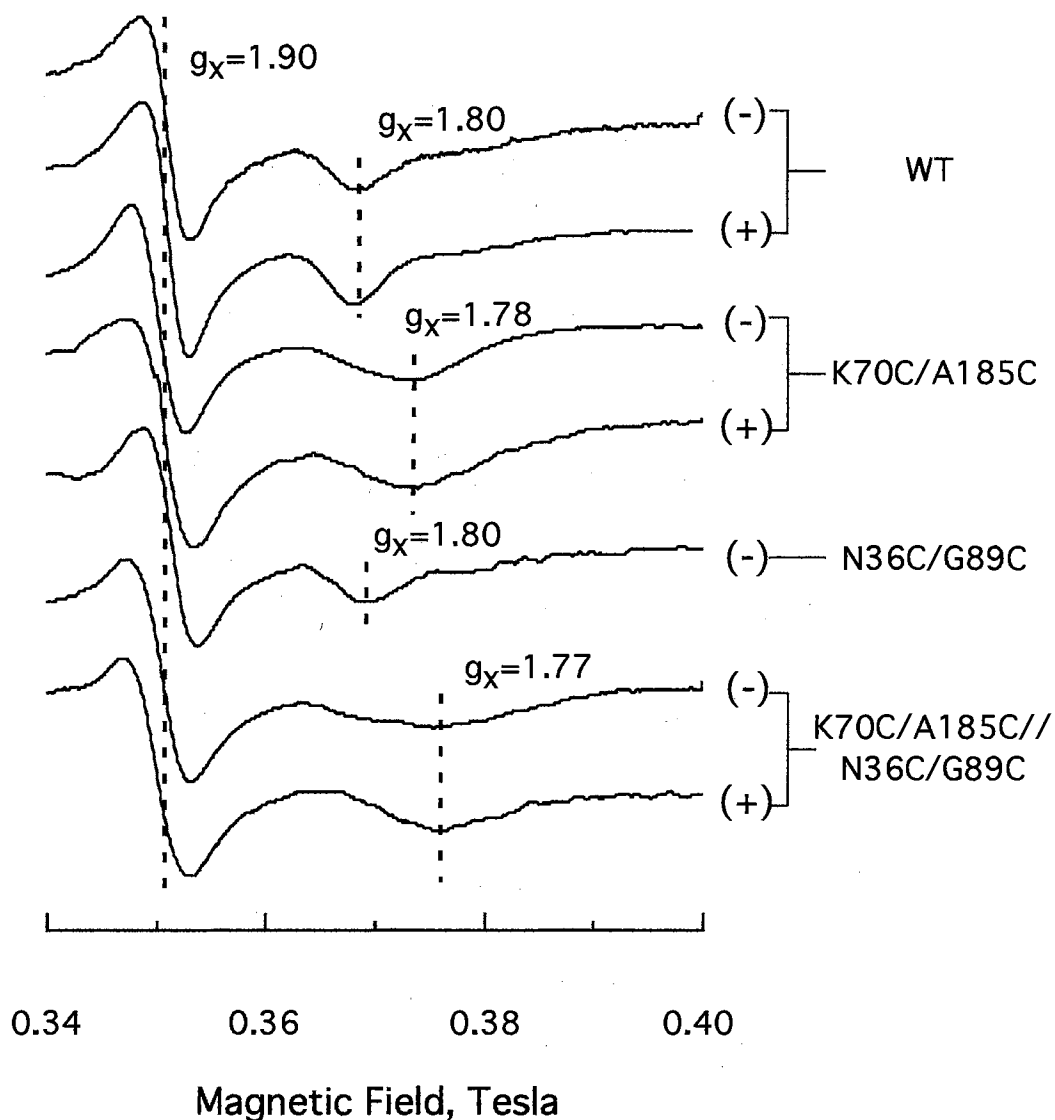


Fig. 3. EPR spectra of the 2Fe₂S cluster in the cytochrome *bc*₁ complexes of wild type (WT) and indicated mutants, with (+) or without (-) 100 mM β -ME treatment. The complexes were incubated with 5 mM sodium ascorbate on ice for 30 minutes and frozen in liquid nitrogen. EPR spectra were recorded at 77 K with the following instruments settings: microwave frequency, 9.28 GHz; microwave power, 20 milliwatts; modulation amplitude, 20 G; modulation frequency, 100 kHz; time constants, 0.1 s; and scan rate, 20 G/s.

complex. The presence of more supernumerary subunits in the mitochondrial cytochrome bc_1 complex apparently contribute to the thermal stability of the complex. When single-cysteine-pair mutant complexes K70C(ISP)/A185C(cytb), P33C(ISP)/G89C(cytb), and N36C(ISP)/G89C(cytb) were subjected to thermodenaturation, all showed a T_m of around 41 °C (an increase of about 3 °C) with an increased ΔH value. This indicates that formation of an intersubunit disulfide bond either between the head domain or tail domain of ISP and cytochrome b increases the structural stability of the complex. It should be noted that single cysteine substitutions at positions K70, P33, or N36 of ISP, or A185 or G89 of cytochrome b do not affect the stability of the bc_1 complex (data not shown). The increase in T_m and ΔH in the double cysteine mutant proteins must result from the formation of the disulfide bond.

REFERENCES

1. Trumpower, B. L. and Gennis, R. B. (1994) *Annu. Rev. Biochem.* **63**, 675-716.
2. Xia, D., Yu, C. A., Kim, H., Xia, J. Z., Kachurin, A. M., Zhang, L., Yu, L., and Deisenhofer, J. (1997) *Science* **277**, 60-66.
3. Iwata, S., Lee, J. W., Okada, K., Lee, J. K., Iwata, M., Rasmussen, B., Link, T. A., Ramaswamy, S., and Jap, B. K. (1998) *Science* **281**, 64-71.
4. Zhang, Z. L., Huang, L-S., Shulmeister, V. M., Chi, Y-I., Kim, K. K., Huang, L-W., Crofts, A. R., Berry, E. A. and Kim, S-H (1998) *Nature* **392**, 677-684.
5. Hunte, C., Koepke, J., Lange, C., Robmanith, T., and Michel, H. (2000) *Structure* **8**, 669-684.
6. Iwata, S., Saynovits, M., Link, T. A., and Michel, H. (1996) *Structure* **4**, 567-569.
7. Link, T. A., Saynovits, M., Assmann, C., Iwata, S., Ohnishi, T., and Von Jagow, G. (1996) *Eur. J. Biochem.* **237**, 71-75.
8. Von Jagow, G., Schagger, H., Riccio, P., Klingenberg, M., and Kolb, H. J. (1977) *Biochim. Biophys. Acta* **462**, 549-558.
9. Nalecz MJ, Azzi A.(1985) *Arch. Biochem. Biophys.* **240**, 921-931.
10. Musatov, A., and Robinson, N. (1994) *Biochemistry* **33**, 13005-13012.
11. Jungas, C., Ranck, J-L., Rigaud, J-L., Joliot, P., and Vermeglio, A. (1999) *EMBO J.* **18**, 534-542.
12. Tian, H., Yu, L., Michael, W., and Yu, C. A. (1998) *J. Biol. Chem.* **273**, 27953-27959.
13. Tian, H., White, S., Yu, L., and Yu, C. A. (1999) *J. Biol. Chem.* **274**, 7146-7152.
14. Xiao, K., Yu, L., and Yu, C. A. (2000) *J. Biol. Chem.* **275**, 38597-38604.

15. Kim, H., Xia, D., Yu, C. A., Kachurin, A., Zhang, L. Yu, L. and Deisenhofer, J. (1998) *Proc. Natl. Acad. Sci. USA* **95**, 8026-8033.
16. Yu, C. A., and Yu, L. (1982) *Biochemistry* **21**, 4096-4101.
17. Mather, M. W., Yu, L., and Yu, C. A. (1995) *J. Biol. Chem.* **270**, 28668-28675.
18. Lowry, O. H., Rosebrough, N. J., Farr, A. L., and Randall, R. J. (1951) *J. Biol. Chem.* **193**. 265-275.
19. Berden, J. A., and Slater, E. C. (1970) *Biochim. Biophys. Acta* **216**, 237-249.
20. Yu, L., Dong, J. H., and Yu, C. A. (1986) *Biochim. Biophys. Acta* **852**, 203-211.
21. Laemmli, U. K. (1970) *Nature* **227**, 680-685.
22. Tso, S-C., Shenoy, S. K., Quinn, B., and Yu, L. (2000) *J. Biol. Chem.* **275**, 15287-15294.
23. Darrouzet, E., Valkova-Valchanova, M., and Daldal, F. (2000) *Biochemistry* **39**, 15475-15478.
24. Obungu, V. H., Wang, Y., Amyot, S. M., Gocke, C. B., and Beattie, D. E. (2000) *Biochim. Biophys. Acta* **1457**, 36-44.
25. McCurley, J. P., Miki, T., Yu, L., and Yu, C. A. (1990). *Biochim. Biophys. Acta*, **1020**, 176-186.
26. Ding, H., Moser C. C., Robertson, D. E., Tokito, M. K., Daldal, F., and Dutton, P. L. (1995) *Biochemistry* **34**, 15979–15996.

CHAPTER IV

Photoinduced Electron Transfer between the Rieske Iron-Sulfur Protein and Cytochrome c_1 in the *Rhodobacter sphaeroides* Cytochrome bc_1 Complex: Effects of pH, Temperature, and Driving Force

Gregory Engstrom, Kunhong Xiao, Chang-An Yu, Linda Yu, Bill Durham, and Francis Millett

The Journal of Biological Chemistry, 277, 31072-8 (2002)

ABSTRACT

Electron transfer from the Rieske iron-sulfur protein to cytochrome c_1 (cyt c_1) in the *Rhodobacter sphaeroides* cytochrome bc_1 complex was studied using a ruthenium dimer complex, Ru₂D. Laser flash photolysis of a solution containing reduced cyt bc_1 , Ru₂D, and a sacrificial electron acceptor results in oxidation of cyt c_1 within 1 μ s, followed by electron transfer from the iron-sulfur center (2Fe-2S) to cyt c_1 with a rate constant of 80,000 s⁻¹. Experiments were carried out to evaluate whether the reaction was rate-limited by true electron transfer, proton gating, or conformational gating. The temperature dependence of the reaction yielded an enthalpy of activation of +17.6 kJ/mol, which is consistent with either rate-limiting conformational gating or electron transfer. The rate constant was nearly independent of pH over the range pH 7 to 9.5 where the redox potential of 2Fe-2S decreases significantly due to deprotonation of His-161. The rate constant was also not greatly affected by the Rieske iron-sulfur protein mutations Y156W, S154A, or S154A/Y156F, which decrease the redox potential of 2Fe-2S by 62, 109, and 159 mV, respectively. It is concluded that the electron transfer reaction from 2Fe-2S to cyt c_1 is controlled by conformational gating.

INTRODUCTION

The cytochrome bc_1 complex (ubiquinol:cytochrome c oxidoreductase) is an integral membrane protein in the energy-conserving electron transport chains of mitochondria and many respiratory and photosynthetic prokaryotes (1). The complex contains the Rieske iron-sulfur protein, cyt c_1 , and two b -type hemes (b_L and b_H) in the cyt b subunit (1,2). In the Q-cycle mechanism, the complex translocates four protons to the positive side of the membrane per two electrons transferred from ubiquinol to cyt c (2). In a key bifurcated reaction at the Q_o site, the first electron is transferred from ubiquinol to the Rieske iron-sulfur center (2Fe-2S) and then to cyt c_1 and cyt c (1-3). The second electron is transferred from semiquinone in the Q_o site to cyt b_L and then to cyt b_H and ubiquinone in the Q_i site. Extensive x-ray crystallographic studies of cyt bc_1 have revealed that the Rieske iron-sulfur protein occurs in several different conformations depending on the crystal form and the presence of Q_o site inhibitors (Fig. 1) (4-6). In native I4₁22 bovine crystals an anomalous signal for 2Fe-2S is found close to cyt b_L , but its intensity is small, suggesting that the Rieske iron-sulfur protein is conformationally mobile (4, 7). Addition of the Q_o inhibitors UHDBT or stigmatellin significantly increased the intensity of 2Fe-2S, indicating that the Rieske iron-sulfur protein was immobilized with 2Fe-2S near the surface of cyt b_L (7). In both chicken and yeast cyt bc_1 crystals, grown in the presence of stigmatellin, the Rieske iron-sulfur protein is in a conformation with 2Fe-2S proximal to the cyt b_L heme, called the b state (5, 8). However, in native chicken or beef P6₅22 crystals, the Rieske iron-sulfur protein is in a conformation with 2Fe-2S close to cyt c_1 , called the c_1 state (Fig. 1) (5, 6). An intermediate conformation of the Rieske iron-sulfur protein was found in P6₅ crystals of

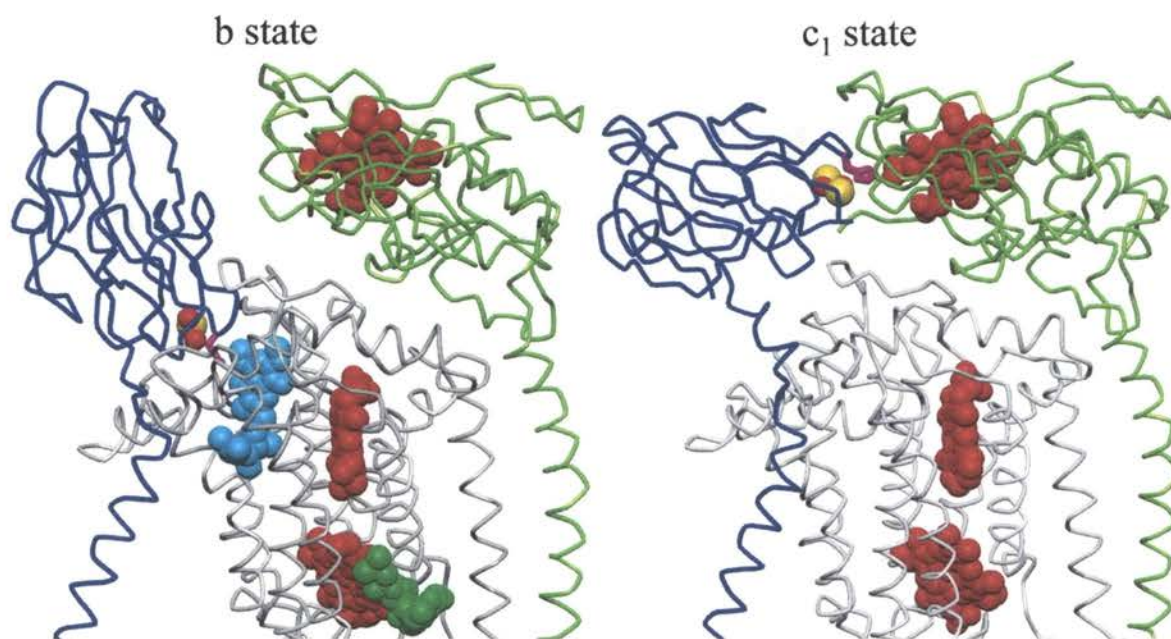


Fig. 1. X-ray crystal structures of cytochrome bc_1 from chicken in the presence of stigmatellin and antimycin (b state), and in the beef P6₅22 crystals (c_1 state). The Rieske, cyt c_1 , and cyt b subunits are colored *blue*, *green*, and *gray*, respectively. The hemes, the 2Fe-2S center, stigmatellin, and antimycin are represented by CPK models colored *red*, *red/yellow*, *cyan*, and *green*, respectively. His-161 is colored *purple*.

the bovine complex (6). These structural studies have suggested a novel shuttle mechanism for the Rieske iron-sulfur protein during electron transfer. It has been proposed that the Rieske iron-sulfur protein changes conformation from the *b* state, where oxidized 2Fe-2S accepts an electron from ubiquinol in the Q_o site, to the c_1 state where reduced 2Fe-2S transfers an electron to cyt c_1 (4-7). This mobile shuttle mechanism has been supported experimentally by the finding that cross-linking the Rieske iron-sulfur domain to the cyt *b* subunit inhibited steady-state electron transfer (9) and by studies involving mutations, which alter the conformation or flexibility of the neck domain of the Rieske iron-sulfur protein (10-18).

A complete understanding of the mobile shuttle mechanism requires determination of the dynamics of conformational changes in the Rieske iron-sulfur protein and the rate constants for electron transfer from quinol to 2Fe-2S and from 2Fe-2S to cyt c_1 . However, the rate constant for electron transfer between 2Fe-2S and cyt c_1 is too fast to be measured by conventional techniques. Flash photolysis experiments in *Rhodobacter sphaeroides* chromatophores established that the rate constant was much larger than 5000 s^{-1} , the rate of diffusion of photooxidized cyt c_2 from the reaction center to cyt bc_1 (19, 20). We have recently introduced a new method to study electron transfer between 2Fe-2S and cyt c_1 that utilizes a ruthenium complex, Ru_2D , to directly add or remove an electron from cyt c_1 within $1 \mu\text{s}$ (11). The net charge of +4 on Ru_2D allows it to bind with high affinity to the negatively charged domain on cyt c_1 . Laser flash photolysis of Ru_2D generates the metal-to-ligand excited state, which rapidly reduces or oxidizes cyt c_1 in the presence of appropriate sacrificial electron donors or acceptors (11).

The rate constant for electron transfer from 2Fe-2S to cyt c_1 was found to be $80,000 \text{ s}^{-1}$ in *R. sphaeroides* cyt bc_1 and $16,000 \text{ s}^{-1}$ in bovine cyt bc_1 (11).

In the present report, we further characterize the electron transfer reaction between 2Fe-2S and cyt c_1 in *R. sphaeroides* cyt bc_1 . Experiments were carried out to evaluate whether the reaction is rate-limited by true electron transfer, proton gating, or conformational gating. The temperature dependence of the reaction is consistent with either a mechanism involving rate-limiting electron transfer according to Marcus theory or a mechanism involving rate-limiting conformational gating. The rate constant was nearly independent of pH over the range pH 7 to 9.5 where the redox potential of 2Fe-2S decreases significantly due to deprotonation of His-161. This result indicates that the reaction is not rate-limited by proton gating. The rate constant was also not greatly affected by the Rieske iron-sulfur protein mutations Y156W, S154A, or S154A/Y156F, which decrease the redox potential of 2Fe-2S by 62, 109, and 159 mV, respectively. These results indicate that the reaction is not rate-limited by electron transfer, because Marcus theory predicts that the increase in the driving force of the reaction for these mutants would increase the rate constant by up to 15-fold. It is concluded that conformational gating controls electron transfer between the Rieske iron-sulfur protein and cyt c_1 .

EXPERIMENT PROCEDURES

Materials-- Ru₂D was prepared by a modification of the method of Downard *et al.* (21). Cytochrome *c* (horse heart, Type III) was purchased from Sigma Chemical Co. *N*-Dodecyl- β -D-maltoside and *N*-octyl- β -D-glucoside were from Anatrace. 2,3-Dimethoxy-

5-methyl-6-geranyl-1,4-benzoquinol (Q_2H_2) was prepared as previously reported (22). Succinate cytochrome *c* reductase (SCR) was purified as previously described (23). Antimycin A, succinate, TMPD, and *p*-benzoquinone were obtained from Sigma; stigmatellin was purchased from Fluka; and $[Co(NH_3)_5Cl]^{2+}$ was synthesized (24).

Generation and Expression of *R. sphaeroides* Cyt *bc*₁ Complexes with

Substitutions on *ISP*-- Mutations were constructed by site-directed mutagenesis using the Altered Sites system from Promega. Single-stranded pSELNB3503 (25) was used as the template for mutagenesis, and oligonucleotides used were as follows: S154A (*ISP*), CCCTGCCACGGAGCGCACTACGACAGT; Y156W (*ISP*), CACGGATCGCACTGGGACAGTGCCGGCCGTA; and S154A/Y156F (*ISP*), TTCTGCCCCTGCCACGGAGCGCACTTCGACAGTGCCGGCCGTAT.

A plate-mating procedure (25) was used to mobilize the pRKD*fb*cF_mBC_HQ plasmid in *Escherichia coli* S17-1 cells into *R. sphaeroides* BC17 cells as previously described (9). Growth of *E. coli* cells and plasmid-bearing *R. sphaeroides* cells were carried out as previously described (9). The identity of the mutations was confirmed by DNA sequencing before and after photosynthetic or semi-aerobic growth of the cells, as described previously (9). Mutant cytochrome *bc*₁ was purified as described by Xiao *et al.* (9).

Determination of Enzyme Activity and Redox Potential of the 2Fe-2S Cluster in

Mutant *cyt bc*₁-- The *cyt bc*₁ activity was determined in an assay mixture containing 100 mM of Na⁺/K⁺ phosphate buffer, pH 7.4, 300 μM of EDTA, 100 μM of *cyt c*, and 25 μM of Q_2H_2 at 23 °C using the method described by Xiao *et al.* (9). *cyt bc*₁ complexes containing partially reduced *cyt c*₁ were prepared by mixing complexes containing fully

reduced and fully oxidized cyt c_1 in 20 mM Tris-Cl buffer, pH 8.0, containing 200 mM NaCl and 0.01% dodecyl maltoside. The concentration of cyt c_1 in the partially reduced complex was adjusted to 10 μ M in the pH 8.0 buffer. The His-tagged bc_1 complex with fully oxidized, or reduced cytochrome c_1 was obtained by addition of $K_3Fe(CN)_6$ or sodium ascorbate, respectively, followed by passage through the nickel-nitrilotriacetic acid column to remove excess oxidant or reductant. The redox status of heme c_1 and the 2Fe-2S in the partially reduced wild-type and mutant complexes were determined as previously described (9). Reduction of cytochrome c_1 was followed by measuring the increase of the α absorption (553-545 nm) in a Shimadzu UV2101 PC spectrophotometer. Reduction of 2Fe-2S was followed by measuring the negative circular dichroism peak, at 500 nm, of partially reduced complex minus fully oxidized complex in a JASCO J-715 spectropolarimeter (26-28). The same samples were used for the absorption and circular dichroism measurements. Instrument settings for the spectropolarimeter were: scan speed, 100 nm/min; step resolution, 1 nm; accumulation, 10 traces for averaging; response, 1 s; bandwidth, 1.0 nm; sensitivity, 10 millidegrees; and slit width, 500 μ m. The redox potentials of 2Fe-2S were calculated from the redox states of heme c_1 and 2Fe-2S, at pH 8.0, using 280 mV for the midpoint redox potential of heme c_1 (29).

Flash Photolysis Experiments-- Transient absorbance measurements were obtained by flash photolysis of 300- μ l solutions in a 1-cm quartz semi-microcuvette. A Phase R model DL1400 flash lamp-pumped dye laser containing coumarin LD490 was used to generate an excitation flash at 480 nm for a duration of <0.5 μ s. The detection system has been previously described by Heacock *et al.* (30). Samples typically contained 5 μ M *R. sphaeroides* bc_1 complex and 20 μ M Ru₂D in 20 mM sodium borate or Tris-Cl

buffer with 0.02% lauryl maltoside. All photooxidation samples contained 5 mM of the sacrificial electron acceptor, $[\text{Co}(\text{NH}_3)_5\text{Cl}]^{2+}$. About 10 μM of the synthetic quinol, $\text{Q}_0\text{C}_{10}\text{Br}$, was used to initially reduce the bc_1 complex. To regenerate reduced quinol throughout the flash experiments, 1 mM succinate and 50 nM SCR were included. Redox mediators included *p*-benzoquinone ($\epsilon_m = +280$ mV) and TMPD ($\epsilon_m = +275$ mV) used in concentrations of 10 and 2 μM , respectively. The temperature dependence data was fitted by Equations 1-3 using the Marquardt-Levenberg nonlinear regression algorithm in SigmaPlot. The error for each parameter reported is the asymptotic standard error representing 95% confidence limits given by the algorithm.

RESULTS

Effects of pH and Redox State on Electron Transfer from 2Fe-2S to cyt c_1 -- The ruthenium dimer Ru_2D was used to rapidly photooxidize $\text{cyt } c_1$ in a solution containing *R. sphaeroides* $\text{cyt } bc_1$ with $\text{cyt } c_1$ and 2Fe-2S fully reduced and $\text{cyt } b_H$ 20% reduced (Fig. 2). The metal-to-ligand excited state of Ru_2D is a strong oxidant and oxidizes $\text{cyt } c_1$ within 1 μs as indicated by the rapid decrease in absorbance at 552 nm (Fig. 2). The sacrificial electron acceptor $[\text{Co}(\text{NH}_3)_5\text{Cl}]^{2+}$ was present in the solution to oxidize $\text{Ru}^{\text{II}*}$ and/or Ru^{I} . The mechanism of $\text{cyt } c_1$ oxidation may involve either pathway shown in Scheme 1. Subsequent reduction of $\text{cyt } c_1$ by 2Fe-2S is biphasic with rate constants of 80,000 and 1,200 s^{-1} at pH 9.0, as indicated by the increase in absorbance at 552 nm (Fig. 2 and Scheme 2). The fast phase has been assigned to electron transfer from 2Fe-2S

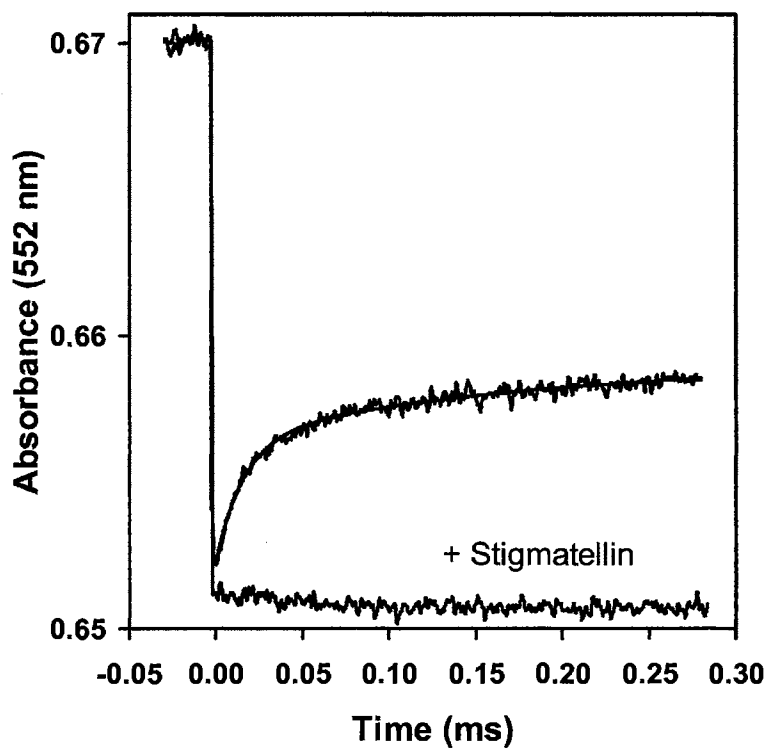
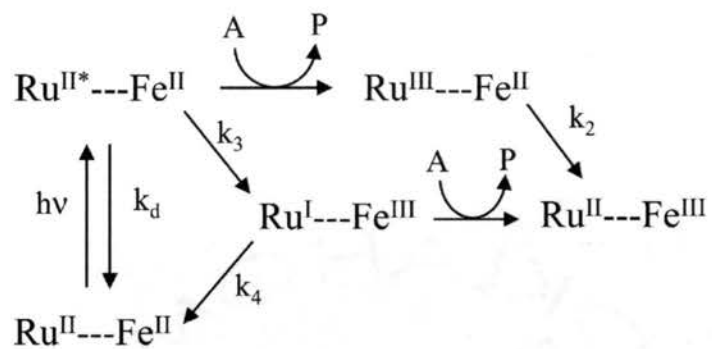
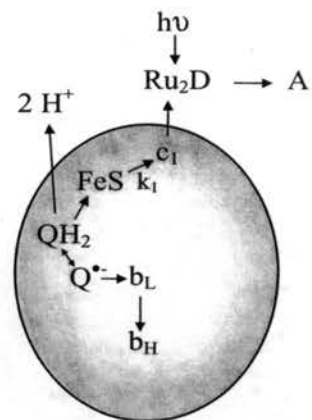


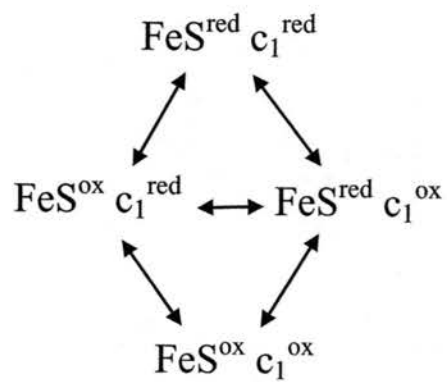
Fig. 2. Electron transfer within *R. sphaeroides* cyt bc_1 following photooxidation of cyt c_1 . A solution containing 5 μM *R. sphaeroides* cyt bc_1 and 20 μM Ru_2D in 20 mM sodium borate, pH 9.0, and 5 mM $[\text{Co}(\text{NH}_3)_5\text{Cl}]^{2+}$ was treated with $\text{Q}_0\text{C}_{10}\text{Br}$ to reduce cyt bc_1 and excited with a laser flash. The *smooth curve* is a biphasic fit with rate constants of 80,000 and 1,200 s^{-1} . The *lower transient* was obtained with the same sample after treatment with 20 μM stigmatellin.



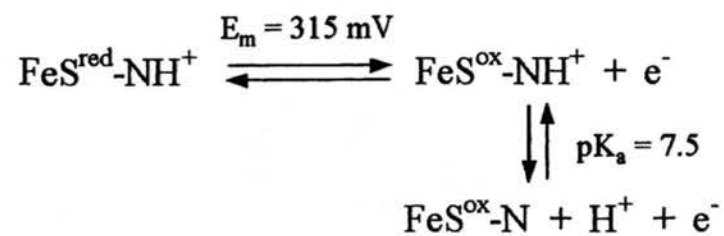
SCHEME 1



SCHEME 2



SCHEME 3



SCHEME 4

to cyt c_1 , whereas the slow phase is due to electron transfer from QH₂ to oxidized 2Fe-2S, which then reduces cyt c_1 (Fig. 2) (12). Both phases of cyt c_1 reduction are completely inhibited by addition of the Q_o inhibitor stigmatellin, which strongly binds reduced 2Fe-2S in the b state and prevents electron transfer to cyt c_1 .

To further investigate the factors affecting the fast phase of cyt c_1 reduction in the bc_1 complex, studies were conducted in the presence of various mediators to control the redox states of the metal centers in cyt bc_1 . The possible redox states of 2Fe-2S and cyt c_1 are shown in Scheme 3. Only the state with both 2Fe-2S and cyt c_1 initially reduced would be active in the flash photolysis experiments described here. When a minimum amount of QH₂ (10 μ M) was added in the presence of the redox mediator *p*-benzoquinone at pH 9.0, the reduction of cyt c_1 after the first flash was biphasic with rate constants of 80,000 s⁻¹ and 1,200 s⁻¹. The absorbance showed that cyt c_1 was fully reduced, and cyt b_H was partially reduced before photooxidation. The amplitudes of both the fast and slow phases of cyt c_1 reduction decreased with subsequent laser flashes until the transient changed to a step function indicating photooxidation of cyt c_1 with no subsequent re-reduction (Fig. 3). Absorption spectra recorded immediately before and after loss of the fast phase indicated that cyt c_1 remained 70-95% reduced while cyt b_H was completely oxidized. The redox potential of 2Fe-2S is lower than that of cyt c_1 at pH 9.0, and 2Fe-2S will be oxidized before cyt c_1 during successive photooxidation flashes, accounting for the loss of the fast phase of cyt c_1 reduction. When ascorbate was used to reduce 2Fe-2S and cyt c_1 in the presence of *p*-benzoquinone, the fast phase of cyt c_1 was observed with the same rate constant as in the presence of excess QH₂. cyt b_H was fully oxidized before the flash, and the absence of a slow reduction phase for cyt b_H at 562 nm indicated that

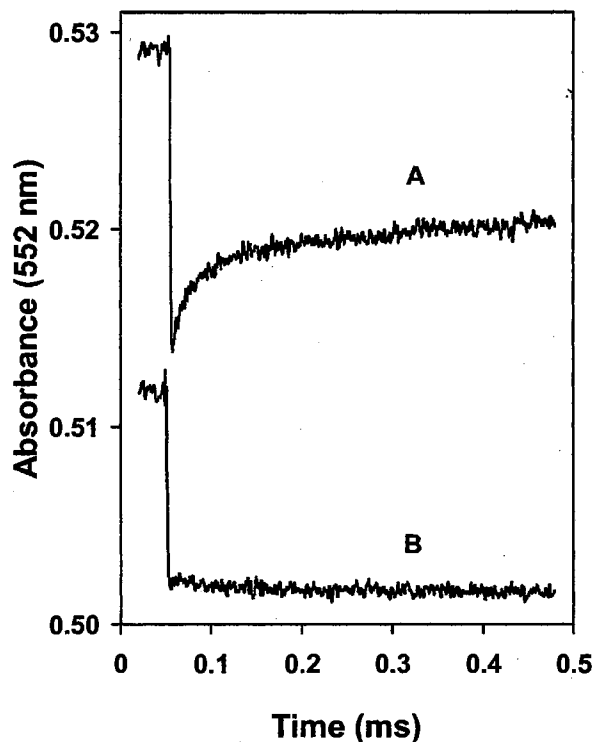


Fig. 3. Electron transfer within *R. sphaeroides* cyt bc_1 following photooxidation of cyt c_1 . A solution containing 5 μM *R. sphaeroides* cyt bc_1 and 20 μM Ru₂D in 20 mM sodium borate, pH 9.0, and 5 mM [Co(NH₃)₅Cl]²⁺ was treated with 10 μM Q₀C₁₀Br to reduce cyt bc_1 and excited with a laser flash. *A*, after the first flash the transient was biphasic with rate constants of 80,000 and 1,000 s⁻¹, respectively. Under these conditions, cyt b_{H} was about 10% reduced. *B*, after about 10 flashes, both the fast and slow phases of the transient disappeared, even though cyt c_1 was still 80% reduced. cyt b_{H} was 100% oxidized under these conditions.

the quinol pool remained oxidized. Addition of the inhibitor myxothiazol did not affect the rate constant of the fast phase of electron transfer from 2Fe-2S to cyt c_1 in the presence of ascorbate or quinol.

The driving force for the electron transfer reaction between 2Fe-2S and cyt c_1 changes significantly over the pH range 7.0-9.5, because the redox potential of 2Fe-2S is pH-dependent whereas that of cyt c_1 is not (27). The redox potential of *R. sphaeroides* 2Fe-2S decreases from +300 to +200 mV as the pH is increased from pH 7.0 to 9.5 (27). The kinetics of cyt c_1 reduction were measured over the pH range 7.0-9.5 in the presence of succinate and SCR to regenerate reduced quinol and maintain 2Fe-2S and cyt c_1 in the fully reduced state. The rate constant for the fast phase of cyt c_1 reduction has a very small pH dependence over the range pH 7.0-9.5 (Fig. 4). In the semiclassical theory developed by Marcus (31), the rate constant for nonadiabatic electron transfer is controlled by the driving force $\Delta G^{0'}$, the reorganization energy λ , and the electronic coupling H_{AB} between the two redox centers,

$$k_{ct} = \frac{4\pi^2 H_{AB}^2}{h(4\pi\lambda RT)^{1/2}} \exp[-\Delta G^{0'} + \lambda)^2/4\lambda RT] \quad (\text{Eq. 1})$$

where R is the gas constant and T is the temperature. The electronic coupling term H_{AB} has been found to decrease exponentially with distance in a broad range of biological systems, and a simplified Equation can be used (32),

$$k_{ct} = k_0 \exp[-\beta(r - r_0)] \exp[-(\Delta G^{0'} + \lambda)^2/4\lambda RT] \quad (\text{Eq. 2})$$

where r is the distance between the closest macrocycle atoms in the two redox centers, the van der Waals contact distance r_0 is usually assumed to be 3.6 Å, β is taken to

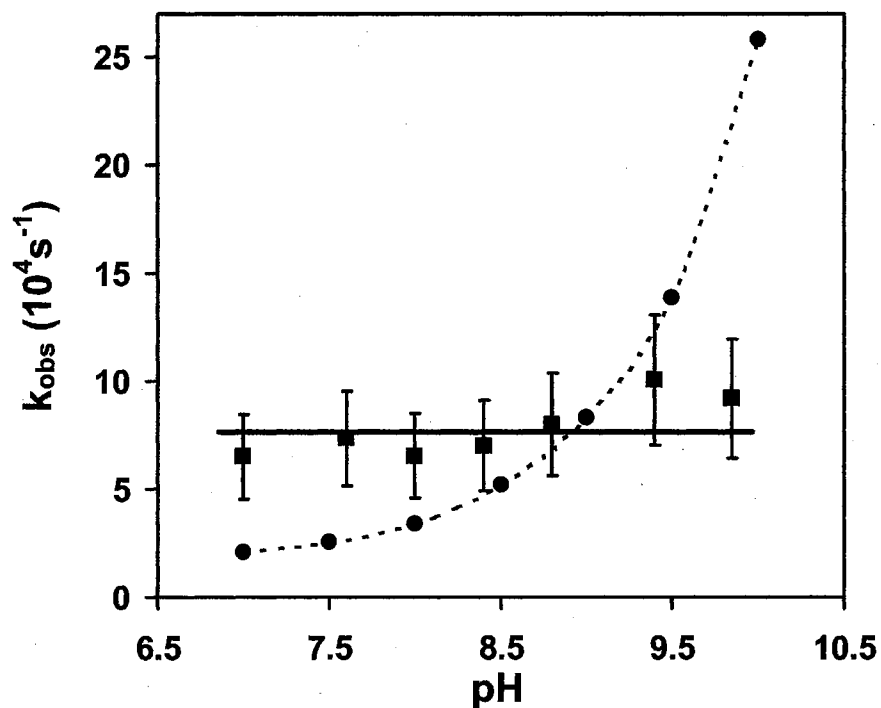


Fig. 4. pH dependence of the rate constant for electron transfer from 2Fe-2S to cyt c_1 . The solutions contained 5 μM *R. sphaeroides* cyt bc_1 , 20 μM Ru₂D, and 5 mM [Co(NH₃)₅Cl]²⁺ in a buffer containing 20 mM sodium borate (pH 8.5-9.5), Tris-Cl (pH 7.5-8.5), or sodium phosphate (pH 7.0-7.5). The sample was treated with 10 μM Q₀C₁₀Br, 1 mM succinate, and 50 nM SCR to reduce cyt bc_1 and excited with a laser flash. ■, rate constant for fast phase of cyt c_1 reduction. ●, theoretical calculations based on Equation 2 with $\lambda = 1$ eV, $r = 10.6$ Å, and ΔG^0 calculated from the difference in redox potentials of 2Fe-2S and cyt c_1 (27). The solid line is the theoretical calculation based on Equation 2 with $\lambda = 1$ eV, $r = 9.4$ Å, and $\Delta G^0 = -0.035$ eV.

be 1.4 \AA^{-1} , and the nuclear frequency k_0 is 10^{13} s^{-1} (32). Equation 2 was used to calculate the rate constant for the fast phase of electron transfer from 2Fe-2S to cyt c_1 , assuming that the nuclear reorganization energy λ is 1 eV (33) and the distance r between the 2Fe-2S ligand His-161 and the closest heme c_1 macrocycle atom is 10.6 \AA . The driving force (ΔG^0) of the reaction was based on the midpoint potential of the 2Fe-2S center at different pH values and the midpoint potential of cyt c_1 , 280 mV, which is independent of pH (27). The Marcus theory prediction is in agreement with the experimental rate constant at pH 9.0, but the large pH dependence predicted by Marcus theory is not in agreement with the experimental results.

Effects of Temperature on Electron Transfer from 2Fe-2S to Cyt c_1 -- The electron transfer reaction between 2Fe-2S and cyt c_1 was studied as a function of temperature from 0 to $30 \text{ }^\circ\text{C}$ to provide further insight into the mechanism. The fast phase of cyt c_1 reduction decreased significantly with decreasing temperature, as shown in Fig. 5. The temperature dependence of the rate constant k was analyzed by transition state theory using the Eyring equation,

$$\ln(k/T) = \Delta H^\ddagger / RT + \Delta S^\ddagger / R + \ln(h/k_B) \quad (\text{Eq. 3})$$

where H^\ddagger is the activation enthalpy, ΔS^\ddagger is the activation entropy, h is Planck's constant, k_B is the Boltzmann constant, and R is the gas constant. The best fit of Equation 3 to the data was obtained with $\Delta H^\ddagger = +17.6 \pm 1.8 \text{ kJ/mol}$ and $\Delta S^\ddagger = -91.1 \pm 5.8 \text{ J/mol}\cdot\text{K}$ (Fig. 5A). The temperature dependence of the fast phase of electron transfer was also analyzed by Marcus theory Equations 1 and 2. The best fit to Equation 2 was obtained with $r = 11.1 \pm 0.7 \text{ \AA}$ and $\lambda = 0.75 \pm 0.09 \text{ eV}$ (Fig. 5B). The driving force, ΔG^0 , of the reaction was set equal to -0.035 eV based on the differences in redox

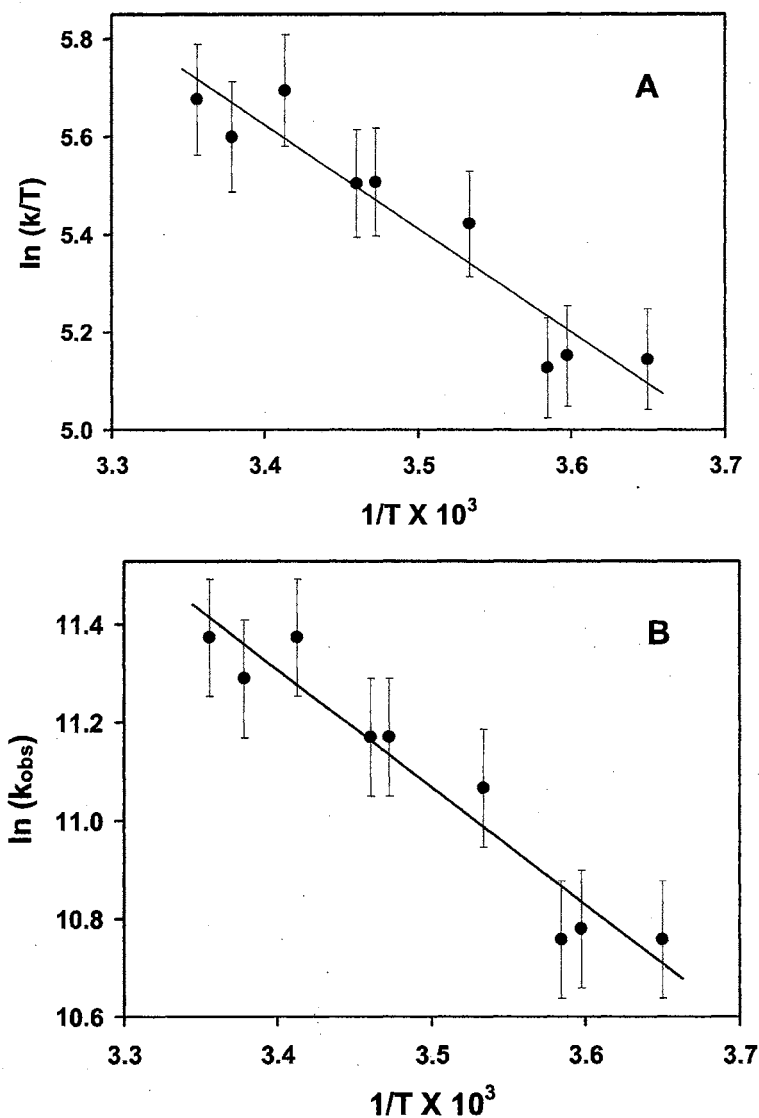


Fig. 5. Temperature dependence of rate constant for electron transfer from 2Fe-2S to cyt c_1 . The solution contained 5 μM *R. sphaeroides* cyt bc_1 , 20 μM Ru_2D , and 5 mM $[\text{Co}(\text{NH}_3)_5\text{Cl}]^{2+}$ in 20 mM sodium borate, pH 9.0. The sample was treated with 10 μM $\text{Q}_0\text{C}_{10}\text{Br}$, 1 mM succinate, and 50 nM of SCR to reduce cyt bc_1 and excited with a laser flash. *A*, the *solid line* is the best fit of Equation 3 to the data with $\Delta H^\ddagger = +17.6 \pm 1.8$ kJ/mol and $\Delta S^\ddagger = -91.1 \pm 5.8$ J/mol·K. *B*, the *solid line* is the best fit to Equation 2 with $r = 11.1 \pm 0.7$ Å, $\lambda = 0.75 \pm 0.09$ eV, and $\Delta G^0 = -0.035$ eV. The *solid line* is also the best fit to Equation 1 with $H_{AB} = 1.3 \pm 0.6$ cm $^{-1}$ and $\lambda = 0.80 \pm 0.09$ eV.

Table I

Kinetic properties of R. sphaeroides cyt bc₁ mutants

Mutant	Enzymatic activity ^a	ΔE_m ^b mV	k_1 (10^4 s ⁻¹) (experimental) ^c	k_1 (10^4 s ⁻¹) (theory) ^d
Wild-type	2.5	0	8.0	8.0
Y156W	0.58	-62	15.0	26.0
S154A	0.23	-109	7.8	60.0
S154A/Y156F	0.03	-159	9.0	140.0

^a Enzymatic activity is expressed as micromoles of cyt *c* reduced/min/ μ mol cyt *b* at 25 °C.

^b ΔE_m is the difference in redox potential between 2Fe-2S and cyt *c*₁ at pH 8.0, 25 °C.

^c k_1 is the experimental rate constant for electron transfer from 2Fe-2S to cyt *c*₁ at pH 8.0, 25 °C.

^d Theoretical rate constant for electron transfer calculated from Equation 2 with $r = 9.9$ Å, $\lambda = 1.0$ eV, and ΔG^0 calculated from the ΔE_m value of the mutant cyt *bc*₁.

midpoint potentials of the protonated 2Fe-2S center and the cyt c_1 heme. The best fit to Equation 1 was obtained with $H_{AB} = 1.3 \pm 0.6 \text{ cm}^{-1}$ and $\lambda = 0.80 \pm 0.09 \text{ eV}$ (Fig. 5B).

Mutations Altering the Redox Midpoint Potential of 2Fe-2S-- To examine the effect of driving force on the fast phase of electron transfer from 2Fe-2S to cyt c_1 , several mutant cyt bc_1 complexes were prepared with altered 2Fe-2S redox potentials. The Rieske iron-sulfur protein mutants were prepared by site-directed mutagenesis and expressed and purified as described under "Experimental Procedures." The 2Fe-2S redox potentials of the Y156W, S154A, and S154A/Y156F mutants were found to be 62, 109, and 159 mV lower than that of cyt c_1 , respectively, at pH 8.0 and 25 °C (Table I). The 2Fe-2S redox potential of wild-type cyt bc_1 was the same as that of cyt c_1 at pH 8.0. The steady-state enzymatic activities of these mutants were 23%, 9%, and 1% that of wild-type cyt bc_1 , respectively (Table I). However, the rate constants for the fast phase of electron transfer from 2Fe-2S to cyt c_1 were not greatly affected by these mutations. The rate constant of the Y156W mutant was $150,000 \text{ s}^{-1}$ compared with $80,000 \text{ s}^{-1}$ for wild-type cyt bc_1 , whereas the rate constants of the S154A and S154A/Y156F mutants were nearly the same as that of wild-type (Table I). The slow phase of reduction of cyt c_1 and cyt b_H due to electron transfer from QH_2 to 2Fe-2S was too slow to measure accurately by the ruthenium method for these mutants. The increase in driving force for electron transfer from 2Fe-2S to cyt c_1 by 62-159 mV for these mutants would be expected to increase the rate constant of the fast phase by 3- to 17-fold according to the Marcus theory in Equation 2 (Table I). It is apparent that the fast phase of electron transfer from 2Fe-2S to cyt c_1 is not rate-limited by true electron transfer.

DISCUSSION

Kinetic characterization of the electron transfer reactions involving cyt bc_1 has proven to be a formidable task, because the rate constants are so large. The cyt bc_1 electron transfer reactions have been studied extensively in chromatophores from *R. sphaeroides* and *R. capsulatus* using a light flash to initiate the electron transfer cycle (13, 16, 19, 20). The time resolution of this technique is limited by the diffusion of photooxidized cyt c_2 from the reaction center to cyt bc_1 , which has a rate constant of about $5,000\text{ s}^{-1}$ (19, 20). The rate constant for electron transfer from quinol to 2Fe-2S in the Q_0 site was found to be $1,650\text{ s}^{-1}$ using this method, whereas electron transfer from 2Fe-2S to cyt c_1 was estimated to be greater than 10^5 s^{-1} (20). Very recently, the electric field generated by the reaction center in *R. sphaeroides* chromatophores was found to induce electron transfer from cyt b_H to cyt b_L with a half-time of 0.1 ms, establishing the rate constant for this important reaction (34). We have developed a ruthenium photoexcitation method to study intracomplex electron transfer of cyt c with cyt b_5 , cyt c peroxidase, cyt c oxidase, and cyt bc_1 (35-38). The rate constant for intracomplex electron transfer between cyt c and cyt c_1 was determined to be $60,000\text{ s}^{-1}$ by this method (38). The development of a binuclear ruthenium complex to rapidly photooxidize cyt c_1 has allowed measurement of the rate constant for electron transfer from 2Fe-2S to cyt c_1 to be $80,000\text{ s}^{-1}$ in the *R. sphaeroides* cyt bc_1 complex (12). The rate constant for electron transfer from quinol to 2Fe-2S in the Q_0 site was found to be 1200 s^{-1} by this technique, in good agreement with flash photolysis studies in chromatophores (20). Here we report the effects of pH, temperature, and driving force on electron transfer between 2Fe-2S and cyt c_1 using the ruthenium flash photolysis technique.

Electron transfer from 2Fe-2S to cyt c_1 was studied in an attempt to elucidate some of the factors controlling the conformational states of the Rieske iron-sulfur protein required for efficient reduction of cyt c_1 . The amplitude of the fast phase of cytochrome c_1 reduction is maximal in the presence of reduced QH₂ to maintain 2Fe-2S and cyt c_1 in the reduced state. As QH₂ is oxidized by successive laser flashes, the amplitude of the fast phase decreases as 2Fe-2S and cyt c_1 become partially oxidized. Addition of ascorbate restored the fast phase of electron transfer from 2Fe-2S to cyt c_1 , even when no reduced quinol was present and cyt b_H was fully oxidized. Furthermore, addition of myxothiazol did not affect the rate constant of the fast phase. X-ray diffraction studies of the bovine enzyme indicate that binding myxothiazol to the Q_o site decreases the fraction of Rieske iron-sulfur protein in the b state (7). The present results suggest that the fast phase of electron transfer may only involve Rieske iron-sulfur protein that is initially in the c_1 state or is undergoing rapid conformational changes between an ensemble of states involving the free state and the c_1 state.

The role of the 2Fe-2S ligand His-161 in electron transfer from quinol to 2Fe-2S has been extensively investigated (27, 39-41). The pH dependence of the redox potential of 2Fe-2S has been interpreted as shown in Scheme 4. His-161 has a very high p*K* value when the iron-sulfur center is reduced and is fully protonated up to pH 9.5. However, His-161 has a p*K*_a of 7.5 when the iron-sulfur center is oxidized (27, 41). The redox potential of the iron-sulfur center is +315 mV when His-161 is protonated at low pH and decreases as His-161 is deprotonated at higher pH (27). Electron transfer from quinol to 2Fe-2S in the Q_o site is coupled to proton transfer from quinol to unprotonated His-161, accounting for the pH dependence of the reaction (27, 39-41). However, much less is

known about the deprotonation of the His-161 ligand after Rieske iron-sulfur protein rotates to the c_1 state and reduces cyt c_1 . If electron transfer from 2Fe-2S to cyt c_1 is coupled to deprotonation of the 2Fe-2S His-161 ligand, then a large dependence on pH would be predicted. Using the equilibrium pH-dependent redox potential of the iron-sulfur center (27) to calculate the driving force ΔG^0 , Marcus theory predicts the pH dependence as shown in the *dashed line* of Fig. 4. However, very little pH dependence was observed for the fast phase of electron transfer from 2Fe-2S to cyt c_1 (Fig. 4), indicating that the reaction is not rate-limited by deprotonation of His-161. Two possible explanations for the small pH dependence of the rate of cyt c_1 reduction will be considered. The first explanation is that proton release occurs after the rate-limiting electron transfer step in the mechanism of Scheme 4 and does not affect the rate constant. In this case the driving force used in the Marcus equation should be calculated from the redox potential of the protonated form, +315 mV, which is independent of pH. With this assumption, Marcus theory is in good agreement with the experimental pH dependence of the rate constant, using an r value of 9.4 Å (Fig. 4). The second explanation is that the observed rate of reduction of cyt c_1 is not limited by electron transfer at all but, rather, is limited by conformational gating (42, 43). This would require that dynamic fluctuations, in the conformation of the Rieske iron-sulfur protein between an electron transfer-active c_1 state and other inactive states, control the observed rate of reduction. It is not possible to distinguish between the two explanations suggested above on the basis of the pH dependence studies alone.

Temperature dependence studies are useful in determining whether electron transfer is rate-limited by conformational gating or by an actual electron transfer step

(43). The temperature dependence of the rate constant for electron transfer from 2Fe-2S to cyt c_1 is in good agreement with the predictions of Marcus theory for electron transfer (Fig. 5). The value of the reorganization energy λ obtained from fitting Equation 2 to the data of Fig. 5 is 0.75 eV, which is in the range expected for electron transfer between an iron-sulfur protein and a cytochrome (31-33). The fitted value of r , 11.1 Å, is quite reasonable for the distance between the Rieske iron-sulfur center and the cyt c_1 heme in the c_1 state (4-7). Moreover, the value of the electronic coupling constant H_{AB} , 1.31 cm^{-1} , obtained by fitting Equation 1 to the data is consistent with a nonadiabatic electron transfer mechanism (31, 43). However, the activation parameters $\Delta H^\ddagger = +17.6 \text{ kJ/mol}$ and $\Delta S^\ddagger = -91.1 \text{ J/mol}\cdot\text{K}$ obtained by fitting the temperature dependence data with the Eyring transition state theory are also compatible with a conformational gating mechanism (42, 43). Thus, it is not possible to distinguish between the two mechanisms for the reaction from the temperature dependence studies.

One of the most useful methods for characterizing electron transfer reactions is by measuring the effect of driving force on the rate constant (31, 32). If the reaction is controlled by a true electron transfer step, then the rate constant should depend on the driving force according to Equation 2. The effect of driving force on electron transfer in yeast cyt bc_1 has been studied using the Rieske iron-sulfur protein mutants Y185W, S183A, and Y185F/S183A, which have 2Fe-2S redox potentials that are lower than that of wild-type bc_1 by 90, 130, and 180 mV, respectively (44). The decrease in redox potential of the mutants is presumably due to removal of the hydrogen bonds between the hydroxyl group of Ser-183 and S-1 of the 2Fe-2S cluster and the hydroxyl group of Tyr-185 and S^γ of Cys-159 (Fig. 6). These yeast mutations decrease the steady-state enzyme

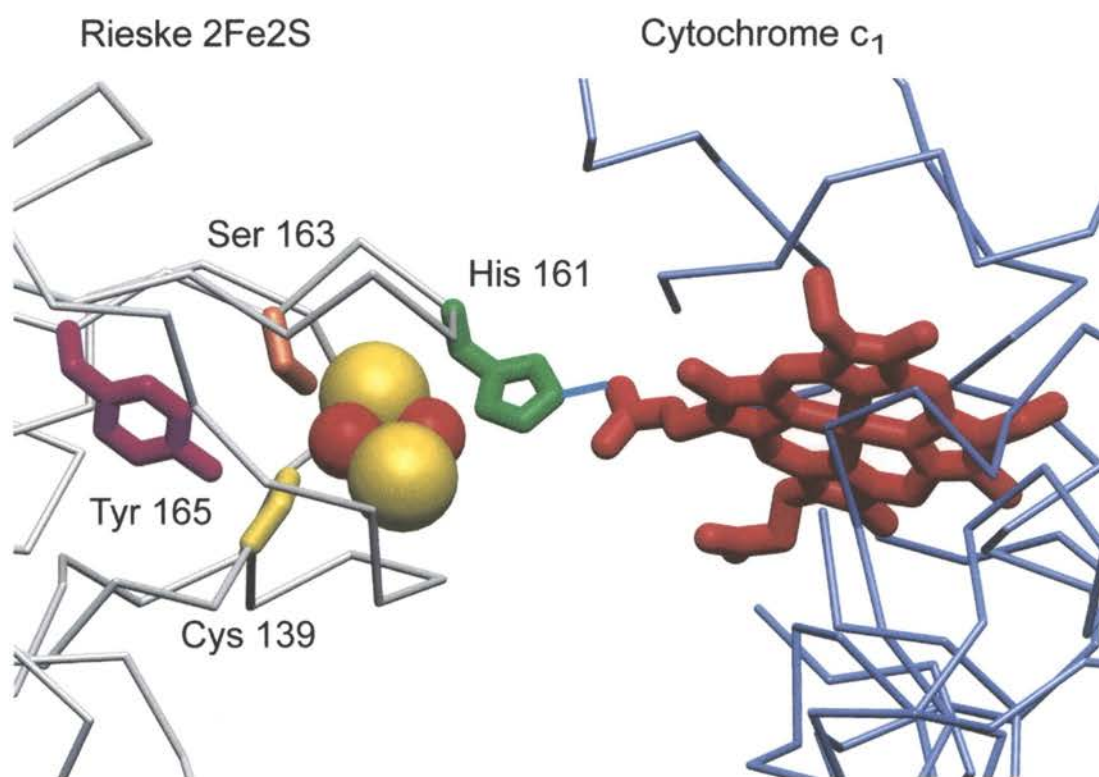


Fig. 6. Structure of bovine cyt bc_1 P6₅22 crystals in the c_1 state. The Rieske and cyt c_1 subunits are colored *gray* and *blue*, respectively, the 2Fe-2S center is shown as a CPK model colored *red/yellow*, and heme c_1 is colored *red*. Tyr-165, Ser-163, His-161, and Cys-139 are shown as *sticks*. Tyr-165, Ser-163, and Cys-139 in bovine Rieske protein are homologous to Tyr-185, Ser-183, and Cys-159 in yeast and Tyr-156, Ser-154, and Cys-130 in *R. sphaeroides*. A *blue line* indicates a hydrogen bond between the Nε2 nitrogen of His-161 and the heme c_1 propionate oxygen, with a separation of 2.96 Å.

activity to 30%, 10%, and 2% that of wild-type, respectively, consistent with decreases in the rate of the reaction between QH_2 and 2Fe-2S due to decreases in driving force (44). Mutation of the homologous residues in the *P. denitrificans* Rieske iron-sulfur protein led to similar decreases in redox potential and steady-state activity (45). Guergova-Kuras *et al.* (39) found that the Y156W mutation in the Rieske iron-sulfur protein of *R. sphaeroides* cyt bc_1 decreased the redox potential by 114 mV at low pH, and increased the pK of the 2Fe-2S ligand His-161 by 1 pH unit. The rate constant for electron transfer from quinol to 2Fe-2S was decreased to 7% that of wild-type by the Y156W mutation, suggesting that this reaction is controlled by proton-coupled electron transfer. In the present studies, the redox potentials of the Y156W, S154A, and S154A/Y156F *R. sphaeroides* mutants were decreased by 62, 109, and 159 mV, respectively, at pH 8.0 compared with that of the wild-type Rieske iron-sulfur protein. 2Fe-2S and cyt c_1 have the same redox potential in wild-type cyt bc_1 at pH 8.0, so the above mutations will significantly increase the driving force for electron transfer from 2Fe-2S to cyt c_1 . Based on Marcus theory calculations using Equation 2, these mutations would be predicted to increase the rate constant for electron transfer from 2Fe-2S to cyt c_1 by 3.3-, 8-, and 17-fold, respectively (Table I). The absence of a significant correlation between the rate constants and the driving force for these mutants indicates that the reaction is not rate-limited by the actual electron transfer event. The discrepancy between the prediction of Marcus theory and the experimentally determined rate constants of the mutants cannot be accounted for by using different values for the Marcus parameters. Changing the value of r simply changes the predicted rate constants of all the mutants by the same amount, whereas changing the value of λ over a reasonable range of 0.7-1.0 eV has a very small

effect on the relative rate constants. The larger rate constant for the Y156W mutant is probably due to a subtle conformational effect.

Taken together, the effects of temperature, pH, and driving force indicate that the electron transfer reaction from 2Fe-2S to cyt c_1 is not rate-limited by true electron transfer but, rather, by some type of dynamic fluctuation in the conformation of the Rieske iron-sulfur protein. If the fluctuations are rapid compared with the rate of electron transfer in an "active" c_1 state, then the observed rate constant is $k_{\text{obs}} = fk_{\text{et}}$, where f is the fraction of molecules in the active c_1 state and k_{et} is the true rate of electron transfer in the c_1 state (43). In this case electron transfer is said to be "conformationally coupled." A recent molecular dynamics simulation suggested that conformational changes in the Rieske iron-sulfur protein from the b state to the c_1 state may occur within 1 ns, which is consistent with the rapid fluctuation model (46). However, the observed rate constant in the conformational coupling case should be affected just as much by changes in the driving force as the true rate of electron transfer, k_{et} (43). Therefore, it appears that electron transfer from 2Fe-2S to cyt c_1 is "conformationally gated." In this case, if the fluctuations are slow compared with electron transfer in the active c_1 state and the population of the c_1 state is small, then the observed rate constant is limited by the rate of the fluctuations and there will be no dependence on the driving force (42, 43). One requirement for this mechanism is that the rate constant for electron transfer in the active c_1 state must be much larger than the observed rate constant. The active c_1 state may be represented by the bovine P6₅22 crystal structure reported by Iwata *et al.* (6), in which the N ϵ 2 nitrogen of His-161 forms a hydrogen bond with the heme c_1 propionate oxygen, with a separation of 2.96 Å (Fig. 6). This provides a direct pathway for electron transfer from the 2Fe-2S

center to the edge of the heme c_1 macrocycle with just four covalent bonds and one hydrogen bond between the His-161 nitrogen and the heme c_1 C3D atom (Fig. 6). The distance from the His-161 N ϵ 2 nitrogen to the heme c_1 macrocycle atom C3D is 7.8 Å (Fig. 6). This distance is somewhat larger (8.2 Å) in the bovine P6₅22 structure reported by Zhang *et al.* (5). The rate constant was calculated from the Marcus equation (Equation 2) to range from 1.5×10^6 to $3 \times 10^7 \text{ s}^{-1}$ assuming $r = 7.8 \text{ Å}$ and λ values between 1.0 and 0.7 eV. Therefore, it appears that the rate constant for electron transfer in the active c_1 state could be considerably faster than the observed value of $8 \times 10^4 \text{ s}^{-1}$. The conformational gating mechanism also requires that the population of the active c_1 state be small. Crystal packing forces in the P6₅22 crystals may constrain the Rieske iron-sulfur protein into a position closer to cyt c_1 than the average position in solution (5, 6). It is significant that the distance between 2Fe-2S and heme c_1 is considerably larger in chicken bc_1 crystals (14.4 Å) (5), and most of the Rieske iron-sulfur protein appears to be conformationally mobile in the bovine I4₁22 crystals (4). The present studies indicate that the experimental rate constant of $80,000 \text{ s}^{-1}$ is governed by the rate of fluctuations between one or more conformations that are inactive in electron transfer and an active c_1 state with a low occupancy. It is not known whether these fluctuations involve the whole ensemble of conformations ranging from the b state to the c_1 state or a smaller ensemble of conformations including the free state and the active c_1 state. It is interesting that a much slower rate of electron transfer from 2Fe-2S to cyt c_1 was observed in pH jump stopped-flow experiments involving *R. sphaeroides* cyt bc_1 (9). The slower rate of electron transfer observed in the pH jump experiments might be rate-limited by a conformational change from the b state to the c_1 state, whereas the fast rate observed in

the ruthenium experiments is associated with fluctuations in an ensemble of conformations, including the free state and the active c_1 state.

REFERENCES

1. Trumpower, B. L., and Gennis, R. B. (1994) *Annu. Rev. Biochem.* **63**, 675-716.
2. Trumpower, B. L. (1990) *J. Biol. Chem.* **265**, 11409-11412.
3. Brandt, U. (1998) *Biochim. Biophys. Acta* **1364**, 261-268.
4. Xia, D., Yu, C.-A., Kim, H., Xia, J.-Z., Kachurin, A. M., Zhang, L., Yu, L., and Deisenhofer, J. (1997) *Science* **277**, 60-66.
5. Zhang, Z., Huang, L., Shulmeister, V. M., Chi, Y.-I., Kim, K. K., Hung, L.-W., Crofts, A. R., Berry, E. A., and Kim, S.-H. (1998) *Nature* **392**, 677-684.
6. Iwata, S., Lee, J. W., Okada, K., Lee, J. K., Wata, M., Rasmussen, B., Link, T. A., Ramaswamy, S., and Jap, B. K. (1998) *Science* **281**, 64-71.
7. Kim, H., Xia, D., Yu, C.-A., Xia, J.-Z., Kachurin, A. M., Zhang, L., Yu, L., and Deisenhofer, J. (1998) *Proc. Natl. Acad. Sci. U. S. A.* **95**, 8026-8033.
8. Hunte, C., Koepke, J., Lange, C., Rossmann, T., and Michel, H. (2000) *Struct. Fold Des.* **8**, 669-684.
9. Xiao, K., Yu, L., and Yu, C.-A. (2000) *J. Biol. Chem.* **275**, 38597-38604.
10. Tian, H., Yu, L., Mather, M. W., and Yu, C.-A. (1998) *J. Biol. Chem.* **273**, 27953-27959.
11. Tian, H., White, S., Yu, L., and Yu, C.-A. (1999) *J. Biol. Chem.* **274**, 7146-7152.
12. Sadoski, R. C., Engstrom, G., Tian, H., Zhang, L., Yu, C.-A., Yu, L., Durham, B., and Millett, F. (2000) *Biochem.* **39**, 4231-4236.
13. Darrouzet, E., Valkova-Valchanova, M., and Daldal, R. (2000) *Biochemistry* **39**, 15474-15483.

14. Nett, J. H., Hunte, C., and Trumpower, B. L. (2000) *Eur. J. Biochem.* **267**, 5777-5782.
15. Gosh, M., Wang, C., Ebert, E., Vadlamuri, S., and Beattie, D. S. (2001) *Biochemistry* **40**, 327-335.
16. Darrouzet, E., Valkova-Valchanova, M., and Daldal, F. (2002) *J. Biol. Chem.* **277**, 3463-3470.
17. Darrouzet, E., and Daldal, F. (2002) *J. Biol. Chem.* **277**, 3471-3476.
18. Brugna, M., Rodgers, S., Schricker, A., Montoya, G., Kazmeier, M., Nitschike, W., and Sinning, I. (2000) *Proc. Nat. Acad. Sci. US.* **97**, 2069-2074.
19. Meinhardt, S. W., and Crofts, A. R. (1982) *FEBS Lett.* **149**, 223-227.
20. Crofts, A. R., and Wang, Z. (1989) *Photosynth. Res.* **22**, 69-87.
21. Downard, A. J., Honey, G. E., Phillips, L. F., and Steel, P. J. (1991) *Inorg. Chem.* **30**, 2259-2260.
22. Yu, C. A., and Yu, L. (1982) *Biochemistry* **21**, 4096-4101.
23. Yu, L., and Yu, C. A. (1982) *J. Biol. Chem.* **257**, 2016-2021.
24. Moeller, T., Ed. (1957) *Inorganic Synthesis*, Vol. V, p. 185, McGraw Hill Book Company, Inc., New York
25. Mather, M. W., Yu, L., and Yu, C. A. (1995) *J. Biol. Chem.* **270**, 28668-28675.
26. Link, T. A., Hatzfeld, O. M., Unalkat, P., Shergill, J. K., Cammack, R., and Mason, J. R. (1996) *Biochemistry* **35**, 7546-7552.
27. Ugulava, N. B., and Crofts, A. R. (1998) *FEBS Lett.* **440**, 409-413.
28. Zhang, L., Tai, C.-H., Yu, L., and Yu, C. A. (2000) *J. Biol. Chem.* **275**, 7656-7661.
29. Yu, L., Dong, J. H., and Yu, C. A. (1986) *Biochim. Biophys. Acta* **852**, 203-211.

30. Heacock, C., Liu, R., Yu, C.-A., Yu, L., Durham, B., and Millett, F. (1993) *J. Biol. Chem.* **268**, 27171-27175.
31. Marcus, R. A., and Sutin, N. (1985) *Biochim. Biophys. Acta* **811**, 265-322.
32. Moser, C. C., Keske, J. M., Warncke, K., Farid, R. S., and Dutton, P. L. (1992) *Nature* **355**, 796-802.
33. Scott, J. R., McLean, M., Sligar, S. G., Durham, B., and Millett, F. (1994) *J. Am. Chem. Soc.* **116**, 7356-7362.
34. Shinkarev, V. P., Crofts, A. R., and Wright, C. A. (2001) *Biochemistry* **40**, 12584-12590.
35. Willie, A., Stayton, P. S., Sligar, S. G., Durham, B., and Millett, F. (1992) *Biochemistry* **31**, 7237-7243.
36. Wang, K., Mei, H., Geren, L., Miller, M. A., Saunders, A., Wang, X., Waldner, J. L., Pielak, G. J., Durham, B., and Millett, F. (1996) *Biochemistry* **35**, 15107-15119.
37. Geren, L. M., Beasley, J. R., Fine, B. R., Saunders, A. J., Hibdon, S., Pielak, G. J., Durham, B., and Millett, F. (1995) *J. Biol. Chem.* **270**, 2466-2472.
38. Tian, H., Sadoski, R., Zhang, L., Yu, C.-A., Yu, L., Durham, B., and Millett, F. (2000) *J. Biol. Chem.* **275**, 9587-9595.
39. Guergova-Kuras, M., Duras, R., Ugalava, N., Hadad, I., and Crofts, A. R. (2000) *Biochemistry* **39**, 7436-7444.
40. Hong, S., Ugalava, N., Guergova-Kuras, M., and Crofts, A. R. (1999) *J. Biol. Chem.* **274**, 33931-33944.
41. Link, T. A. (1994) *Biochim. Biophys. Acta* **1185**, 81-84.
42. Hoffman, B. M., and Ratner, M. A. (1987) *J. Am. Chem. Soc.* **109**, 6237-6243.

43. Davidson, V. L. (1996) *Biochemistry* **35**, 14035-14039.
44. Denke, E., Merbitz-Zahradnik, T., Hatzfeld, O. M., Snyder, C. H., Link, T. A., and Trumpower, B. L. (1998) *J. Biol. Chem.* **273**, 9085-9093.
45. Schroter, T., Hatzfeld, O. M., Gemeinhardt, S., Korn, M., Friedrich, T., Ludwig, B., and Link, T. A. (1998) *Eur. J. Biochem.* **255**, 100-106.
46. Izrailev, S., Crofts, A. R., Berry, E. A., and Schluten, K. (1999) *Biophys. J.* **77**, 1753-1768.

CHAPTER V

Effect of Famoxadone on Photoinduced Electron Transfer between the Iron-Sulfur Center and Cytochrome c_1 in the Cytochrome bc_1 Complex

Kunhong Xiao, Gregory Engstrom, Sany Rajagukguk, Chang-An Yu,
Linda Yu, Bill Durham, and Francis Millett

The Journal of Biological Chemistry, 278, 11419-26 (2003)

ABSTRACT

Famoxadone is a new cytochrome bc_1 Q_0 site inhibitor that immobilizes the iron-sulfur protein (ISP) in the b conformation. The effects of famoxadone on electron transfer between the iron-sulfur center (2Fe-2S) and cyt c_1 were studied using a ruthenium dimer to photoinitiate the reaction. The rate constant for electron transfer in the forward direction from 2Fe-2S to cyt c_1 was found to be $16,000\text{ s}^{-1}$ in bovine cyt bc_1 . Binding famoxadone to the Q_0 site decreased this rate constant to $1,480\text{ s}^{-1}$, consistent with a decrease in mobility of the ISP. Reverse electron transfer from cyt c_1 to 2Fe-2S was found to be biphasic in bovine cyt bc_1 , with rate constants of $90,000\text{ s}^{-1}$ and $7,300\text{ s}^{-1}$. In the presence of famoxadone, reverse electron transfer was monophasic, with a rate constant of $1,420\text{ s}^{-1}$. It appears that the rate constants for release of the oxidized and reduced ISP from the b conformation are the same in the presence of famoxadone. The effects of famoxadone binding on electron transfer were also studied in a series of *R. sphaeroides* cyt bc_1 mutants involving residues at the interface between the Rieske protein and cyt c_1 and/or cyt b .

INTRODUCTION

The cytochrome bc_1 complex (ubiquinol:cytochrome c oxidoreductase) is an integral membrane protein in the electron transport chains of mitochondria and many respiratory and photosynthetic prokaryotes (1). The complex translocates four protons to the positive side of the membrane per two electrons transferred from ubiquinol to cyt c in a Q-cycle mechanism (2). A key bifurcated reaction occurs at the Q_o -site, in which the first electron is transferred from ubiquinol to the Rieske iron-sulfur center (2Fe-2S), and then to cyt c_1 and cyt c (1-3). The second electron is transferred from semiquinone in the Q_o site to cyt b_L and then to cyt b_H and ubiquinone in the Q_i site. Q_o site inhibitors can be divided into three classes. Class Ia inhibitors such as myxothiazol and MOA-stilbene alter the heme spectrum of cyt b_L , class Ib inhibitors such as UHDBT alter the EPR spectrum of 2Fe-2S, and class Ic inhibitors such as stigmatellin alter both (1-3). X-ray crystallographic studies have revealed that these different classes of inhibitors occupy different subsites in the Q_o pocket, and have different effects on the mobility of the extramembrane domain of the Rieske iron-sulfur protein (ISP) (4-8). Stigmatellin binding increases the midpoint redox potential E_m of 2Fe-2S by about 200-250 mV (9), and immobilizes the ISP in the b conformation with the His-161 ligand on reduced 2Fe-2S in hydrogen-bonding contact with stigmatellin in the Q_o site (4-8). In contrast, MOA-stilbene binding to the Q_o site completely eliminates the anomalous scattering signal for 2Fe-2S close to cyt b_L , indicating release of the ISP from the b conformation to a mobile state (7). These studies led to the proposal that the ISP functions as a mobile shuttle as it transfers an electron from QH_2 in the Q_o site to cyt c_1 (4-8). Experimental support for the

mobile shuttle mechanism has been obtained from cross-linking and mutational studies that immobilize the ISP or alter the conformation of the neck region (10-19).

Famoxadone and azoxystrobin are new Q_o site inhibitors that have significantly different effects on *cyt bc*₁ than other Q_o site inhibitors (20-22). X-ray crystallographic studies revealed that famoxadone binding in the Q_o site is stabilized by a network of interactions between the three aromatic groups on famoxadone and aromatic residues in the binding pocket (23) (Figure 1A). Famoxadone binding leads to extensive conformational changes on the surface of *cyt b*, and triggers a long-range conformational change in the ISP from the mobile state to a state with 2Fe-2S proximal to *cyt b* (23). In contrast to stigmatellin, famoxadone increases the E_m of 2Fe-2S by only 26 mV, and immobilizes both the oxidized and reduced ISP in the *b* conformation (unpublished results). This is consistent with the finding that famoxadone is more deeply buried in the Q_o site than stigmatellin, and does not form a hydrogen bond with the His-161 ligand on reduced 2Fe-2S (5,8,23). Azoxystrobin also immobilizes the ISP in the *b* conformation, but has only a minor effect on the E_m of 2Fe-2S, decreasing it by 24 mV (unpublished results).

In the present paper the effects of famoxadone and azoxystrobin on electron transfer between the Rieske iron-sulfur center and *cyt c*₁ are studied using the binuclear ruthenium complex, Ru₂D, to rapidly photooxidize or photoreduce *cyt c*₁ (10). Binding famoxadone to the Q_o site of bovine *cyt bc*₁ decreased the rate constant for electron transfer from 2Fe-2S to *cyt c*₁ from 16,000 s⁻¹ to 1,480 s⁻¹, consistent with a decrease in mobility of ISP. Famoxadone binding also decreased the rate constant for reverse

electron transfer from cyt c_1 to 2Fe-2S to $1,420 \text{ s}^{-1}$, indicating that the rate constants for release of oxidized and reduced ISP from the b conformation are the same in the presence of famoxadone. Famoxadone binding was also found to decrease the rate of electron transfer from 2Fe-2S to cyt c_1 in *R. sphaeroides* cyt bc_1 as well as mutants involving residues at the interface between the Rieske protein and cyt c_1 and/or cyt b .

EXPERIMENT PROCEDURES

Materials---Ru₂D was prepared by a modification of the method of Downard et al. (24). Bovine cyt bc_1 was purified as described by Yu et al. (25). Native and mutant *R. sphaeroides* cyt bc_1 were prepared as described by Tian et al. (11). Paraquat, succinate, TMPD, *p*-benzoquinone and antimycin A were obtained from Sigma, stigmatellin was purchased from Fluka, and $[\text{Co}(\text{NH}_3)_5\text{Cl}]^{2+}$ was synthesized (26). N-Dodecyl- β -D-maltoside was obtained from Anatrace. Succinate cytochrome c reductase (SCR) was purified as previously described (27).

Generation and Expression of *R. sphaeroides* Cyt bc_1 Mutants---Mutations were constructed by site-directed mutagenesis using the Altered Sites system from Promega. The single stranded pSELNB3503 (28) was used as the template for mutagenesis, and oligonucleotides used were as follows: K70C (ISP),

GTCAAGTTCCTCGGCTGCCCGATCTTCATCCGCCGCCGCACCGAGGCCGACAT
CG;

D143C (ISP), GGCGGCGTGTCTGGGTTGCTTCGGGGGCTGGTTCT;

F148C (ISP), GGGGGCTGGTGCTGCCCT;

P150C (ISP), TTCGGGGGCTGGTTCTGCTGCTGCCACGGATCGCACTA;
G153C (ISP), TGGTTCTGCCCCTGCCACTGCTCGCACTACGACAGTGCC;
S154A (ISP), CCCTGCCACGGAGCGCACTACGACAGT;
Y156W (ISP), CACGGATCGCACTGGGACAGTGCCGGCCGTA;
K164C (ISP), ACAGTGCCGGCCGTATCCGGTGCGGCCCGCGCCCGAGAACC;
P166C (ISP), CGTATCCGGAAGGGCTGCGCGCCCGAGAACCTG;
V64C (*cytb*), GTCACCGGCATCTGCCTTGCGATGCAT;
G89C (*cytb*), AACGTGAACTGCGGCTTCATGCT;
M92C(*cytb*), AACGGCGGCTTCTGCCTGCGCTACCTGCATGC;
A185C (*cytb*), GCTGCTCGGCGGCCCGTGCGTGGACAATGCCA;
Y302C (*cytb*), CTGCCCTTCTGCGCGATCCTGCGCGC;
I326C (*cytb*),
CATCAGCTTCGGCATCTGCGACGCCAAGTTCTTCGGCGTGCTCGCGATGT;
K70C(ISP)/A185C(*cytb*),
GTCAAGTTCCTCGGCTGCCCCGATCTTCATCCGCCGCCGCACCGAGGCCGACAT
CG/G
CTGCTCGGCGGCCCGTGCGTGGACAATGCCA;
P33C(ISP)/G89C(*cytb*), GGGGCCGCCGTCTGGTGCCTGATCAACCAAATG/
AACGTGAACTGCGGCTTCATGCT;
N36C(ISP)/G89C(*cytb*), TGGCCGCTGATCTGCCAAATGAATCCGTC/
AACGTGAACTGCGGCTTCATGCT.

A plate-mating procedure (28) was used to mobilize the pRKD $bc_1F_mB_mCHQ$ plasmid in *E. coli* S17-1 cells into *R. sphaeroides* BC17 cells as previously described (12). Growth of *E. coli* cells and plasmid-bearing *R. sphaeroides* cells was carried out as previously described (12). As previously described, the identity of the mutations was confirmed by DNA sequencing before and after photosynthetic or semi-aerobic growth of the cells (12). Mutant cytochrome bc_1 was purified as described by Xiao et al. (12).

Determination of Enzyme Activity and Redox Potential of the 2Fe-2S Cluster in

Mutant Cyt bc_1 --- The cyt bc_1 activity was determined in an assay mixture containing 100 mM of Na⁺ /K⁺ phosphate buffer, pH 7.4, 300 μ M of EDTA, 100 μ M of cyt c , and 25 μ M of Q₂H₂ at 23 °C using the method described by Xiao et al. (12). The redox potentials of 2Fe-2S in cyt bc_1 mutants were determined as previously described (12). Reduction of cyt c_1 was followed by measuring the increase of the α -absorption (553-545 nm) in a Shimadzu UV2101 PC spectrophotometer. Reduction of 2Fe-2S was followed by measuring the negative circular dichroism (CD) peak, at 500 nm, of partially reduced complex minus fully oxidized complex in a JASCO J-715 spectropolarimeter (29-31). The same samples were used for the absorption and CD measurements. The redox potentials of 2Fe-2S were calculated from the redox states of heme c_1 and 2Fe-2S, at pH 8.0, using 280 mV for the midpoint redox potential of heme c_1 (32).

Flash Photolysis Experiments--- Transient absorbance measurements were carried

out by flash photolysis of 300 μ L solutions contained in a 1-cm glass semimicrocuvette. The excitation light flash was provided by a Phase R model DL1400 flash lamp-pumped dye laser using coumarin LD 490 to produce a 480 nm light flash of < 0.5 μ s duration.

The detection system has been described by Heacock *et al.* (33). Samples typically contained 5 μM cyt bc_1 in a buffer with 0.01% dodecylmaltoside. In photoreduction experiments, 10 mM aniline and 1 mM 3CP were used as sacrificial donors, and catalytic concentrations of horse cyt c and bovine cyt oxidase (20 nM) were present to maintain cyt bc_1 in the oxidized state. In photooxidation experiments, paraquat or $[\text{Co}(\text{NH}_3)_5\text{Cl}]^{2+}$ were used as sacrificial acceptors, and 2,3-dimethoxy-5-methyl-6-(10-bromodecyl)-1,4-benzoquinol ($\text{Q}_0\text{C}_{10}\text{BrH}_2$) was used to reduce cyt bc_1 . In order to regenerate reduced quinol throughout the flash experiments, 1mM succinate and 50 nM of SCR were included. Redox mediators included *p*-benzoquinone ($\epsilon_m = +280$ mV) and TMPD ($\epsilon_m = +275$ mV) used in concentrations of 10 μM and 2 μM , respectively. The experiments were carried out aerobically, in order to rapidly reoxidize the highly absorbing reduced paraquat.

RESULTS AND DISCUSSION

Effects of Famoxadone and Azoxystrobin on Electron Transfer between 2Fe-2S

and Cyt c_1 in Bovine Cyt bc_1 --- An important goal towards understanding the mechanism of electron transfer in cyt bc_1 is to determine what factors control the conformation of the ISP in each state of the complex, the dynamics of the changes between the different conformations, and the rate of electron transfer in each of the conformations. X-ray crystallographic studies are providing valuable information on the conformations of the ISP, including the b conformation (Figure 1A), the c_1 conformation (Figure 1B), and intermediate and mobile conformations (4-8). However, it has been difficult to determine

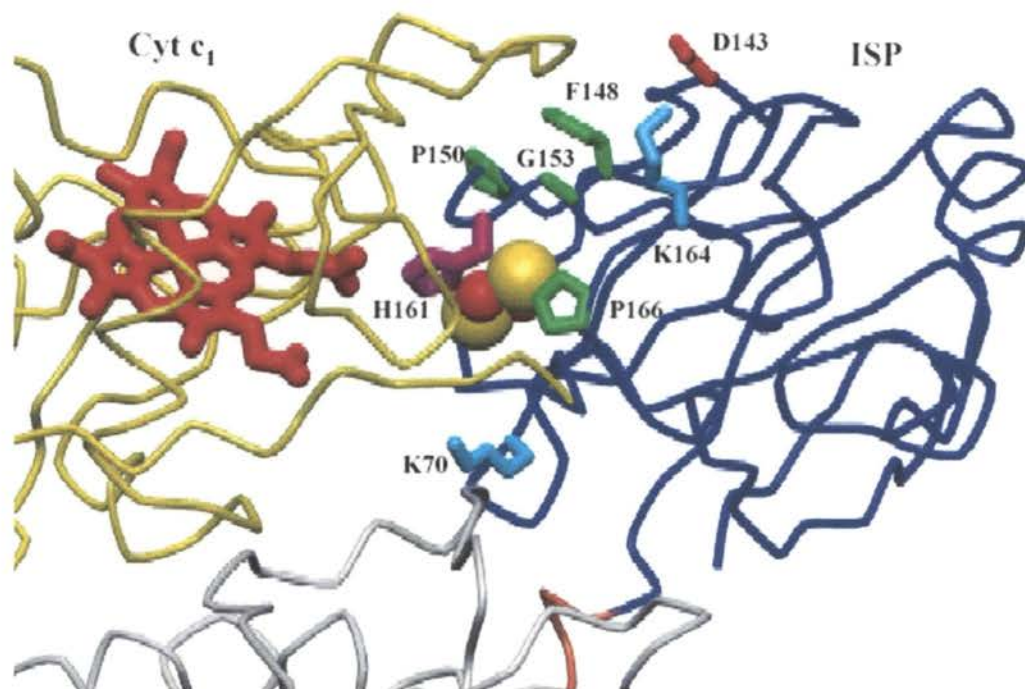


Figure 1B

Fig. 1. (B) X-ray crystal structure of bovine *cyt bc*₁ P6₅₂₂ crystals (*c*₁ conformation) (6). ISP is blue, *cyt c*₁ is yellow and the residues that were mutated are shown as sticks. *R. sphaeroides* numbering is used.

Table I

Spectral and Electrochemical Properties of Ruthenium Complexes

Complex	$E^0(\text{III/II})^a$	$E^0(\text{II/I})^a$	$E^0(\text{III/II}^*)^b$	$E^0(\text{II}^*/\text{I})^b$	$\lambda_{\text{max}}(\text{abs})^c$	$\lambda_{\text{max}}(\text{em})^d$
$\text{Ru}(\text{bpy})_3^{+2}$	1.26 V	-1.35 V	-0.87 V	0.78 V	452 nm	582 nm
Ru_2D	1.24 V	-1.10 V	-0.81 V	0.95 V	480 nm	605 nm

^aDetermined by cyclic voltammetry at a platinum disc working electrode in acetonitrile with respect to a saturated calomel reference electrode (24).

^bCalculated from the excited state energy and the ground state potential as described in (39).

^cRecorded in air-saturated 1 mM aqueous phosphate buffer, pH 7.

^dRecorded in 4:1 ethanol/methanol glass at 77 K.

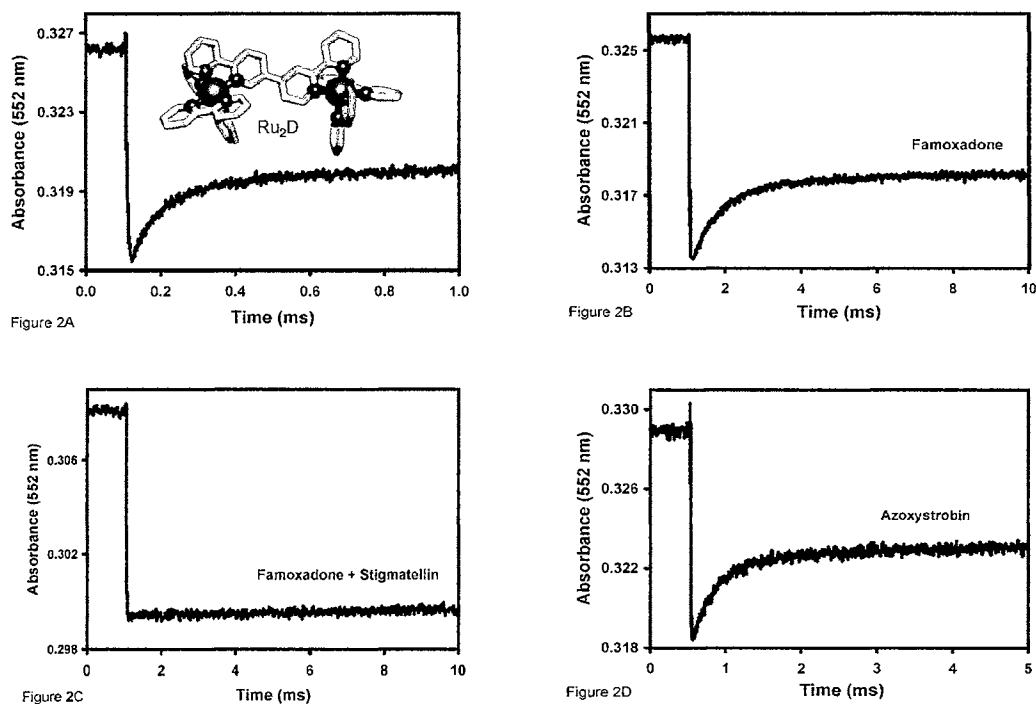
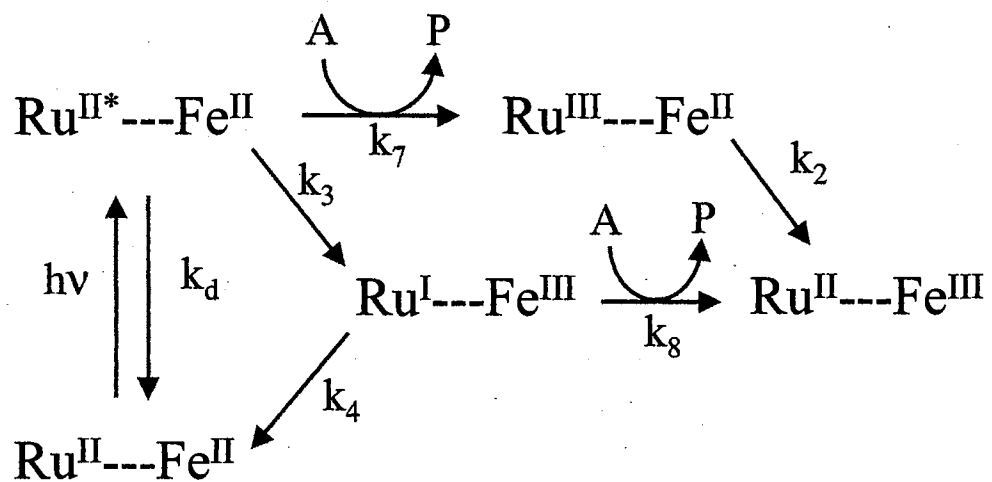


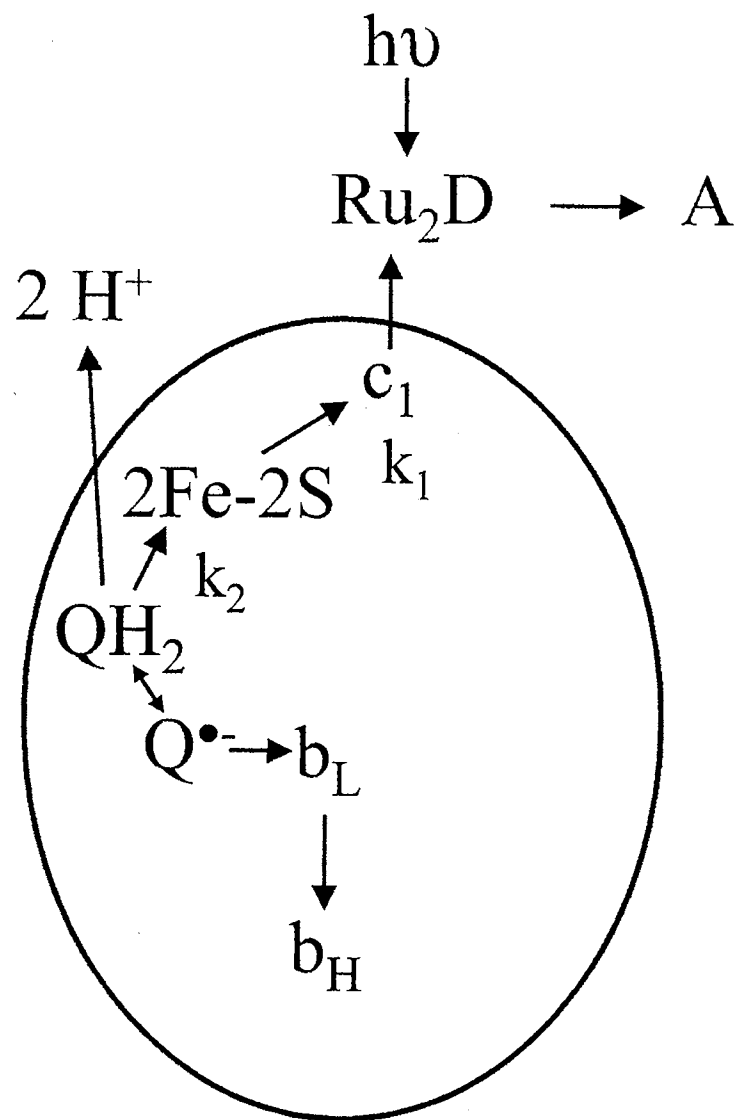
Fig. 2. Electron transfer from 2Fe₂S to cyt *c*₁ in bovine cyt *bc*₁ following photooxidation of cyt *c*₁. (A) A sample containing 5 μ M bovine cyt *bc*₁, 20 μ M Ru₂D and 10 mM paraquate in 20 mM TrisCl, pH 8 at 24 °C was treated with 10 μ M Q₀C₁₀Br, 1 mM succinate and 50 nM of SCR to reduce 2Fe-2S and cyt *c*₁. The sample was subjected to a 480 nm laser flash to photooxidize cyt *c*₁, and electron transfer from 2Fe₂S to cyt *c*₁ was followed at 552 nm. The smooth curve is a biphasic fit with rate constants of $16,000 \pm 3,000 \text{ s}^{-1}$ and $250 \pm 50 \text{ s}^{-1}$, and relative amplitudes of 66% and 34%. (Inset) Ru₂D, with ruthenium atoms represented by CPK models, and nitrogens by small balls. (B) Famoxadone (30 μ M) was added to the sample in (A) and subjected to a laser flash to photooxidize cyt *c*₁. Note the change in time scale. The monophasic transient has a rate constant of $1,480 \pm 250 \text{ s}^{-1}$. (C) Sigmatellin (45 μ M) was added to the sample in (B) and subjected to flash photolysis. (D). The sample in (A) was treated with 50 μ M axoxytrobilin and subjected to flash photolysis. The monophasic transient has a rate constant of $3,400 \pm 600 \text{ s}^{-1}$.

the kinetics of electron transfer from 2Fe-2S to cyt c_1 (34, 35), as well as the dynamics of ISP conformational changes. The development of the ruthenium photoreduction method provides an opportunity to measure electron transfer between 2Fe-2S and cyt c_1 in both the forward and reverse directions, and thus provide kinetic information on two different initial redox states of cyt bc_1 (10). Moreover, it is becoming clear that measured rates of electron transfer are probably rate-limited by conformational changes in the ISP (36). The binuclear complex Ru₂D contains the 2,2':4',4'':2'',2'''-quaterpyridine ligand which bridges the two ruthenium atoms (Figure 2A inset) (24). Ru₂D has a charge of +4, which allows it to bind with high affinity to the negatively charged domain on cyt c_1 (10). The electrochemical properties of Ru₂D are similar to those of the widely used ruthenium trisbipyridine complex (Table 1). The metal-to-ligand excited state of Ru₂D, with a lifetime of 0.5 μ s, is both a strong oxidant and a strong reductant, and can rapidly oxidize or reduce cyt c_1 in the presence of appropriate sacrificial electron acceptors or donors (10).

In order to study electron transfer in the forward direction, the ruthenium dimer Ru₂D was used to rapidly photooxidize cyt c_1 in bovine cyt bc_1 with cyt c_1 and 2Fe-2S initially reduced (Figure 2A). The excited state of Ru₂D oxidizes cyt c_1 within 1 μ s according to Scheme 1. Only one of the two ruthenium centers in Ru₂D is photoexcited in this experiment, and this one is represented in Scheme 1. The sacrificial electron acceptor paraquat was present in the solution to oxidize Ru(II*) and/or Ru(I). The rapid photooxidation of cyt c_1 shown by the initial decrease in 552 nm absorbance was followed by biphasic reduction of cyt c_1 with rate constants of $k_1 = 16,000 \pm 3,000 \text{ s}^{-1}$ and



Scheme 1



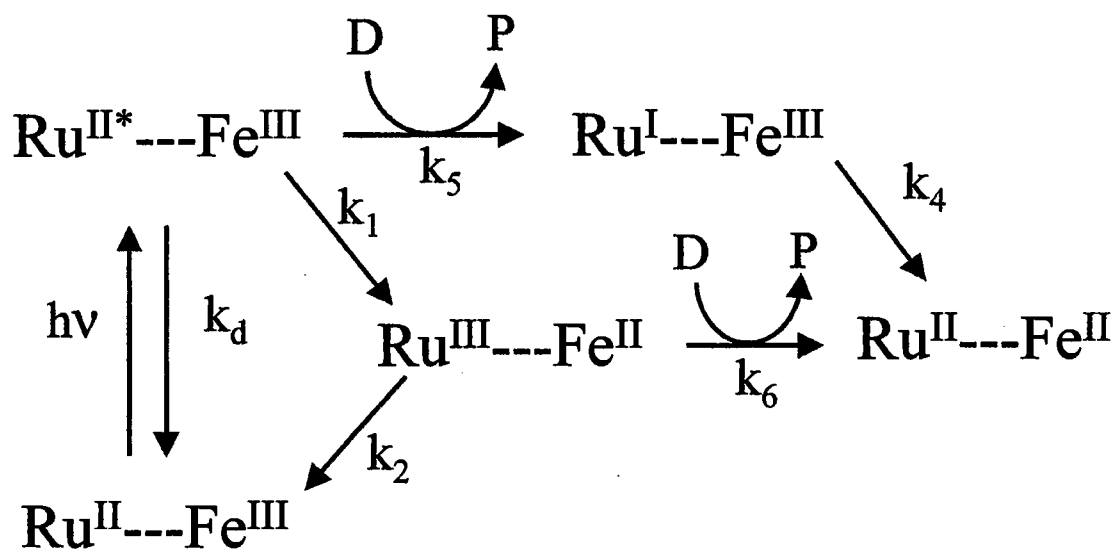
Scheme 2

$k_2 = 250 \pm 50 \text{ s}^{-1}$ (Figure 2A). The rate constant k_1 has been assigned to electron transfer from reduced 2Fe-2S to photooxidized cyt c_1 , while k_2 is correlated with the oxidant-induced reduction of cyt b_H (Scheme 2) (10). The rate constant k_2 thus represents electron transfer of the first electron from QH₂ to 2Fe-2S and cyt c_1 , followed rapidly by transfer of the second-electron from the semiquinone to cyt b_L and cyt b_H (10). The experimental rate constant k_1 is much smaller than the theoretical value predicted for electron transfer between 2Fe-2S and cyt c_1 in the crystallographic c_1 state, $1 \times 10^6 - 2 \times 10^7 \text{ s}^{-1}$ (5,10). It therefore appears that the measured rate constant for electron transfer is “gated” by changes in the conformation of the ISP (10). This interpretation is consistent with previous studies showing that k_1 has a large temperature dependence, with an activation energy of 59 kJ/mol (10). X-ray diffraction studies have indicated that the ISP is largely in the b conformation when both cyt c_1 and 2Fe-2S are reduced (37). Therefore, the rate constant of $16,000 \text{ s}^{-1}$ could represent the rate of the conformational change from the b state of the ISP to the c_1 state where rapid electron transfer can occur.

Addition of 30 μM famoxadone to bovine cyt bc_1 led to a single phase of reduction of photooxidized cyt c_1 with a rate constant of $1,480 \pm 250 \text{ s}^{-1}$, and no reduction of cyt b_H observed at 562 nm (Figure 2B). The rate constant was independent of the concentration of famoxadone over the range 10 μM to 100 μM , consistent with a large binding constant. These results indicate that famoxadone binds strongly to the Q_o site and decreases the rate constant for electron transfer from 2Fe-2S to cyt c_1 from $16,000 \text{ s}^{-1}$ to $1,480 \text{ s}^{-1}$. It appears that famoxadone binding significantly decreases the rate constant for the conformational change from the b state to the c_1 state. The amplitude of the 552 nm

transient for cyt c_1 reduction in the presence of famoxadone is 31% of the amplitude of the initial photooxidation, about the same as in the absence of famoxadone, 28%. Since 2Fe-2S and cyt c_1 have the same redox potentials at pH 8.0, electron transfer from 2Fe-2S to cyt c_1 would reach equilibrium with cyt c_1 50% reduced, and the amplitude of the cyt c_1 reduction would be expected to be 50% of the initial photooxidation. It is quite possible that the ISP is lost from a fraction of cyt bc_1 molecules during purification, accounting for the smaller amplitude of the observed cyt c_1 reduction. The similar reduction amplitudes in the presence and absence of famoxadone is consistent with the finding that famoxadone binding has only a small effect on the redox potential of 2Fe-2S, increasing it by 26 mV. Addition of stigmatellin completely eliminated the reduction of cyt c_1 , indicating that stigmatellin displaced famoxadone from the Q_o site and locked reduced ISP strongly in the b conformation (Figure 2C). This indicates that stigmatellin has a much higher affinity for the Q_o site than famoxadone. Addition of 30 μ M azoxystrobin to bovine cytochrome bc_1 resulted in a single phase of cyt c_1 reduction with a rate constant of $3,400 \pm 600 \text{ s}^{-1}$ (Figure 2D). This result is consistent with X-ray crystallographic studies showing that azoxystrobin binding immobilizes the ISP in the b conformation (unpublished results). Addition of 30 μ M stigmatellin to bovine cyt bc_1 treated with 30 μ M azoxystrobin led to elimination of cyt c_1 reduction, indicating that stigmatellin displaced azoxystrobin from the Q_o site.

In order to study reverse electron transfer from cyt c_1 to 2Fe-2S, Ru₂D was used to photoreduce cyt c_1 in oxidized bovine cyt bc_1 according to Scheme 3 (Figure 3). Electron transfer from excited-state Ru(II*) to cyt c_1 was complete in 1 μ s, the lifetime of the



Scheme 3

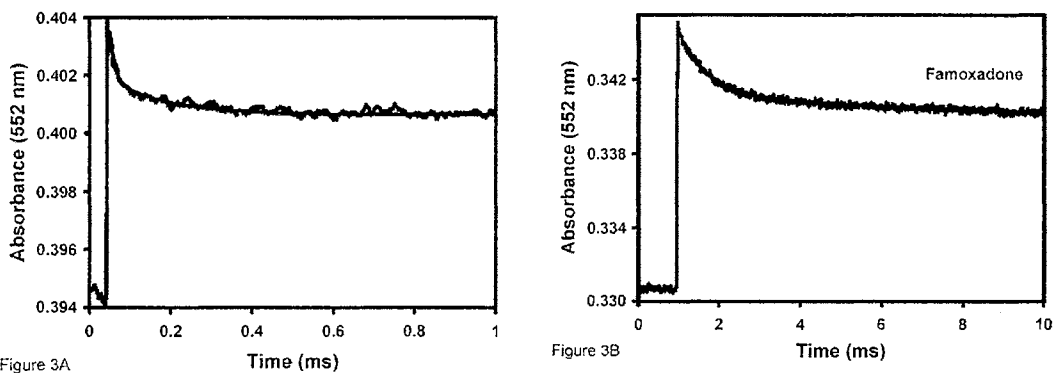


Fig. 3. Reverse electron transfer from *cyt c*₁ to 2Fe-2S in bovine *cyt bc*₁ following photoreduction of *cyt c*₁. (A) A sample containing 5 μM oxidized bovine *cyt bc*₁ and 25 μM Ru₂D in 5 mM sodium phosphate, pH 7.0, 10 mM aniline, 1 mM 3CP, and 0.01% lauryl maltoside at 24 °C was excited with a 480 nm laser flash to photoreduced *cyt c*₁. Electron transfer from *cyt c*₁ to 2Fe2S was followed at 552 nm. Catalytic concentrations (50 nM) of *cyt c* and *cyt oxidase* were present in the solution to reoxidize *cyt bc*₁ between flashes. The smooth curve is a biphasic fit with rate constants of $90,000 \pm 15,000 \text{ s}^{-1}$ and $7,300 \pm 1,200 \text{ s}^{-1}$ and relative amplitudes of 57% and 43%. (B) Famoxadone (30 μM) was added to the solution in (A) and subjected to flash photolysis. The monophasic transient has a rate constant of $1,420 \pm 200 \text{ s}^{-1}$.

excited state of Ru₂D. The sacrificial electron donors aniline and 3CP were present in the solution to reduce Ru(III). The photoreduction of cyt *c*₁ was followed by biphasic oxidation with rate constants of $90,000 \pm 15,000 \text{ s}^{-1}$ and $7,300 \pm 1,200 \text{ s}^{-1}$ and relative amplitudes of 57% and 43%, respectively (Figure 3A). The difference in kinetics compared with forward electron transfer is apparently due to the initial redox states of the enzyme. X-ray diffraction studies have indicated that a smaller fraction of ISP is in the *b* conformation in the fully oxidized complex than in the complex with cyt *c*₁ and 2Fe-2S reduced (37). It is reasonable to assign the fast phase to the mobile conformation of the ISP, and the slow phase to the conformation initially in the *b* state (10). With this assumption, the fast phase would be gated by fluctuations in conformation between the mobile state and the *c*₁ state, while the slow phase would be gated by the conformational change from the *b* state to the mobile state. Addition of famoxadone resulted in a single phase of cyt *c*₁ oxidation with a rate constant of $1,420 \pm 200 \text{ s}^{-1}$ (Figure 3B). The amplitude of the single phase in the presence of famoxadone was nearly the same as the sum of the two phases in the absence of inhibitor. This result is consistent with the finding that ISP is nearly all in the *b* conformation in the presence of famoxadone (23). The rate constant k_d for the change in conformation from the *b* state to the mobile state must therefore be much smaller than the rate constant k_f from the mobile state to the *b* state in the presence of famoxadone. The rate constant k_d is $1,420 \text{ s}^{-1}$ in the presence of famoxadone, while the rate constant k_f could be $90,000 \text{ s}^{-1}$ or even higher. It is interesting that the rate constants for forward and reverse electron transfer are the same in the presence of famoxadone. This indicates that the rate constant k does not depend on the redox state of 2Fe-2S,

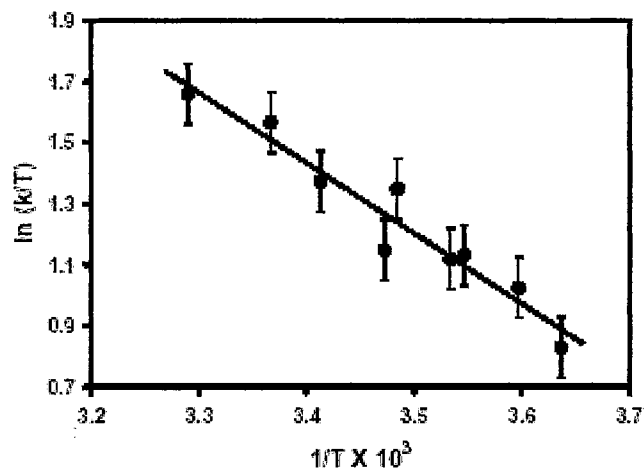


Fig. 4. Temperature dependence of rate constant for electron transfer from cyt c_1 to 2Fe-2S in bovine cyt bc_1 inhibited with famoxadone. The 552 nm transients were recorded under the same conditions as in Figure 3B. The solid line is the best fit to the Eyring equation: $\ln(k/T) = -\Delta H^\ddagger/RT + \Delta S^\ddagger/R + \ln(h/k_B)$ with $\Delta H^\ddagger = 19.1 \pm 1.8$ kJ/mol and $\Delta S^\ddagger = -121 \pm 6$ J/mol \cdot K.

consistent with the finding that famoxadone binding changes the redox potential of 2Fe-2S by only 26 mV. The temperature dependence of k_d gives activation parameters of $\Delta H^\ddagger = 19.1 \pm 1.8$ kJ/mol and $\Delta S^\ddagger = -121 \pm 6$ J/mol·K for the conformational change from the b state to the mobile state in the presence of famoxadone (Figure 4).

The present studies indicate that famoxadone binding significantly decreases the rate constant for release of the ISP from the b conformation in cyt *bc*₁. X-ray crystallography studies have revealed that famoxadone binding leads to significant conformational changes in three domains on the surface of cyt *b*: residues 163-171 which contact the neck region of the ISP, residues 262-268 in the *ef* loop which are part of the ISP docking crater, and residues 252-256 in the middle of the *ef* loop which connects the Q_o site to the other two surface domains (23) (Figure 1A). The *ef* loop may play a role in relaying famoxadone-induced conformational changes in the Q_o pocket to the ISP crater and the neck contact domain to decrease the rate of release of the ISP. The linkage between the conformation of the Q_o site and the dynamics of the ISP movement could be a key to how the enzyme promotes the transfer of the first electron from QH₂ to 2Fe-2S, but inhibits the transfer of the second electron from semiquinone to 2Fe-2S. The potential role of the *ef* loop in regulating the dynamics of ISP domain movement during the catalytic cycle is particularly intriguing.

Effects of Famoxadone on Electron Transfer between 2Fe-2S and Cyt c₁ in R.

sphaeroides Cyt bc₁—Electron transfer in the forward direction was studied using Ru₂D to photooxidize cyt *c*₁ in *R. sphaeroides* cyt *bc*₁ according to Scheme 1 in the presence of the sacrificial electron acceptor, [Co(NH₃)₅Cl]²⁺. The reduction of photooxidized cyt *c*₁

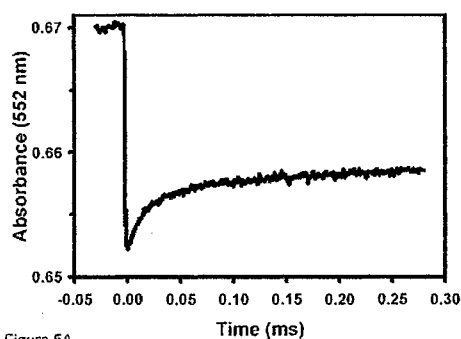


Figure 5A

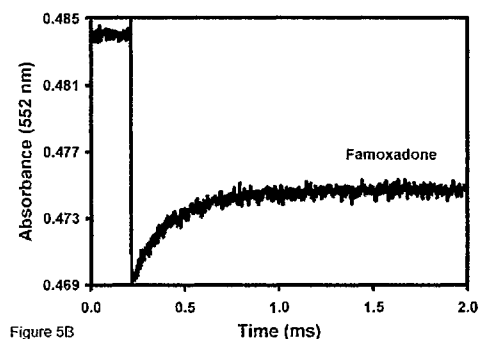


Figure 5B

Fig. 5. Electron transfer from 2Fe-2S to cyt c_1 in *R. sphaeroides* cyt bc_1 following photooxidation of cyt c_1 . (A) A solution containing 5 μM *R. sphaeroides* cyt bc_1 and 20 μM Ru₂D in 20 mM sodium borate, pH 9.0, and 5 mM $[\text{Co}(\text{NH}_3)_5\text{Cl}]^{2+}$ was treated with $\text{Q}_6\text{C}_{10}\text{Br}$ to reduce cyt bc_1 , and excited with a 480 nm laser flash. The smooth curve is a biphasic fit with rate constants of $80,000 \pm 15,000 \text{ s}^{-1}$ and $1,500 \pm 300 \text{ s}^{-1}$. (B) Famoxadone (30 μM) was added to the sample in (A) and subjected to flash photolysis. The monophasic transient has a rate constant of $6,800 \pm 1,200 \text{ s}^{-1}$.

was biphasic, with rate constants of $k_1 = 80,000 \pm 15,000 \text{ s}^{-1}$ and $k_2 = 1,500 \pm 300 \text{ s}^{-1}$ (Figure 5A). k_1 is due to electron transfer from 2Fe-2S to cyt c_1 , while k_2 is due to subsequent electron transfer from QH₂ to 2Fe-2S and cyt c_1 , followed by electron transfer from the semiquinone to cyt b_L and cyt b_H (Scheme 2) (10). Previous studies of the effects of temperature, pH, and redox potential demonstrated that k_1 is not rate-limited by true electron transfer in the c_1 state, but rather is gated by conformational changes from the b state and the mobile state to the active c_1 state (36). According to this analysis, the population of the c_1 state is small, but the rate constant for electron transfer from 2Fe-2S to cyt c_1 in the c_1 state is much larger than the observed value of k_1 , $80,000 \text{ s}^{-1}$. Addition of famoxadone leads to monophasic reduction of cyt c_1 with a rate constant of $4,800 \pm 800 \text{ s}^{-1}$ (Figure 5B). There is no reduction of cyt b_H in the presence of famoxadone, consistent with displacement of QH₂ from the Q₀ site. The most reasonable explanation of these results is that famoxadone binding stabilizes the b state of the ISP, and the observed rate constant k_1 is gated by the rate constant k_d for release of the ISP from the b state to the mobile state and the c_1 state. The rate constant k_f for the conformational change from the mobile state to the b state is expected to be much larger than k_d in the presence of famoxadone, and could be $80,000 \text{ s}^{-1}$ or larger. Electron transfer was also studied in the reverse direction using Ru₂D to photoreduce cyt c_1 in the oxidized complex according to Scheme 3 in the presence of the sacrificial electron donors aniline and 3CP. Oxidation of photoreduced cyt c_1 was biphasic with rate constants of $84,000 \pm 15,000 \text{ s}^{-1}$ and $4,800 \pm 800 \text{ s}^{-1}$ and relative amplitudes of 60% and 40%, respectively. Addition of famoxadone led to monophasic oxidation of cyt c_1 with a rate constant of $6,800 \pm 1,200 \text{ s}^{-1}$. It appears

Table II

Kinetic Properties of R. sphaeroides cyt bc₁ mutants

Mutant	Subunit	Enzymatic activity ^a	k ₁ (s ⁻¹) ^b	k ₂ (s ⁻¹) ^c
Wild type	---	2.5	80,000	1,200
K70C	Rieske	1.40	70,000	250
D143C	Rieske	0.98	20,000	1,500
F148C	Rieske	2.20	60,000	1,300
P150C	Rieske	0.23	50,000	4
G153C	Rieske	0.78	13,000	450
K164C	Rieske	0.98	82,000	1,300
P166C	Rieske	0.08	0	0
V64C	cyt <i>b</i>	2.5	58,000	1,400
G89C	cyt <i>b</i>	2.4	59,000	1,600
M92C	cyt <i>b</i>	2.5	82,000	1,600
A185C	cyt <i>b</i>	2.08	60,000	1,800
Y302C	cyt <i>b</i>	0.98	12,000	1,000
I326C	cyt <i>b</i>	0.80	86,000	1,200
K70C:A185C	cross-link	0	0	0
P33C:G89C	cross-link	1.3	48,000	1,100
N36C:G89C	cross-link	2.5	64,000	1,100

^aEnzymatic activity is expressed as $\mu\text{mol cyt } c \text{ reduced/min} / \mu\text{mol cyt } b$ at 25 °C. The error limits are $\pm 15\%$.

^bk₁ is the experimental rate constant for electron transfer from 2Fe-2S to cyt *c*₁ measured from the 552 nm transient at pH 9.0, 25 °C. The error limits are $\pm 20\%$.

^ck₂ is the rate constant for electron transfer from QH₂ to 2Fe-2S measured from the rate of cyt *b*_H reduction at 562 nm in the presence of antimycin A at pH 9.0. The error limits are $\pm 20\%$.

Table III

*Effect of famoxadone on electron transfer from 2Fe-2S to cyt c_1 in *R. sphaeroides* cyt bc_1 mutants*

Mutant	Subunit	Enzymatic activity ^a	Em (mV) ^b	k ₁ (s ⁻¹) (without famoxadone) ^c	k ₁ (s ⁻¹) (with famoxadone) ^d
Wild type	---	2.5	0	80,000	4,800
K70C	Rieske	1.40	+3	70,000	2,400
D143C	Rieske	0.98	nd	20,000	10,700
P150C	Rieske	0.23	-34	50,000	2,000
G153C	Rieske	0.78	-24	13,000	1,470
S154A	Rieske	0.23	-109	78,000	5,300
Y156W	Rieske	0.58	-62	150,000	12,000
V64C	cyt <i>b</i>	2.4	nd	58,000	5,000
Y302C	cyt <i>b</i>	0.98	nd	12,000	7,600

^aEnzymatic activity is expressed as μmol cyt *c* reduced/min /nmol cyt *b* at 25 °C. The error limits are $\pm 15\%$.

^bEm is the difference in redox potential between 2Fe-2S and cyt c_1 at pH 8.0, 25 °C. The error limits are ± 5 mV.

^ck₁ is the rate constant for electron transfer from 2Fe-2S to cyt c_1 measured from the 552 nm transient at pH 9.0, 25 °C. The error limits are $\pm 20\%$.

^dk₁ is the rate constant for electron transfer from 2Fe-2S to cyt c_1 in the presence of 30 μM famoxadone at pH 9.0, 25 °C. The error limits are $\pm 20\%$.

the Rieske protein is largely in the *b* conformation in the presence of famoxadone, and the rate of release to the *c*₁ conformation is decreased. The fact that the rate constants for forward and reverse electron transfer are nearly the same in the presence of famoxadone, indicates that the rate constant k_d does not depend on the redox state of 2Fe-2S.

Effect of Mutations in the iron-sulfur protein and cyt b on electron transfer in cytochrome bc₁—Mutations in *R. sphaeroides* *bc*₁ were generated by site-directed mutagenesis in order to characterize the interaction of the ISP with *cyt c*₁ and with *cyt b* (Figure 1). Flash photolysis studies were carried out to determine the effects of these mutations on the rate constants k_1 for electron transfer from 2Fe-2S to *cyt c*₁, and k_2 for electron transfer from QH₂ to 2Fe-2S as described above (Table 2). The effects of famoxadone on the kinetics of selected mutants was also examined (Table 3). The ISP mutant P166C is completely inactive in photoinduced electron transfer, suggesting that this mutation may have led to a critical alteration in the conformation of the ISP. The P150C mutation near the 2Fe-2S center dramatically decreases the rate constant k_2 for electron transfer from QH₂ to 2Fe-2S down to only $4 \pm 1 \text{ s}^{-1}$, but does not significantly affect the rate constant k_1 for electron transfer from 2Fe-2S to *cyt c*₁. It appears that the structural change caused by this mutation greatly affects the interaction of the ISP with the *cyt b* peptide, but does not affect the dynamics of the interaction of the ISP with *cyt c*₁. Famoxadone binding decreased the rate constant k_1 somewhat more than for wild-type *cyt bc*₁, indicating that the ISP was held more tightly in the *b* conformation (Table 3). The K70C mutation on the ISP decreases k_2 down to $250 \pm 50 \text{ s}^{-1}$, but does not affect k_1 , indicating a significant effect on the interaction of ISP with the *cyt b* peptide, but no

effect on the interaction with cyt c_1 . In contrast, the D143C mutation decreases k_1 down to $20,000 \pm 4,000 \text{ s}^{-1}$, but does not affect k_2 . This suggests that the acidic residue D143 on the surface of the ISP may be involved in the interaction with cyt c_1 . Surprisingly, famoxadone binding only decreased k_1 to $10,700 \pm 2,000 \text{ s}^{-1}$, indicating that this mutant is not held as tightly in the b conformation as wild-type ISP. The G153C mutation affects both rate constants, decreasing k_1 to $13,000 \pm 2,600 \text{ s}^{-1}$ and k_2 to $450 \pm 80 \text{ s}^{-1}$. This residue close to the 2Fe-2S center appears to be important for the interaction with both cyt b and cyt c_1 . Famoxadone binding to the G153C mutant decreased the rate of electron transfer from 2Fe-2S to cyt c_1 to $1,500 \pm 300 \text{ s}^{-1}$, indicating that this mutant is held more tightly in the b conformation than wild-type ISP. Among the cyt b mutations, only Y302C affected the photoinduced kinetics, decreasing k_1 to $12,000 \pm 2,000 \text{ s}^{-1}$ but not greatly affecting k_2 . It appears that the ISP is held more tightly in the b conformation in this mutant than in wild-type enzyme. Earlier studies have shown that the rate constant k_1 for electron transfer from 2Fe-2S to cyt c_1 was not greatly affected by ISP mutations S154A and Y156W, which decrease the redox potential of 2Fe-2S significantly (36). These results provided evidence that k_1 is not rate-limited by true electron transfer in the c_1 state, but is gated by conformational changes from the b state and the mobile state to the c_1 state. The effects of famoxadone binding on k_1 in the S154A and Y156W mutants were comparable to the effect on wild-type cyt bc_1 . Xiao et al. (12) have previously shown that formation of a disulfide cross-link between ISP and cyt b in the K70C:A185C mutant led to complete loss of steady-state activity, providing experimental evidence for the mobile shuttle mechanism of the ISP. The K70C:A185C mutant was totally inactive in

photoinduced electron transfer, providing further confirmation of the mobile shuttle mechanism. Xiao et al. (38) previously prepared the P33C:G89C and N36C:G89C mutants which each have a disulfide cross-link between the tail region of the ISP and cyt *b*. These mutants both have good steady-state enzyme activity, providing evidence for the intertwined dimer structure of cyt *bc*₁. The photoinduced electron transfer kinetics is not greatly affected by cross-linking in these mutants, providing further evidence that the tail region of the ISP is not involved in the mobile shuttle mechanism.

References

1. Trumpower, B. L. and Gennis, R. B. (1994) *Annu. Rev. Biochem.* **63**, 675-716.
2. Trumpower, B. L. (1990) *J. Biol. Chem.* **265**, 11409-11412.
3. Brandt, U. (1998) *Biochim. Biophys. Acta* **1364**, 261-268.
4. Xia, D., Yu, C.-A., Kim, H., Xia, J.-Z., Kachurin, A. M., Zhang, L., Yu, L., and Deisenhofer, J. (1997) *Science* **277**, 60-66.
5. Zhang, Z., Huang, L., Shulmeister, V. M., Chi, Y.-I., Kim, K. K., Hung, L.-W., Crofts, A. R., Berry, E. A., and Kim, S.-H. (1998) *Nature* **392**, 677-684.
6. Iwata, S., Lee, J. W., Okada, K., Lee, J. K., Wata, M., Rasmussen, B., Link, T. A., Ramaswamy, S., and Jap, B. K. (1998) *Science* **281**, 64-71.
7. Kim, H., Xia, D., Yu, C.-A., Xia, J.-Z., Kachurin, A. M., Zhang, L., Yu, L., and Deisenhofer, J. (1998) *Proc. Natl. Acad. Sci. U.S.A.* **95**, 8026-8033.
8. Hunte, C., Koepke, J., Lange, C., Rossmann, T., and Michel, H. (2000) *Structure Fold Des.* **8**, 669-84.
9. von Jagow, G., and Ohnishi, T. (1985) *FEBS Lett.* **185**, 311-315.
10. Sadoski, R. C., Engstrom, G., Tian, H., Zhang, L., Yu, C.-A., Yu, L., Durham, B., and Millett, F. (2000) *Biochem.* **39**, 4231-4236.
11. Tian, H., Yu, L., Mather, M., and Yu, C. A. (1998) *J. Biol. Chem.* **273**, 27953-27959.
12. Xiao, K., Yu, L., and Yu, C.-A. (2000) *J. Biol. Chem.* **275**, 38597-38604.
13. Tian, H., White, S., Yu, L., and Yu, C.-A. (1999) *J. Biol. Chem.* **274**, 7146-7152.
14. Darrouzet, E., Valkova-Valchanova, M. and Daldal, R. (2000), *Biochemistry* **39**, 15474-15483.
15. Nett, J. H., Hunte, C., and Trumpower, B. L. (2000) *Eur. J. Biochem.* **267**, 5777-

5782.

16. Gosh, M., Wang, C., Ebert, E., Vadlamuri, S., and Beattie, D. S. (2001) *Biochemistry* **40**, 327-335.

17. Darrouzet, E., Valkova-Valchanova, M., and Daldal, F. (2002) *J. Biol. Chem.* **277**, 3463-3470.

18. Darrouzet, E., and Daldal, F. (2002) *J. Biol. Chem.* **277**, 3471-3476.

19. Brugna, M, Rodgers, S., Schricker, A., Montoya, G., Kazmeier, M, Nitschike, W., and Sinning, I. (2000) *Proc. Nat. Acad. Sc. US.* **97**, 2069-2074.

20. Jordan, D. B., Livingston, R. S., Bisaha, J. J., Duncan, K. E., Pember, S. O., Piccollelli, M. A., Schwartz, R. S., Sternberg, J. A. and Tang, X. S. (1999) *Pestic Sci* **55**, 197-218.

21. Joshi, M. M. and Sternberg, J. A. (1996) Proc 1996 Brighton Crop Prot Conf-Pests and Diseases, British Crop Protection Council, Farnham, England, pp 21-26.

22. Beaument, K, Clough, J. M., de Fraine P. J. and Godfrey, C. R. A. (1991) *Pestic Sci* **31**, 499- 519.

23. Gao, X., Wen, X., Yu, C.-A., Esser, L., Tsao, S., Quinn B., Zhang, L., Yu, L., and Xia, D., (2002) *Biochemistry* **41**, 11692-11702.

24. Downard, A. J., Honey, G. E., Phillips, L. F., and Steel, P. J. (1991) *Inorg. Chem.* **30**, 2259-2260.

25. Yu, C.-A., Xia, J.-Z., Kachurin, A. M., Yu, L., Xia, D., Kim, H., and Deisenhofer, J. (1996) *Biochim. Biophys. Acta* **1275**, 47-53.

26. Moeller, T., Ed. (1957) *Inorganic Synthesis*, Vol. V, p. 185, McGraw Hill Book Company, Inc., New York.

27. Yu, L., and Yu, C. A. (1982) *J. Biol. Chem.* **257**, 2016-2021.

28. Mather, M. W., Yu, L., and Yu, C. A. (1995) *J. Biol. Chem.* **270**, 28668-28675.
29. Link, T. A., Hatzfeld, O. M., Unalkat, P., Shergill, J. K., Cammack, R., and Mason, J. R. (1996) *Biochemistry* **35**, 7546-7552.
30. Ugulava, N. B., and Crofts, A. R., (1998) *FEBS Lett.* **440**, 409-413. 31. Zhang, L., Tai, C-H., Yu, L., and Yu, C. A. (2000) *J. Biol. Chem.* **275**, 7656-7661.
32. Yu, L., Dong, J. H., and Yu, C. A. (1986) *Biochim. Biophys. Acta* **852**, 203-211.
33. Heacock, C., Liu, R., Yu, C.-A., Yu, L., Durham, B., and Millett, F. (1993) *J. Biol. Chem.* **268**, 27171-27175.
34. Meinhardt, S. W., and Crofts, A. R. (1982) *FEBS lett.* **149**, 223-227.
35. Crofts, A. R., and Wang, Z. (1989) *Photosynth. Res.* **22**, 69-87.
36. Engstrom, G., Xiao, K., Yu, C.-A., Yu, L., Durham, B., and Millett, F. (2002) *J. Biol. Chem.* **277**, 31072-31078.
37. Yu, C.A, Wen, X., Xiao, K., Xia, D., Yu, L. (2002) *Biochimica et Biophysica Acta* **1555**, 65-
38. Xiao, K., Chandrasekaran, A., Yu, L., and Yu, C.-A. (2001) *J. Biol. Chem.* **276**, 46125- 46131.
39. Juris, A., Balzani, V., Barigelletti, F., Campagna, S., Belser, P., and Von Zelewsky, A. (1988) *Coord. Chem. Rev.* **84**, 85-277.

CHAPTER VI

**The Extra Fragment of Iron-Sulfur Protein (Residues 96-107)
of *R. sphaeroides* Cytochrome *bc*₁ Complex is Required for
Protein Stability**

Kunhong Xiao, Chang-An Yu, and Linda Yu

The Journal of Biological Chemistry, submitted

ABSTRACT

Sequence alignment of the Rieske iron-sulfur protein (ISP) of cytochrome bc_1 complex from various sources reveals that bacterial ISPs contain an extra fragment. To study the role of this fragment in bacterial cytochrome bc_1 complex, *R. sphaeroides* mutants expressing His tagged cytochrome bc_1 complexes with deletion or single or multiple alanine substitution at various positions of this fragment (residues 96-107) were generated and characterized. The $ISP\Delta(96-107)$, $ISP(96-107)A$, and $ISP(104-107)A$ mutant cells, in which residues 96-107 of ISP are deleted, and residues 96-107 and 104-107 are substituted with alanine, respectively, do not grow photosynthetically and show no bc_1 complex activity in intracytoplasmic membranes prepared from these mutant cells. The $ISP(96-99)A$, in which residues 96-99 are substituted with alanine, grows photosynthetically at a rate comparable to that of the complement cells, whereas $ISP(100-103)A$, in which residues 100-103 are substituted with alanine, has a longer lag period prior to photosynthetic growth. Chromatophores prepared from these two mutant cells have 48% and 9% of the bc_1 activity found in the complement chromatophores. Studies of absorption spectra of cytochromes b and c_1 , EPR characteristics of ISP, Western and Northern blottings indicate that the loss (or decrease) of bc_1 activity in these mutant membranes results from a decrease in the amount of ISP in the membrane due to ISP instability and not from mutations affect the assembly of cytochromes b and c_1 into the membrane, the binding affinity of cytochrome b to cytochrome c_1 , or the ability of these two cytochromes to interact with ISP or subunit IV. The order of essentiality of residues in this fragment is: residues 104-107 > 100-103 > 96-99.

INTRODUCTION

Rhodobacter sphaeroides cytochrome bc_1 complex catalyzes electron transfer from ubiquinol to cytochrome c_2 with concomitant translocation of protons across the membrane to generate a proton gradient and membrane potential for ATP synthesis (1). Purified complex contains four protein subunits: the largest three, housing two b -type cytochromes (b_{566} & b_{562}), one c -type cytochrome (c_1), and one high potential Rieske iron-sulfur cluster ([2Fe-2S]), respectively, are the core subunits; the smallest one (subunit IV), containing no redox prosthetic group, is a supernumerary subunit (2). The genes for these four subunits were cloned and sequenced (3, 4). The protocol for generation of *R. sphaeroides* expressing His₆-tagged, wild-type and mutant cytochrome bc_1 complexes, has been well developed (5, 6). Since this four-subunit bacterial complex is functionally analogous to the mitochondrial enzyme, has simpler subunit composition, and is readily manipulated genetically, it has been used as a model for structural and functional studies of mitochondrial cytochrome bc_1 complexes.

Recently, the 3-D structures of mitochondrial bc_1 complexes from beef (7, 8), chicken (9), and yeast (10), which contain 7-8 supernumerary subunits in addition to the three core subunits, have been obtained. This structural information suggests an unexpected feature for this complex; e.g., the movement of the head domain of Rieske iron-sulfur protein (ISP) during bc_1 catalysis (7-9, 11, 12). The structure of ISP can be divided into three domains: the membrane-spanning N-terminal domain (tail), the soluble C-terminal extramembrane domain (head), and the flexible linking domain (neck). The [2Fe-2S] cluster, located at the tip of the head, accepts the first electron from ubiquinol and transfers it to heme c_1 in the proposed Q-cycle mechanism (13).

Biochemical evidence for this movement hypothesis was first provided by molecular genetic studies of the ISP neck in the *R. sphaeroides* complex (5, 14). Because the three-dimensional structures of the head and tail domains are rigid and are the same in the fixed and released states, a bending of the neck is required for movement of the head domain. For the neck region to bend, some flexibility is imperative (5, 14). Mutants with increased neck rigidity, generated by deletion or double- or triple-proline substitution, have greatly reduced electron transfer activity with increased activation energy (5). Formation of a disulfide bond between two engineered cysteines, having only one amino acid residue between them, in the neck region near the transmembrane helix, drastically reduces electron transfer activity (14), presumably because of increased neck rigidity. Cleavage of the disulfide bond by reduction or alkylation restores activity to that of the wild-type enzyme. These results clearly demonstrate a need for neck flexibility during catalysis. Molecular genetic studies of the ISP neck of the yeast (15-17) and *R. capulatus* (18) bc_1 complexes support this conclusion.

The movement hypothesis is further supported by the loss of bc_1 activity in *R. sphaeroides* bc_1 complexes having the ISP head locked in the fixed position by formation of an inter-subunit disulfide bond from a pair of engineered cysteines, one each at the head domain of ISP and cytochrome *b* (19). The rates of intra-electron transfer between heme c_1 and [2Fe-2S], induced by pH change (19) or by photoinduced ruthenium compound (20, 21), in this inter-subunit disulfide bond forming mutant complex are much lower than that in the wild-type or in their respective single cysteine mutant complexes, indicating that formation of an inter-subunit disulfide bond between

cytochrome *b* and ISP arrests the head domain of ISP in the “fixed state” position, too far away for electron transfer to heme c_1 (19, 21).

Since the redox potentials and EPR characteristics of [2Fe-2S] in *R. sphaeroides bc₁* complex are similar to those of the mitochondrial complex, the microenvironments of [2Fe-2S] cluster in these two complexes must be quite similar. However, sequence alignment of ISP in *R. sphaeroides bc₁* complex with its counter part in the beef heart mitochondrial complex reveals an extra fragment in the bacterial protein, corresponding to residues 96-107 (2) (see Fig. 1). This extra fragment is also present in ISPs from other bacterial *bc₁* complexes containing no supernumerary subunit, such as *Rhodobacter capsulatus* and *Paracoccus denitrificans*. ISPs from mitochondrial complexes with more supernumerary subunits, such as human and yeast, lack this extra fragment, it probably plays some role similar to that of the supernumerary subunits of the mitochondrial complex.

This extra fragment, located at the near middle portion of the ISP, is modeled into the 3-D structure of *R. sphaeroides bc₁* complex as an α -helical structure (see Fig. 2) using coordinates from residues 34-52 of subunit IX from the bovine complex (2). The α -helical structure of this extra fragment was recently confirmed by the X-ray crystallographic analysis of this bacterial *bc₁* complex at low resolution (Personal communication with E.A. Berry).

Does a mitochondrial-like ISP structure function in the bacterial complex? In the 3-D structural model of *R. sphaeroides bc₁* complex, the extra fragment is 20.77 -24.83 Å (Thr 96---Fe II, 20.77Å; ASN 102---Fe II, 21.42 Å; ALA 107---Fe II, 24.83 Å) away from the [2Fe-2S] cluster of ISP. Thus, direct participation of this fragment in electron

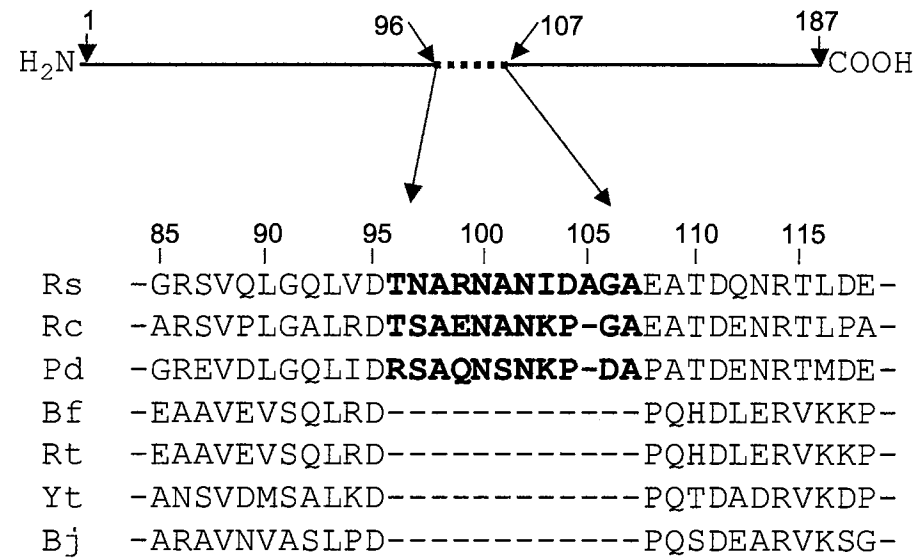


Fig. 1. Partial sequence comparison in the extra fragment of various ISPs: Rs, *Rhodobacter sphaeroides*; Rc, *Rhodobacter capsulatus*; Pd, *Paracoccus denitrificans*; Bf, beef; Rt, rat; Yt, yeast; Bj, *Bradyrhizobium japonicum*.

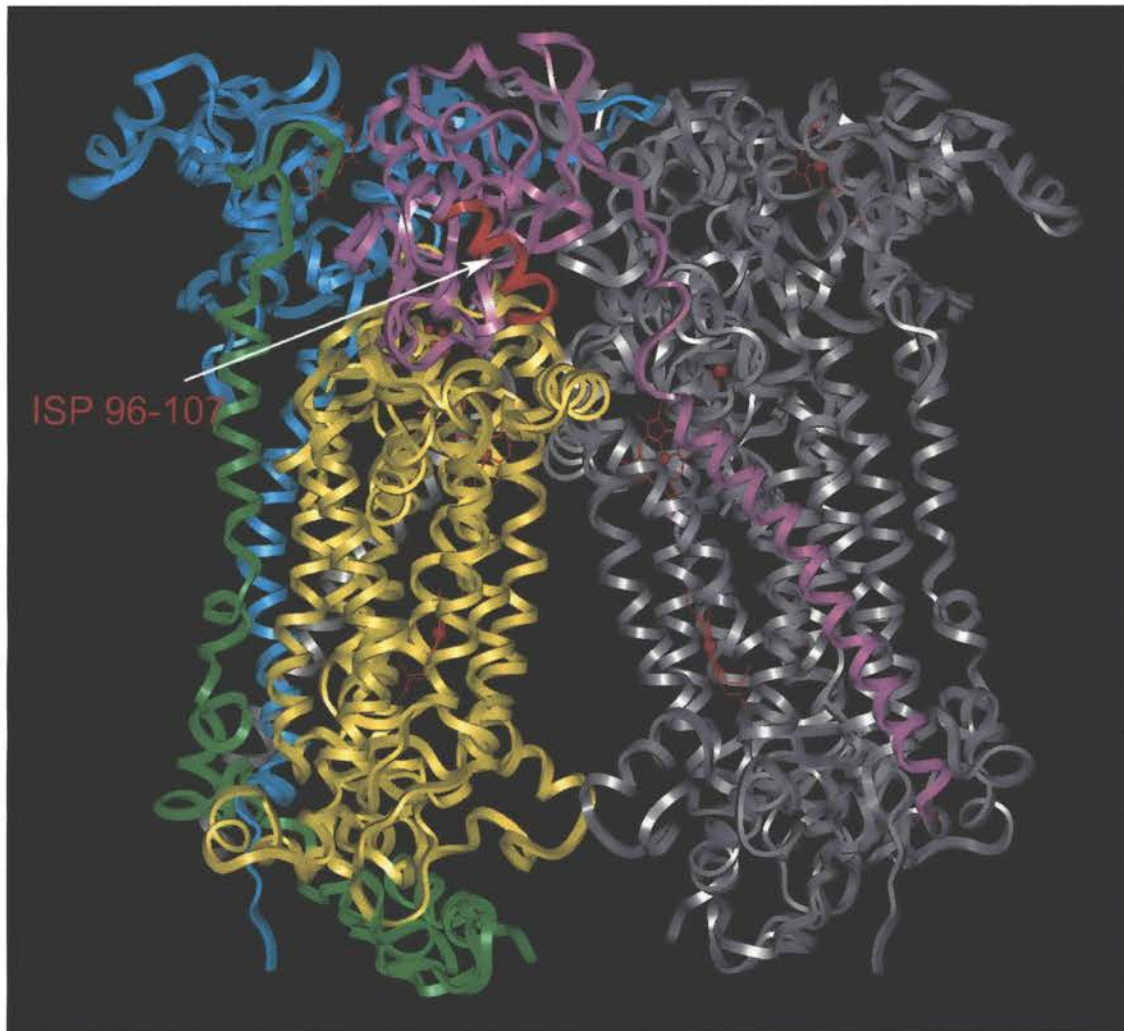


Fig. 2. The location of the extra fragment of ISP in the proposed structural model of *Rhodobacter sphaeroides* cytochrome bc_1 complex. In the left monomer, the cytochrome b is yellow, cytochrome c_1 blue, and subunit IV green; the ISP of the right monomer is in purple with the extra fragment (residues 96-107) colored in red. The other subunits are in gray for clarity.

transfer activity of ISP is unlikely. Perhaps this extra fragment is required for bacterial ISP's structural stability in the bc_1 complex, a function similar to that suggested for supernumerary subunits in the mitochondrial complex.

Mitochondrial cytochrome bc_1 complexes contain 7-8 supernumerary subunits whereas bacterial complexes have none or one supernumerary subunit (2). The structure of ISP in the mitochondrial complex may be stabilized through interactions between ISP and its neighboring supernumerary subunits. Since bacterial complexes lack a supernumerary subunit in the vicinity of ISP, interactions between the extra fragment and another part of ISP or between cytochrome b or cytochrome c_1 may contribute to the stability of ISP. The feasibility of using coordinates of supernumerary subunit IX of mitochondria to model this fragment into the structure of bacterial bc_1 complex (2) supports the idea that the extra fragment of ISP functions like a supernumerary subunit.

To investigate the role of this extra fragment of ISP in the bc_1 complex we generated *R. sphaeroides* mutants expressing His₆-tagged bc_1 complexes with deletion or substitution at various positions in this fragment. The photosynthetic behavior of mutants were examined and compared with those of the complement strain to see whether or not this extra fragment of ISP is an essential component of the bc_1 complex and to identify the critical amino acid residue(s). The bc_1 activity, the amount of ISP protein, and the EPR characteristics of ISP, in the membrane and the purified state, of complement and mutants were examined and compared.

ISP (T96A): CAGCTGGTCGACGCCAATGCCCGCAACGCG

ISP (N97A): CAGCTGGTCGACACCGCCGCCCGCAACGCGAACA

ISP (R99A): TGGTCGACACCAATGCCGCCAACGCGAACATCGACGCC

ISP (N100A): GTCGACACCAATGCCCGGCCGCGAACATCGA

ISP (N102A): ACCAATGCCCGCAACGCGGCCATCGACGCCGGCGCCG

ISP (I103A): CGCAACGCGAACGCCGACGCCGGCGCCGAGGCGACGG

ISP (D104A): GCAACGCGAACATCGCCGCCGGCGCCGAGGCG

ISP (G106A): AACGCGAACATCGACGCCGCCGCCGAGGCGACGGACCA

ISP (G106L): AACGCGAACATCGACGCCCTCGCCGAGGCGACGGACCA

The ISP Δ (96-107), ISP(96-99)A, ISP(100-103)A, ISP(104-107)A were constructed by the QuickChange[®] site-directed mutagenesis method, using a supercoiled double-stranded pGEM7Zf(+)-*fbcFB* as template and a forward and a reverse primer for PCR amplification. The pGEM7Zf(+)-*fbcFB* plasmid was constructed by ligating the *EcoRI*-*Bam*HI fragment from pSELNB3503 into *EcoRI* and *Hind*III sites of pGEM7Zf(+) plasmid. The primers used were as follows:

ISP Δ (96-107):

Forward primer---

CAGCTCGGCCAGCTGGTCGACGAGGCGACGGACCAGAACCGC

Reverse primer--- GCGGTTCTGGTCCGTCGCCTCGTCGACCAGCTGGCCGAGCTG

ISP(96-99)A:

Forward primer--- CGGCCAGCTGGTCGACGCCGCCCGCCGCCAACGCGAAC

Reverse primer--- GTTCGCGTTGCGGCGGCGGCGTCGACCAGCTGGCCG

ISP(100-103)A:

Forward primer ---

CAATGCCCGCGCCGCCGCCGCCGACGCCGGCGCCGAGGCGACG

Reverse primer---

CGTCGCCTCGGCGCCGGCGTCCGCCGCCGCCGCCGCGGGCATTG

ISP(104-107)A:

Forward primer--- GCAACGCGAACATCGCCGCCGCCGCCGAGGCGACGGAC

Reverse primer--- GTCCGTCGCCTCGGCCGCCGCCGCCGATGTTTCGCGTTGC

A plate-mating procedure (24) was used to mobilize the pRKD*fb*C_mBC_HQ plasmid in *E.coli* S17-1 cells into *R. sphaeroides* BC17 cells. The presence of engineered mutations were confirmed twice by DNA sequencing before and after photosynthetic or semi-aerobic growth of the cells as previously reported (24). DNA sequencing and oligonucleotide syntheses were performed by the Recombinant DNA/Protein Core Facility at Oklahoma State University.

Enzyme Preparations and Activity Assay-- Chromatophores were prepared and His₆-tagged cytochrome *bc*₁ complexes were purified from chromatophores or ICM as previously reported (5). To assay the cytochrome *bc*₁ complex activity, membrane or purified cytochrome *bc*₁ complexes were diluted with 50 mM Tris-Cl, pH 8.0, containing 200 mM NaCl and 0.01% dodecylmaltoside to a final concentration of cytochrome *b* of 3 μM. Appropriate amount of the diluted samples were added to 1-ml of assay mixture containing 100 mM of Na⁺/K⁺ phosphate buffer, pH 7.4, 300 μM of EDTA, 100 μM of cytochrome *c*, and 25 μM of Q₀C₁₀H₂. Activities were determined by measuring the reduction of cytochrome *c* (the increase of absorbance at 550 nm) in a Shimadzu UV 2101 PC spectrophotometer at 23 °C, using a millimolar extinction coefficient of 18.5 for

calculation. The nonenzymatic oxidation of $Q_0C_{10}H_2$, determined under the same conditions, in the absence of enzyme, was subtracted.

Other Biochemical and Biophysical Techniques-- Protein concentration was measured by the method of Lowry *et al.*(25). Cytochrome *b* (26) and cytochrome *c*₁ (27) were determined according to published methods. SDS-PAGE was performed according to Laemmli (28) using a Bio-Rad Mini-protean dual slab vertical cell. Western blotting used rabbit polyclonal antibodies raised against ISP of *R. sphaeroides*. The polypeptides separated in the SDS-PAGE gel were transferred to a 0.22 μ M Nitrocellulose membrane for immunoblotting. Protein A conjugated to horseradish peroxidase was used as the second antibody. Total RNA from wild-type or mutant *R. sphaeroides* was prepared from cells harvested at mid-log phase using the RNeasy[®] Mini Kit from Qiagen. The DNA probe containing the ISP gene was prepared by polymerase chain reaction using 5'ACGCCACGGCCGGAGCCGGGGCGGTG3' and 5'CTCCGCTGCCTGGTCTTGGC3' as forward and reverse primers, respectively. Northern blot was performed by using the North2South[®] Direct HRP Labeling and Detection Kit from Pierce. EPR spectra were recorded with a Bruker ER 200D equipped with a liquid N₂ Dewar at 77 K. Instrument settings are detailed in legends of the relevant figures.

RESULTS AND DISCUSSION

The Essentiality of ISP Extra Fragment for the Cytochrome *bc*₁ Complex-- The *R. sphaeroides* ISP extra fragment that corresponds to residues 96-107 with a sequence of TNARNANIDAGA is located at the near middle portion of the ISP sequence (see Fig. 1).

To probe the role of this fragment, *R. sphaeroides* mutants expressing His₆-tagged *bc*₁ complexes with deletion or substitution at various positions of the extra fragment were generated and characterized. Because the *bc*₁ complex is absolutely required for the photosynthetic growth of *R. sphaeroides*, whether or not this ISP extra fragment is critical to the complex can be determined by assaying photosynthetic growth.

When this extra fragment is deleted from the ISP sequence, the resulting cells [ISPΔ(96-107)] are unable to support photosynthetic growth, indicating that this region is required for *bc*₁ complex activity. To further confirm that the inability of the ISPΔ(96-107) mutant cells to grow photosynthetically results from the essentiality of the extra fragment for the *bc*₁ complex, and not from improper protein assembly or folding due to the large deletion, a mutant with an extra fragment substituted with alanines [ISP(96-107)A] was generated and shown to be unable to grow photosynthetically. This result supports the essentiality of this ISP extra fragment in the bacterial *bc*₁ complex, and suggests that the amino acid residues, rather than the length or α -helical structure of the extra fragment, are critical, since the alanine substituted fragment should have the same length as the wild-type fragment and the same α -helical structure.

To identify critical amino acid residues in the ISP extra fragment, we first located the critical regions. Residues in three portions of the extra fragment were replaced with alanine to generate three mutants: ISP(96-99)A, ISP(100-103)A, and ISP(104-107)A, which were subjected to photosynthetic growth conditions. The ISP(96-99)A mutant grows photosynthetically at a rate comparable to that of wild type cells; the ISP(100-103)A mutant, after a long lag time (when the wild-type cells have grown to stationary phase under the same condition), starts to grow at a rate comparable to that of the wild-

type cells; and the ISP(104-107)A mutant does not grow photosynthetically (see Fig. 3). These results indicate that the first four residues (residues 96-99) in the ISP extra fragment are not critical; the second four residues (residues 100-103) may possess the supernumerary subunit's function, since the ISP(100-103)A mutant has a growth behavior similar to that of the subunit IV-lacking *R. sphaeroides* (RS Δ IV) cells (29); and the last four residues (104-107) are critical.

Since residues 104-107 of ISP have an amino acid sequence of -D-A-G-A-, the inability of ISP(104-107)A mutant to grow photosynthetically must result from alanine replacement at D-104 and/or G-106. Hence, two single alanine mutants, D104A and G106A, were generated and subjected to anaerobic photosynthetic growth conditions. Both mutants grow at a rate comparable to that of wild-type cell. This indicates that the inability of the ISP(104-107)A mutant to grow photosynthetically results from the combined effect of alanine substitutions at both D104 and G106.

Table I shows ubiquinol-cytochrome *c* reductase activities in membranes prepared from complement and mutant cells. Intracytoplasmic membranes (ICMs) from mutants ISP Δ (96-107) and ISP(96-107)A have no ubiquinol-cytochrome *c* reductase activity. This is as expected, since *bc*₁ complex is required for photosynthetic growth and neither mutant grows photosynthetically. The ISP(96-99)A, ISP(100-103)A, and ISP(104-107)A mutant membranes have, respectively, 48, 9, and 0% of the ubiquinol-cytochrome *c* reductase activity found in the complement chromatophores, suggesting the essentiality of the ISP extra fragment to the *bc*₁ complex is in the order of : residues 104-107 > residues 100-103 > residues 96-99. It should be noted that all the single substitution mutant chromatophores, ISPs(T96A), (N97A), (R99A), (N100A), (N102A), ISP(I103A),

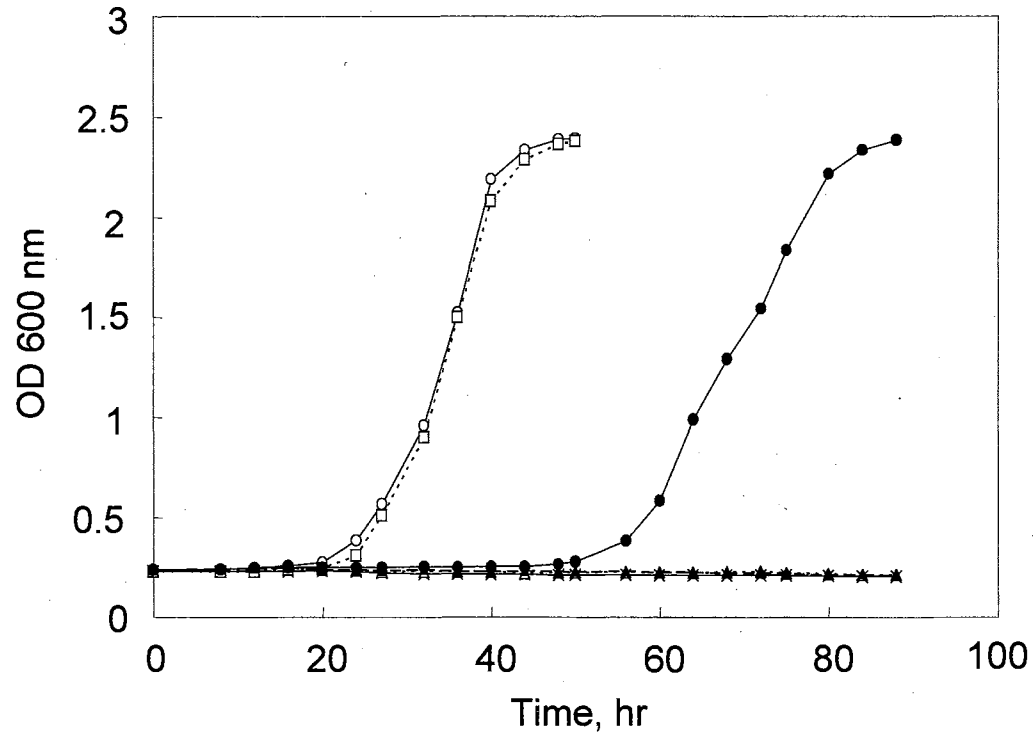


Fig. 3. Photosynthetic growth of various *R. sphaeroides* strains. 60 ml of mid-log phase aerobic grown complement (—○—), ISPΔ(96-106) (—×—), ISP (96-106)A (—△—), ISP (96-99)A (···□···), ISP (100-103)A (—●—), and ISP (104-107)A (···▲···) with the same cell intensity were inoculated into 1-liter Sistrom medium containing 25 μg/ml kanamycin and 30 μg/ml of thrimethoprim and subjected to photosynthetic growth conditons as described in Experimental Procedure. Growth was moitored at OD660 nm.

Table I.

Characterization of the ISP extra fragment mutants

Strains	Ps ^a	Cytochrome <i>bc</i> ₁ complex		
		Membrane	Purified Complex	
		Specific Activity ^e	Specific Activity	Subunit Composition
Complement	+++ ^b	2.3	2.5	FBCQ ^f
ISPΔ(96-107)	- ^c	0	0	BC
ISP(96-107)A	-	0	0	BC
ISP(96-99)A	+++	1.1	0.9	FBCQ
ISP(100-103)A	++ ^d	0.2	0	BC
ISP(104-107)A	-	0	0	BC
ISP(D104A)	+++	2.2	2.4	FBCQ
ISP(G106A)	+++	2.2	2.4	FBCQ
ISP(G106L)	+++	2.2	2.4	FBCQ
ISP(N100A)	+++	2.2	2.4	FBCQ
ISP(I103A)	+++	2.3	2.3	FBCQ
ISP(T96A)	+++	2.2	2.4	FBCQ
ISP(N97A)	+++	2.2	2.5	FBCQ
ISP(R99A)	+++	2.3	2.5	FBCQ

^aPs, photosynthetic growth.

^b+++, the growth rate was essentially the same as that of the complement cells.

^c-, no photosynthetic growth within 4 days.

^d++, the cells can grow photosynthetically but the growth rate was slower than that of the complement cells.

^e Enzymatic activity is expressed as μmol cytochrome *c* reduced/min/nmol cytochrome *b*.

^fFBCQ indicates gene products of the *fbcF* (ISP) (F), *fbcB* (cytochrome *b*) (B), *fbcC* (cytochrome *c*₁) (F), and *fbcQ* (subunit IV) (Q), respectively.

(D104A), (G106A) and (G106L), have ubiquinol-cytochrome c reductase activity similar to that found in complement chromatophores. This indicates that the role played by the extra fragment of ISP is not individual amino acid specific but is a combination effect of several residues.

The Requirement of the ISP Extra Fragment for ISP Protein Stability-- To determine whether the loss (or decrease) of the cytochrome bc_1 complex activity in the mutant membranes of ISP Δ (96-107), ISP(96-107)A, ISP(96-99)A, ISP(100-103)A, ISP(104-107)A results from a lack (or decrease) of ISP protein in the membrane, the amount of ISP protein and its EPR characteristics, in mutant and complement membranes, were compared. Western blot analysis with antibodies against *R. sphaeroides* ISP revealed that mutant membranes of ISP Δ (96-107), ISP(96-107)A, and ISP(104-107)A contain no detectable ISP protein, and the ISP(96-99)A and ISP(100-103)A mutant membranes have, respectively, 50 and 5%, of the amount of ISP found in complement membrane (see Fig. 4). Absorption spectral analyses show that the content of cytochrome b and c_1/c_2 in all of these mutant membranes is the same as that in the complement membrane (data not shown). These results indicate that the mutation on the extra fragment affects the assembly of ISP, but not of cytochrome b and c_1/c_2 , into the membrane. Although the ISP(96-99)A and ISP(100-103)A mutant membranes had decreased amounts of ISP, the [2Fe-2S] in these membranes had an EPR spectrum identical to that observed in complement chromatophores, with resonance at $g_x=1.80$ and $g_y=1.90$ (see Fig. 5). As expected, no [2Fe-2S] cluster is detected in mutant membranes of ISP(104-107)A, ISP Δ (96-107), and ISP(96-107), since they contain no ISP protein.

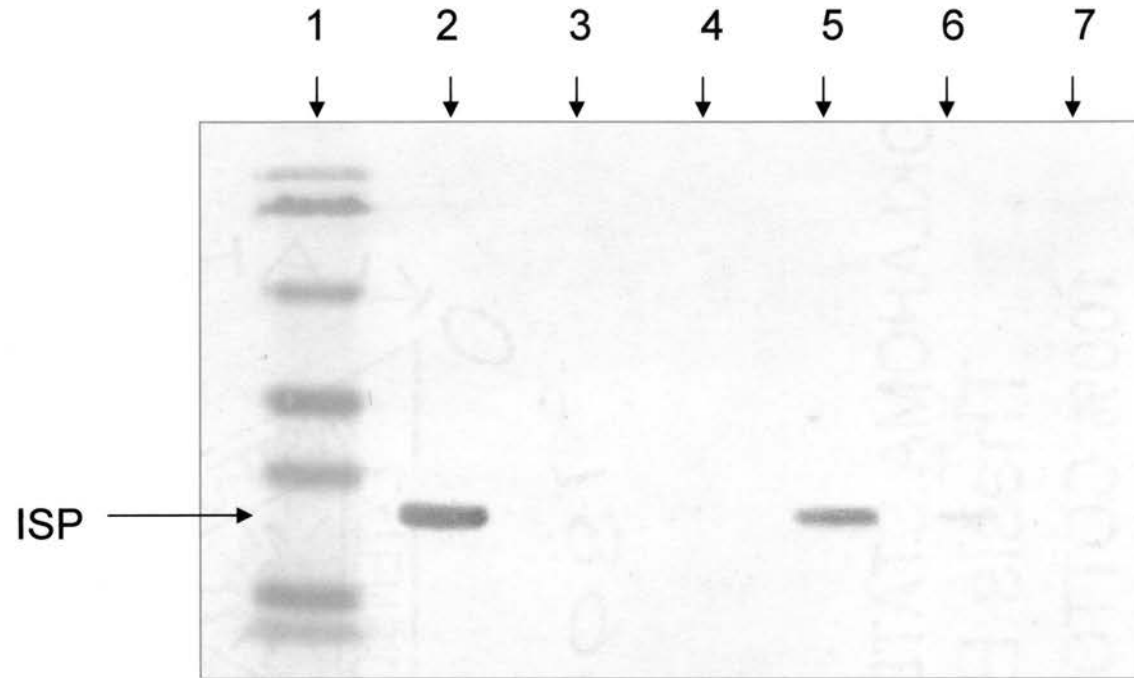


Fig. 4. Western blot analysis of ISP in complement and mutant membranes. Membrane samples containing 35 pmol of cytochrome *b* were loaded into each well and subjected to SDS-PAGE. The proteins in the gel were transferred electrophoretically to a 0.22 μ M Nitrocellulose membrane and treated with antibodies against *R. sphaeroides* ISP. Protein A horseradish peroxidase was used as the second antibody. Lane 1, prestained molecular mass standards; lanes 2-5, membranes from complement, ISP Δ (96-107), ISP(96-107)A, ISP(96-99)A, ISP(100-103)A, and ISP(104-107)A, respectively.

These results further confirm that the mutations affect the assembly of ISP into the membrane, but not the microenvironments of the iron-sulfur cluster.

The observation of a lack of (or decrease in) ISP in mutant membranes can result from mutant ISP protein instability, mutant ISP mRNA instability, or inability of mutant ISP to be assembled into the membrane. To test these possibilities, the amounts of ISP in the cell lysate, 200,000 x g supernatant and precipitate fractions from mutant cells during membrane preparation were determined and compared with those obtained from complement cells (see Fig. 6). Mutant cell lysates of ISP Δ (96-107), ISP(96-107)A, ISP(96-99)A, ISP (100-103)A, and ISP (104-107)A have, respectively, 10%, 10%, 50%, 30%, and 10% of the ISP content of complement cell lysates, based on Western Blotting. When these cell lysates are centrifuged at 200,000 x g for 2.5 hrs to separate the supernatant from the membrane fraction, no ISP is found in any supernatant fraction. While nearly all of the ISP in the complement cell lysates is recovered in the membrane fraction, less than 60% and 10% of the ISPs in the ISP(96-99)A and ISP(100-103)A mutant cell lysates is recovered in the membrane fractions, respectively. The low recovery of ISP from cell lysate to membrane fraction of these mutants is apparently due to degradation of ISP during the duration of centrifugation. No ISP in cell lysates of the ISP Δ (96-107), ISP(96-107)A, and ISP(104-107)A mutants is recovered in their respective membrane fractions. The fact that no ISP is detected in any supernatant fraction together with the observation that the rates of *bc*₁ activity decay in the cell lysates and in the membrane fraction are similar for ISP(96-99)A and ISP(100-103)A mutant cells, suggests that the low recovery of ISP in the membrane fractions of these mutant cells results from the instability of mutant ISP, not from the inability of mutant

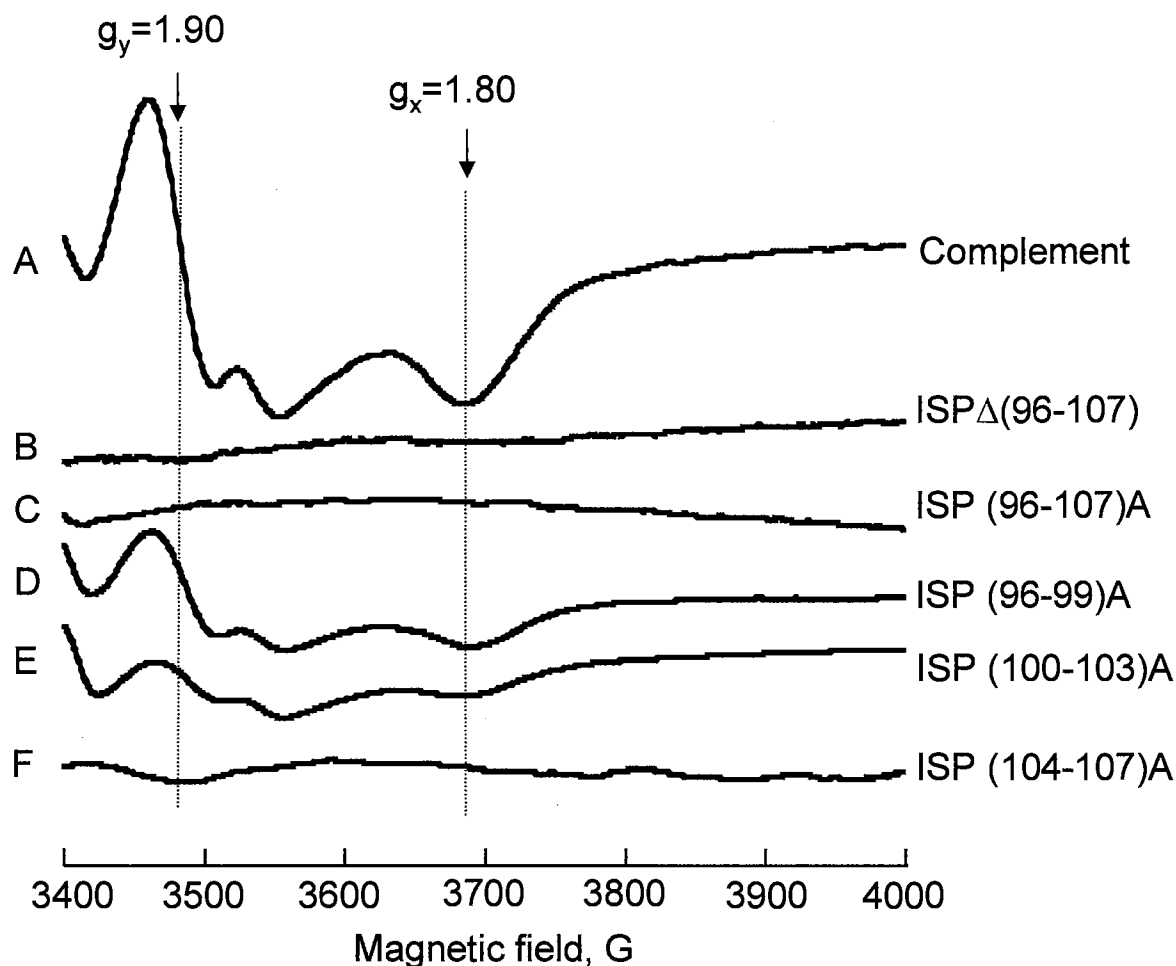


Fig. 5. EPR spectra of the 2Fe₂S cluster of Rieske iron-sulfur protein in membranes from the complement and mutants ISP Δ (96-107), ISP(96-107)A, ISP(96-99)A, ISP(100-103)A, and ISP(104-107)A. Membrane pastes were partially reduced by addition of 5 mM sodium ascorbate on ice for 30 min and frozen in liquid nitrogen. EPR spectra were recorded at 77 °K with the following instruments settings: microwave frequency, 9.28 Hz; microwave power, 20 milliwatts; modulation amplitude, 20 G; modulation frequency, 100 kHz; time constants, 0.1 s; and scan rate, 20 G/s.

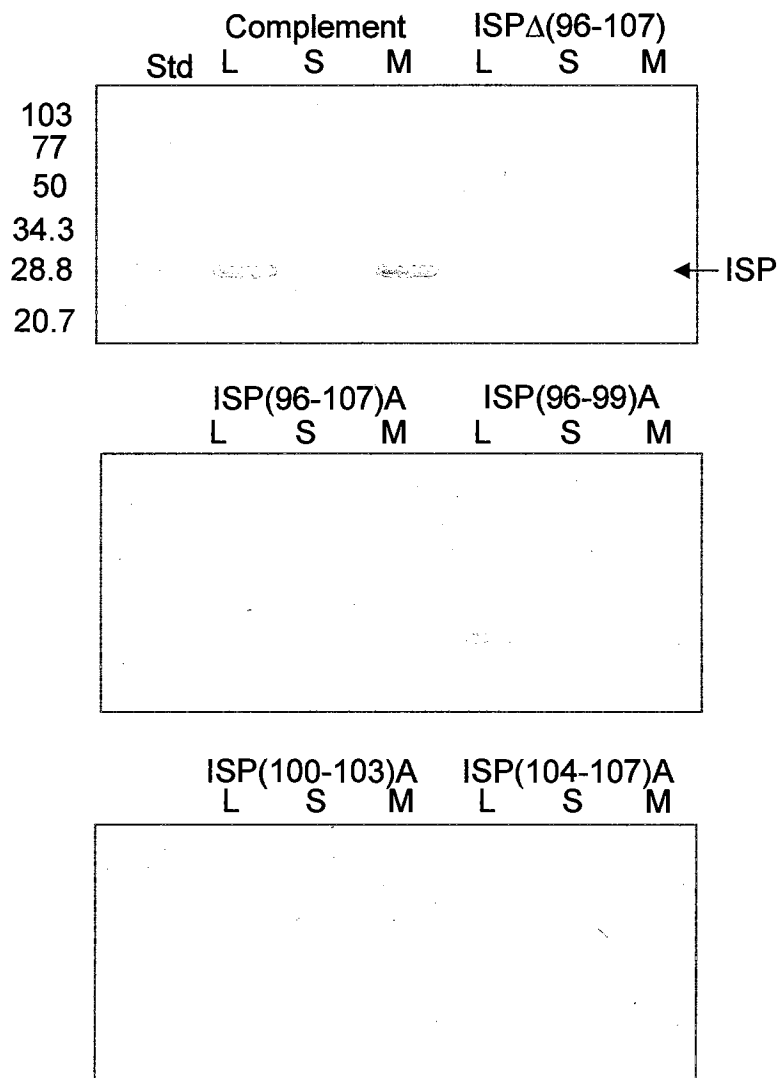


Fig. 6. Western blot analysis of ISP in cell lysates, 200,000 x g supernatant and 200,000 x g precipitate fractions from complement and mutant cells. 30 grams wet weight of complement, $ISP\Delta(96-107)$, $ISP(96-107)A$, $ISP(96-99)A$, $ISP(100-103)A$, and $ISP(104-107)A$ were suspended with 50 mM Tris-Cl, pH 8.0, containing 200 mM NaCl to a final volume of 90 ml, subjected to sonification to break the cells, and centrifuged at 12,000 xg for 15 min to remove unbroken cells. The cell lysates were then centrifuged at 200,000 x g for 2.5 hrs to separate the soluble fractions from the membrane fractions. The membrane fractions were suspended with 50 mM Tris-Cl, pH 8.0, containing 1 mM EDTA to a final volume of 90 ml. Forty- μ l aliquots were withdrawn from the cell lysate (L), 200,000 xg supernatant (S) and membrane (M) suspension fractions, mixed with 10 μ l of 5X digestion buffer, and incubated 2 hrs at 37 $^{\circ}$ C. Five- μ l aliquots of digested samples were applied to each well of SDS-PAGE gel. Western blotting was performed as described for Fig. 4.

ISP to be incorporated into the membrane. Apparently, the protein instability increases with mutation of residues toward the end (residues 104-107) of the extra fragment.

To further confirm that a lack of (or decrease) ISP protein in mutant membranes of ISP Δ (96-107), ISP(96-107)A, ISP(104-107)A, ISP(100-103)A, and ISP(96-99)A results from mutant protein instability, and not mutant mRNA instability, the amount of ISP mRNAs from complement and mutant cells were compared by Northern blotting using an HRP-labeled-DNA probe containing the ISP gene. Since all mutant cells have the same amount of ISP mRNAs as the complement cells (data not shown), mutation of the ISP extra fragment did not affect the stability of ISP mRNA.

The Effect of Mutation on Cytochrome *b* and Cytochrome *c*₁-- Absorption spectral analysis revealed that mutant membranes of ISP Δ (96-107)A, ISP(96-107)A, ISP(104-107)A, ISP(100-103)A, and ISP(96-99)A have the contents and spectral characteristics of cytochromes *b* and *c*₁/*c*₂ similar to those of complement chromatophores. Moreover, Western blot analysis, using antibodies against subunit IV, showed that all these mutant membranes have the same amount of subunit IV as does the complement membrane. Thus, mutation does not affect assembly of cytochromes *b* and *c*₁ and subunit IV into the membrane.

When the cytochrome *bc*₁ complexes were purified from mutant membranes by dodecylmaltoside solubilization and Ni-NTA column chromatography, all but the ISP(96-99)A complex contain two subunits corresponding to cytochromes *b* and *c*₁ (see Fig. 7). Purified ISP(96-99)A complex contains four protein subunits with ISP and subunit IV in decreased amounts compared to purified wild-type complex. The ratio of *b/c*₁ in all purified mutant complexes is similar to that in the wild-type complex, indicating that

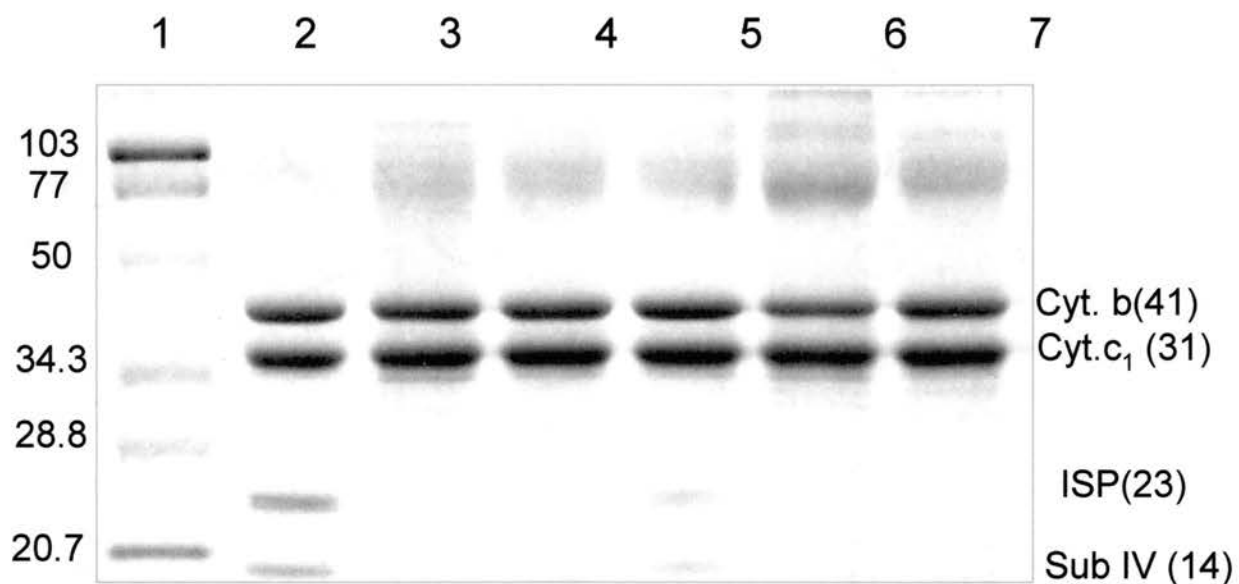


Fig. 7. SDS-PAGE analysis of the purified cytochrome bc_1 complexes from complement and mutant membranes. Aliquots of complement (lane 2), $ISP\Delta(96-107)$ (lane 3), $ISP(96-107)A$ (lane 4), $ISP(96-99)A$ (lane 5), $ISP(100-103)A$ (lane 6), $ISP(104-107)A$ (lane 7) were incubated with 1% SDS and 0.4% β -ME at 37 ° C for 2 h. Digested samples containing 150 pmol of cytochrome *b* were subjected to electrophoresis. *Lane 1*, protein standard (*Std*) containing: phosphorylase B (103 kDa), bovine serum albumin (77 kDa), ovalbumin (50 kDa), carbonic anhydrase (34.3 kDa), soybean trypsin inhibitor (28.8 kDa), and lysozyme (20.7 kDa).

mutation did not affect the binding affinity of cytochrome *b* to c_1 , but greatly decreased the binding affinity of subunit IV to cytochrome c_1 or to cytochrome *b*. Since it has been reported that incorporation of recombinant subunit IV into the bc_1 complex does not require the presence of ISP (30), the simultaneous loss of ISP and subunit IV when the ISP extra fragment is altered may result from induced changes on subunit IV which decrease its affinity for cytochrome *b* or c_1 .

To determine whether the two-subunit bc_1 complexes purified from $ISP\Delta(96-107)$, $ISP(96-107)A$, $ISP(100-103)A$, and $ISP(104-107)A$ are functionally active, the effect of the addition of ISP was examined. The two-subunit mutant complexes were incubated with purified recombinant subunit IV for 30 min at 0 °C prior to the addition of purified, wild-type ISP. Activity of cytochrome bc_1 complex is restored after the addition of ISP indicating that cytochromes *b* and c_1 subunits are indeed functionally active.

REFERENCES

1. Trumpower, B. L., and Gennis, R. B. (1994) *Annu. Rev. Biochem.* **63**, 675-716.
2. Yu, L., Tso, S-C., Shenoy, S. K., Quinn, B. N., and Xia, D. (1999) *J. Bioenerg. Biomembr.* **31**, 251-257.
3. Yun, C.H., Beci, R., Croft, A. R., Kaplan, S., and Gennis, R. (1991) *Eur. J. Biochem.* **194**, 399-411.
4. Usui, S., and Yu, L. (1991) *J. Biol. Chem.* **266**, 15644-15649.
5. Tian, H., Yu, L., Mather, M. W., and Yu, C. A. (1998) *J. Biol. Chem.* **273**, 27953-27959.
6. Guergova-Kuras, M., Salcedo-Hernandez, R., Bechmann, G., Kuras, R., Gennis, R. B., and Crofts, A. R. (1999) *Protein Expr. Purif.* **15**, 370-380.
7. Xia, D., Yu, C. A., Kim, H., Xia, J. Z., Kachurin, A. M., Zhang, L., Yu, L., and Deisenhofer, J. (1997) *Science* **277**, 60-66.
8. Iwata, S., Lee, J. W., Okada, K., Lee, J. K., Iwata, M., Rasmussen, B., Link, T. A., Ramaswamy, S., and Jap, B. K. (1998) *Science* **281**, 64-71.
9. Zhang, Z. L., Huang, L-S., Shulmeister, V. M., Chi, Y-I., Kim, K. K., Huang, L-W., Crofts, A. R., Berry, E. A. and Kim, S-H (1998) *Nature* **392**, 677-684.
10. Hunte, C., Koepke, J., Lange, C., Robmanith, T., and Michel, H. (2000) *Structure* **8**, 669-684.
11. Kim, H., Xia, D., Yu, C. A., Kachurin, A., Zhang, L. Yu, L. and Deisenhofer, J. (1998) *Proc. Natl. Acad. Sci. USA* **95**, 8026-8033.
12. Berry, E. A., Guergova-Kuras, M., Huang, L. S., and Crofts, A. R. (2000) *Annu. Rev. Biochem.* **69**, 1005-1075.

13. Mitchell, P. (1976) *J. Theor. Biol.* **62**, 327-367.
14. Tian, H., White, S., Yu, L., and Yu, C. A. (1999) *J. Biol. Chem.* **274**, 7146-7152.
15. Obungu, V. H., Wang, Y., Amyot, S. M., Gocke, C. B., and Beattie, D. S (2000) *Biochim. Biophys. Acta.* **1457**, 36-44.
16. Ghosh, M., Wang, Y., Ebert, C. E., Vadlamuri, S., and Beattie, D. S. (2001) *Biochemistry* **40**, 327-335.
17. Nett, J. H., Hunte, C., and Trumpower, B. L. (2000) *Eur. J. Biochem.* **267**, 5777-5782.
18. Darrouzet, E., Valkova-Valchanova, M., Moser, C. C., Dutton, P. L., and Daldal, F. (2000) *Proc. Natl. Acad. Sci. U S A.* **97**, 4567-4572.
19. Xiao, K., Yu, L., and Yu, C. A. (2000) *J. Biol. Chem.* **275**, 38597-38604.
20. Engstrom, G., Xiao, K., Yu, C.A., Yu, L., Durham, B., and Millett, F. (2002) *J Biol Chem.* **277**, 31072-31078.
21. Xiao, K., Engstrom, G., Rajagukguk, S., Yu, C. A., Yu, L., Durham, B., and Millett, F. (2002) *J. Biol. Chem.* **278**, 11419-11426.
22. Yu, C. A., and Yu, L. (1982) *Biochemistry* **21**, 4096-4101.
23. Tian, H., Yu, L., Mather, M. W., and Yu, C. A. (1997) *J. Biol. Chem.* **272**, 23722-23728.
24. Mather, M. W., Yu, L., and Yu, C. A. (1995) *J. Biol. Chem.* **270**, 28668-28675.
25. Lowry, O. H., Rosebrough, N. J., Farr, A. L., and Randall, R. J. (1951) *J. Biol. Chem.* **193**, 265-275.
26. Berden, J. A., and Slater, E. C. (1970) *Biochim. Biophys. Acta* **216**, 237-249.
27. Yu, L., Dong, J. H., and Yu, C. A. (1986) *Biochim. Biophys. Acta* **852**, 203-211.

28. Laemmli, U. K. (1970) *Nature* **227**, 680-685.
29. Chen, Y-R., Usui, S., Yu, C. A., and Yu, L. (1994) *Biochemistry* **33**, 10207-10214.
30. Tso, S.C., Shenoy, S.K., Quinn, B.N., and Yu, L. (2000) *J Biol Chem.* **275**, 15287-15294.

VITA 2

Kunhong Xiao

Candidate for the Degree of

Doctor of Philosophy

Thesis: STRUCTURE AND FUNCTION STUDIES OF *RHODOBACTER SPHAEROIDES* CYTOCHROME *bc*₁ COMPLEX

Major Field: Biochemistry and Molecular Biology

Biographical:

Personal Data: Born in Hunan, China, on April 20, 1970, the son of Quanhua Xiao and Yucui Zeng.

Education: Graduated from the Second High School of Wugang, Hunan, China in July 1988; received Bachelor of Medicine degree in Medicine from Beijing Medical University, Beijing, China in July 1993. Completed requirements for the Doctor of Philosophy degree with a major in Biochemistry and Molecular Biology at Oklahoma State University in May, 2003.

Professional Memberships: American Association for the Advancement of Science; American Biophysical Society; The Honor Society of Phi Kappa Phi.